EXTENDING THE SUPERSYMMETRIC LITTLE HIERARCHY

A DISSERTATION
SUBMITTED TO THE DEPARTMENT OF PHYSICS
AND THE COMMITTEE ON GRADUATE STUDIES
OF STANFORD UNIVERSITY
IN PARTIAL FULFILLMENT OF THE REQUIREMENTS
FOR THE DEGREE OF
DOCTOR OF PHILOSOPHY

Kiel Howe

August 2015

This dissertation is online at: http://purl.stanford.edu/xb659nv9064

I certify that I have read this dissertation and that, in my opinion, it is fully adequate in scope and quality as a dissertation for the degree of Doctor of Philosophy.

Peter Graham, Primary Adviser

I certify that I have read this dissertation and that, in my opinion, it is fully adequate in scope and quality as a dissertation for the degree of Doctor of Philosophy.

Savas Dimopoulos

I certify that I have read this dissertation and that, in my opinion, it is fully adequate in scope and quality as a dissertation for the degree of Doctor of Philosophy.

JoAnne L. Hewett

Approved for the Stanford University Committee on Graduate Studies.

Patricia J. Gumport, Vice Provost for Graduate Education

This signature page was generated electronically upon submission of this dissertation in electronic format. An original signed hard copy of the signature page is on file in University Archives.

Abstract

Particle physics describes particles and their interactions at many energy scales, and different models can be characterized by the relationships between these scales. In a natural model, particle properties are insensitive to perturbations at higher energy scales, while in a tuned model particle properties are determined by delicate cancellations between processes even at energy scales separated by large hierarchies. Is our universe natural or tuned? The answer to this question can have dramatic consequences for the interpretation of fundamental theories and for our understanding of the inflationary birth of our universe. The discovery of a Standard Model-like Higgs Boson at the CERN Large Hadron Collider (LHC) has made concrete the possibility that our universe may be tuned. However, the observed particles of the Standard Model may still form part of a natural model if new particles and symmetries are present at energies observable at the LHC and future colliders. Supersymmetry is one possible extension of the Standard Model motivated by the idea of naturalness, but its minimal version is highly constrained by searches from the first run of the LHC. We describe extensions of the minimal supersymmetric model in which a little hierarchy between the masses of the new supersymmetric particles and the Standard Model particles is consistent with naturalness and current LHC searches. We also discuss the potential for discovering these models in the upcoming collisions at the upgraded LHC and future colliders.

Acknowledgements

To...
My best friend Rachel,
My mom Olivia, my dad Rick,
My sister Tara, and my brothers Keith and Sean.

Thank you for being there every time.

Contents

List of Tables

List of Figures

Chapter 1

Introduction

What are the connections between physical phenomena observed at different distance scales? The Standard Model (SM), which describes all known direct observations of fundamental particles, can be defined as a local quantum field theory in terms of the properties of particles observed at a distance scale 1000 times smaller than an atomic nucleus. This scale is known as the weak scale, and corresponds to energies of $m_{\text{weak}} \approx 100$ GeV. It is a remarkable property of quantum field theories that observations made around a single short (UV) distance scale define in principle the behavior of the theory at *all* longer (IR) distance scales. The Standard Model leads to predictions for the properties of physics from the weak scale all the way through the scales of hadrons, nuclei, atoms, chemistry, materials, stars, and galaxies. The experimental and theoretical exploration of the Standard Model at the weak scale has been the great success of the past fifty years of particle physics, culminating in the discovery of the Higgs Boson at the Large Hadron Collider [18, 19]. This success has also led to a puzzling question: *is local quantum field theory the only principle connecting UV and IR physics?* This question is most commonly framed as the naturalness problem, and has driven much of the experimental and theoretical inquiry into theories of physics beyond the Standard Model (BSM).

1.1 The naturalness principle

The Standard Model defined at the weak scale has a striking feature– small changes in the properties of particles at the weak scale lead to proportionately small changes in the physics at *all* longer distance scales! Such a theory is called a *natural* theory [20]. In a natural theory, it appears as though the properties of particles at the weak scale were 'chosen' with no special regard for the behavior at longer distance scales– any choice of similar properties at the weak scales would lead to similar behavior at long distances! In a natural theory, the properties in the UV 'explain' the properties in the IR, while in a unnatural, or 'tuned' theory, the special IR properties appear as a coincidence.

There is compelling experimental and theoretical evidence that the Standard Model itself is part of a larger theory defined at a distance scale much shorter than the weak scale, corresponding to an energy $\Lambda_{\rm bsm} > m_{\rm weak}$. This evidence includes observations of dark matter, matter anti-matter asymmetry, structure of quark and lepton flavor, neutrino masses, inflationary early universe physics, and the high energy behavior of gravity. There are a number of experimental constraints on such theories, for example precision flavor and CP observables, proton decay, dark matter detection, BBN and CMB observations, and collider constraints. These experiments are all more sensitive to physics at longer distance scales, and set lower bounds on $\Lambda_{\rm bsm}$. In many cases $\Lambda_{\rm bsm}$ could be far out of reach of any experiments, leading to a crucial question: is there any principle that suggests upper limits on the scale $\Lambda_{\rm bsm}$?

The principle of naturalness is one possible guide. Although the Standard Model defined at the weak scale on its own is a natural theory, generic extensions of the Standard Model are not natural! Theories which are natural have a scale $\Lambda_{\rm bsm} \lesssim$ 1 TeV, and generally predict new 'partner' particles with properties related to those of the known SM particles. The masses of the W and Z bosons in the SM are the most sensitive, and the concept of naturalness can be quantified with a quantity called tuning,

$$\Delta \sim \frac{\partial \ln m_Z^2}{\partial \ln \lambda_i},$$

where λ_i are the properties of the theory at Λ_{bsm}. When Δ is large, small changes in

the UV parameters λ_i are enhanced by a factor of Δ in the IR, and the theory is no longer natural.

Should we expect the universe to be natural? Discovering a tuned theory of the weak scale would challenge the notion that the *only* connection between physics at different energy scales is through local quantum field theory. Anthropic landscape selection is one well-studied example of an additional principle connecting UV and IR observables which could explain observed tunings in field theories (for a review, see [21]). The anthropic principle has had some success in tackling the naturalness problems of both the CC and the weak scale, while no field theory solution to the former is known. However, the anthropic landscape still suffers from fundamental questions about how to define a predictive measure. Recently, dynamical landscape selection mechanisms have been proposed, using assumptions about the early cosmology of the universe to explain a tuning of the weak scale [22, 23, 24]. More dramatic departures from the normal point of view of the Standard Model as an effective quantum field theory may also be possible [25]. Or perhaps there simply is no further principle that can simplify our description of the world beyond a tuned quantum field theory. In this context, the exclusion of natural theories of the weak scale is as interesting as their potential discovery (though rather less decisive), with either result shedding light on the fundamental question of the connections between UV and IR distance scales.

1.2 Natural theories of the weak scale

The weak scale is set by the mass term m_H^2 in the Higgs potential at the weak scale,

$$V = m_H^2|h|^2 + \lambda|h|^4 + ..., \tag{1.1}$$

as

$$|\langle H\rangle|^2 \equiv \frac{v^2}{2} = \frac{-m_H^2}{2\lambda} \tag{1.2}$$

where the ellipses indicate non-renormalizable terms generated in the effective potential at the weak-scale, the qualitatively important effects of which can be absorbed

in m_H^2 and λ, and where λ is fixed by the observed value of the Higgs pole mass m_{h^0}. It is the sensitivity of the Higgs mass squared parameter m_H^2 to physics at the scale Λ_{bsm} which introduces the naturalness problem.

Theories of BSM physics predict new particles at the scale $\Lambda_{\rm bsm}$. There are strong arguments that such theories must include new partner states with couplings to the Higgs boson *of comparable strengh* to the couplings of the Standard Model (for a review of these arguments and a study of alternative possibilities see Refs. [26, 27] and references therein). Taking into account couplings and multiplicities, the two particles most strongly coupled to the Higgs boson in the Standard Model are the top quark which gives loop-level contributions to the potential of order $3y_t^2$ where $y_t \approx 0.9$ is the top Yukawa coupling, and the SU(2) gauge bosons which give loop-level contributions of order $\frac{3}{4}g_2^2$ where $g_2 \approx 0.6$ is the $SU(2)$ gauge coupling. At one-loop, contributions from new 'partner' states at $\Lambda_{\rm bsm}$ feed into the Higgs potential as

$$\Delta m_{H,EW}^2 \approx \frac{3g_2^2}{32\pi^2}\Lambda_{bsm}^2, \tag{1.3}$$

$$\Delta m_{H,top}^2 \approx \frac{3y_t^2}{8\pi^2}\Lambda_{\rm bsm}^2. \tag{1.4}$$

In 'supersoft' theories, the new states at Λ_{bsm} contribute to the higgs potential only over a narrow energy range, while if the new states at $\Lambda_{\rm bsm}$ contribute to the Higgs potential over many decades of energy up to a scale $\Lambda_{\rm mess}$, then the contributions are enhanced by factors of $\ln \frac{\Lambda_{\rm mess}^2}{\Lambda_{\rm bsm}^2}$ until the weak coupling is saturated and $\Delta m_H^2 \approx \Lambda_{bsm}^2$. For supersoft theories the weak coupling of the SM establishes a small hierarchy between the electroweak scale and the new states; top partner states appear at a natural scale of ~ 600 GeV and SU(2) partners at ~ 2 TeV (see for example ref. [28, 27]).

A major component of the remaining experimental program for the LHC and its upgrades is to explore the space of natural theories. The most generic feature of such theories is that they contain new particles coupled to the Higgs boson, leading to deviations from SM precision measurements at loop level [29, 30] and often tree-level if the Higgs sector is non-minimal (see e.g. [31, 32]). Often even more constraining than

Higgs property measurements are the constraints on the partners of the top quark. In models where the top is related by a continuous symmetry to its partner, such as SUSY or minimal composite Higgs, the top partners are colored and have a large production cross section at the LHC. The 8 TeV LHC run has deeply probed such states up to ~ 600 GeV [1, 2], approaching the edge of the natural window, with the detailed limits depending on how the new states decay (for phenomenological studies of different decays possibilities, see for example Ref. [33, 34] in the SUSY context and Ref. [32] for the composite Higgs). On the other hand, models where the top partners are related by a discrete symmetry to the top do not require new colored states [35, 36, 37], and are dominantly constrained at colliders by Higgs precision measurements. Direct limits on the partners of the SU(2) gauge states are less constraining and generally leave open a natural mass range.

These general arguments require that new partner particles exist at a scale $\Lambda_{bsm} \lesssim 1$ TeV for the theory beyond the Standard Model to remain natural; this is the largest natural hierarchy that can be maintained at one-loop given the strength of the Higgs couplings. A further question is: can the full theory remain natural up to a scale $\Lambda_{UV} \gg \Lambda_{bsm}$? One simple solution is to study models where there are no further scales, $\Lambda_{UV} \sim$ TeV [38]. Such models however must address many more problems than naturalness at the TeV scale, for example dark matter, baryogenesis, the axion, and the UV completion of gravity, and generally suffer from far more stringent constraints than those implied only by naturalness. On the other hand, if Λ_{UV} is as high as the scale of gauge coupling unification $\sim 10^{16}$ GeV or the naive scale of the UV completion of gravity $\sim 10^{19}$ GeV, then many of these issues can be resolved at high scales with no experimental constraints, but the sector at Λ_{bsm} must be extended to protect the Standard Model beyond one loop order. These additional particles are also experimentally constrained, often giving even stronger constraints on the naturalness of the theory than direct constraints on the top partners and Higgs properties.

1.3 The minimal supersymmetric solution

Supersymmetric models are one such possibility. In the minimal version, the softly broken minimal supersymmetric standard model (MSSM), partner states for all of the SM particles (not just the most strongly coupled ones) are introduced [39]. In the MSSM, these new states are introduced at a scale $\Lambda_{bsm}^2 \sim m_{\rm soft}^2$ where supersymmetry is softly broken, and no new states enter until a scale $\Lambda_{\rm mess}$ characterizing the messenger sector that communicates the spontaneous breaking of supersymmetry to MSSM states. This framework has a number of advantages besides naturalness, including a variety of dark matter candidates, improved gauge coupling unification, and a deep connection with string completions of gravity [40].

In the MSSM, the dominant collider limits are on the most abundant colored particles. The 1st and 2nd generation squarks (which are motivated to be approximately degenerate by flavor constraints) and the gluinos are constrained from 8 TeV LHC results to haves masses $\gtrsim 1.5 - 2$ TeV assuming their simplest decay topologies [17]. If all the superpartners are at this scale including the top partners (stops), then the theory is significantly tuned. However, the limits on the the third generation squarks are by comparison much weaker, with limits $\gtrsim 600$ GeV for the simplest decays [1, 2]. Modifications of the most typical decay signatures of superparticles, for example through R-parity violation [34] or compressed spectra [41], accentuate this situation– although the overall limits tend to decrease, the strength of limits on gluinos tends to increase relative to limits on the third generations squarks. Since at one-loop the mass scale of the stops is the dominant source of tuning, current experimental limits and naturalness together strongly motivate 'Natural SUSY' models [28, 42, 43, 44], where the stops are the lightest colored states, and there is a significant hierarchy before the 1st and 2nd generation squarks and gluino appear.

While it is clear that 'Natural SUSY' models defined at the scale $\Lambda_{bsm} \sim m_{\tilde{t}} \sim 600$ GeV satisfy the naturalness criterion while remaining consistent with experimental constraints, in the softly broken MSSM framework additional complications arise. For typical models, $\Lambda_{\rm mess} \gtrsim 100 \times m_{\rm soft} \sim 100$ TeV. The one-loop formulae of

Eqs. 1.3,1.4 are enhanced by a factor $\ln \Lambda^2_{\rm mess}/m^2_{\rm soft} \gtrsim 10$ – these models are a factor of ten times more tuned than the naive natural model defined at the TeV scale! Furthermore, the hierarchy between the gluino and the stop in the Natural SUSY spectrum becomes another source of tuning, with the natural ratio $m_{\tilde{t}} \gtrsim M_3/2$ after even a decade of running [45]. In fact, for a variety of realistic scenarios incorporating natural spectra and other mechanisms for hiding superpartners, the tuning of the weak scale in MSSM-like models is $\Delta^{-1} \sim 1\%$ given current experimental limits [46, 45, 47, 48, 49, 50]. The experimental absence of superpartners at a low enough scale for the MSSM to be fully natural is part of the supersymmetric little hierarchy problem – although SUSY can still in principle protect the SM from the big hierarchy to the highest gravitational scales $\sim 10^{19}$GeV, it appears there is a little hierarchy between the natural scale $m_{\rm soft} \sim m_{\rm weak}$ and the actual value of $m_{\rm soft}$ if the MSSM is realized in nature.

There is another significant experimental constraint on the tuning of Natural SUSY models from the Higgsinos, the superpartners of the Higgs bosons. The Higgsino mass μ is related directly at tree level to a contribution to the Higgs potential, $m_H^2 = \mu^2 + ...$ In MSSM-like models with a low scale $\Lambda_{\rm mess}$, LHC8 limits on Higgsinos decaying to light gravitinos or other lighter states give $\mu \gtrsim 300$ GeV [51], leading to a tuning of $\sim 10\%$.

The observation of a $m_{h_0} \approx 125$ GeV Standard Model-like Higgs Boson at the LHC provides another source of tension in the MSSM. For the pure MSSM particle content, this mass requires a radiative contribution from the stop sector $\gg 600$GeV, leading to $\lesssim 5\%$ tuning [52]. Extensions to the MSSM particle content can increase the Higgs mass without as large contributions to the tuning of the weak scale [52, 53], and thus naturalness combined with the Higgs properties suggests a much richer structure than the pure MSSM at the scale $m^2_{\rm soft}$.

1.4 Extending supersymmetry in natural directions

In the light of LHC8 results, the interplay of naturalness, Higgs properties, and experimental limits on colored particles has been well characterized for the softly broken MSSM and its simple extensions such as the NMSSM or Dirac gauginos. The (un)naturalness of such models given current LHC results is tied to two important structural assumptions of the softly broken MSSM:

1. The Higgs sector in the low energy theory below the scale $m_{\rm soft}$ is the SM Higgs sector or a small perturbation from it.

2. There is a hierarchy between the MSSM states at $m_{\rm soft}$ and the states responsible for communicating SUSY breaking at $\Lambda_{\rm mess}$.

In this work, we study supersymmetric solutions to the naturalness problem that violate these assumptions in order to extend the natural hierarchy between the weak scale and the observable superpartners. These models introduce a significant increase in complexity and many new experimental constraints, but nonetheless we find models which are calculable, satisfy all the new constraints, and decrease the tuning by a factor of ~ 10 compared to MSSM-like models.

In Chapter 2 we study the Twin SUSY model, which violates (1) and essentially decreases the tuning by modifying the relationship between the scales of the Higgs potential and the electroweak scale, Eq. 1.2. Because these models modify the IR Higgs sector, the principle collider constraints and novel signatures are Higgs coupling deviations, precision electroweak, and new scalar resonances. Substantial portions of Chapter 2 have been published in Ref. [54] in collaboration with Nathaniel Craig. K.H. made important contributions to all aspects of the work presented in this section.

In Chapter 3 we study the Maximally Natural SUSY model, which violates (2) – the theory becomes extra dimensional at the TeV scale and the MSSM gauginos and their extra-dimensional partners communicate SUSY breaking directly to the 3rd generation. A heavy Higgsino mass and a large splitting between the gluino and the stops are consequences of the extra-dimensional nature of the SUSY breaking. Limits on the third generation squarks are the dominant constraint on these models,

while the presence of extra dimensions leads to new signatures not present in other natural SUSY models: a unique degenerate spectrum, potentially observable KK excitations, and in some cases novel decay topologies into large extra dimensions. Substantial portions of Chapter 3 have been published in Refs. [55, 56] and are being prepared for publication in Refs. [57, 58] in collaboration with Savas Dimopoulos, John March-Russell, Isabel Garcia-Garcia, and James Scoville. K.H. made important contributions to all aspects of the work presented in this section.

The models studied in this work demonstrate that supersymmetric solutions to the naturalness problem can remain untuned even after the results of LHC8. The imminent 13 TeV run of the LHC will probe these models to tunings of $\sim 10\%$ level, and potential future ~ 100 TeV hadron colliders will either explore the rich dynamics of these models discovered at 13 TeV, or very deeply probe the possibility of a fully natural solution to the hierarchy problem even beyond the framework of the MSSM.

Chapter 2

Twin SUSY

2.1 Introduction

Just as the discovery of a Standard Model (SM)-like Higgs boson at the LHC [18, 19] sharpens the urgency of the hierarchy problem, the onward march of null results in searches for new physics places increasing stress upon conventional ideas for electroweak naturalness. Perhaps electroweak naturalness is a dead end, with the solution to the hierarchy problem lying somewhere in the landscape. But perhaps electroweak naturalness is still close at hand, concealed only by its unexpected properties. This latter possibility raises a pressing question: *Can we learn anything new about electroweak naturalness from null results at the LHC?* More specifically,

- Are there signatures of naturalness other than conventional top partners?
- Are there wholly natural theories where the conventional signs of naturalness – especially supersymmetric naturalness – may be out of reach of the LHC?

To a certain extent these possibilities are illustrated by composite Higgs models [59, 60], where the Higgs mass is protected by a global symmetry and heavy resonances lie in the multi-TeV range – but even here, one expects light fermionic top partners to accommodate the observed Higgs mass [61], as well as copious production of heavy resonances in the second LHC run. Moreover, such models are typically in tension with precision electroweak constraints and hints of gauge coupling unification,

at variance with what few indirect indications we have about physics in the ultraviolet. While there is also still room for conventional supersymmetric models with light superpartners whose signatures are muddled by reduced event activity [62] or missing energy [63], these solutions are under increasing pressure from evolving search strategies at the LHC – and, in any event, have little intrinsic connection between naturalness and the lack of natural signals.

An attractive possibility is to consider theories enjoying *double protection* of the Higgs potential, for example via both supersymmetry and a spontaneously broken global symmetry [64, 65, 66]. This raises the prospect of partially decoupling the signals of each symmetry mechanism without imperiling the naturalness of the weak scale. In this work we explore the double protection provided by the combination of the twin Higgs mechanism [35] and supersymmetry.[1] In these models an exact $\mathbf{Z}_2$ symmetry between the MSSM and a mirror MSSM leads to an approximate U(4) symmetry, and the light Higgs is primarily composed of the pseudo-goldstones of the broken U(4). Although supersymmetry plays a role in the ultraviolet completion, the stops need not be light. Moreover, the fermionic top partner furnished by double protection is *neutral under the Standard Model gauge group*. Rather, the predominant signals of naturalness emerge through the Higgs portal: modifications of Higgs couplings, an invisible Higgs width, resonant Higgs pair production, and an invisibly-decaying heavy Higgs. Thanks to double protection of the Higgs potential, the conventional signs of supersymmetric naturalness are absent even at the 13/14 TeV LHC, with percent-level tuning in the Higgs vev (comparable to the "fine-tuning" of the QCD scale) compatible with stops at ~ 3.5 TeV and higgsinos at ~ 1 TeV.

The supersymmetric UV completion of the twin Higgs model we study has the attractive features of maintaining perturbative gauge coupling unification, calculable and safe precision electro-weak and flavor observables, and a light CP-even Higgs mass naturally in the experimentally observed window. While many interesting conclusions about twin Higgs phenomenology can be reached from an effective theory of only the scalar Higgs and SM degrees of freedom in twin models[68], studying a full UV

[1] For recent work in a similar spirit combining supersymmetry and the composite Higgs, see e.g. [67].

completion also has the advantage of an unambiguous tuning measure to compare to other perturbative solutions to the naturalness problem like the NMSSM and a direct understanding of collider limits on all of the new colored and electroweak states. Although supersymmetric completions of mirror and left-right twin Higgs models were considered prior to Higgs discovery [69, 70], they focused on eliminating the intrinsic tuning from supersymmetric quartics at the cost of additional model-building complexity and a loss of MSSM-like gauge coupling unification. In this work we explore the simplest supersymmetric mirrow twin Higgs in light of the observed mass and couplings of the SM-like Higgs, taking the tuning arising from supersymmetric quartics at face value. Venturing beyond the pseudo-goldstone limit and accounting for the contributions of the full Higgs effective potential, we find that this simple model has tuning comparable to the more complicated efforts.

This chapter is organized as follows: In section 3.3 we begin by reviewing the simplest supersymmetric twin Higgs model and the parametrics of the Higgs potential in the pseudo-goldstone limit. We then turn to an analysis of the Higgs mass and full effective potential at one loop, computing the fine-tuning of the theory as a function of the superpartner mass scales. In section 2.3, we give a more detailed discussion of the possible UV completions of the twin Higgs singlet portal. In section 3.5 we study the phenomenology of the model in light of the Higgs discovery, focusing on the implications of Higgs couplings for the allowed parameter space and detailing the most relevant signals of naturalness. In section 2.5 we consider ancillary limits from precision electroweak, flavor, and cosmological considerations.

2.2 A Supersymmetric Twin Higgs

2.2.1 Basic Set-up

Mirror Twin Higgs models are based on the idea that a $\mathbf{Z}_2$ symmetry exchanging the SM Higgs and a "mirror" Higgs field charged under a distinct identical copy of the Standard Model gauge group leads to an accidental U(4) symmetry in the quadratic terms of the Higgs potential [35, 68]. If the $\mathbf{Z}_2$ symmetry is exact – implying a

complete mirror copy of the matter and gauge fields coupled to the mirror Higgs – then the full quadratic effective potential including UV-sensitive mass corrections possesses the accidental U(4) symmetry. The light SM Higgs doublet is identified with some of the pseudo-goldstones of the spontaneously broken U(4) and is therefore protected from quadratic sensitivity to the cutoff. The sensitivity to UV scales only re-emerges through the (presumably small) quartic and higher order terms explicitly breaking the U(4) symmetry, and is suppressed by the (presumably large) coefficient of the U(4) preserving quartic terms in a perturbative completion (or equivalently $\sim (4\pi)^2$ in a composite model). As with any pseudo-goldstone mechanism for protecting the Higgs mass, a UV completion such as supersymmetry is required for the theory above a few TeV.

Our perturbative SUSY twin Higgs model comprises two complete copies of the MSSM, an "A-sector" which will correspond to the observed sector with the light fields of the Standard Model, and a "B-sector" with identical copies of the MSSM gauge group and field content. The couplings and soft SUSY breaking masses of the two sectors are set equal by a $\mathbf{Z}_2$ symmetry exchanging the A and B sectors. A single singlet superfield S couples the A and B sectors. The combination of supersymmetry and the $\mathbf{Z}_2$ symmetry yields a theory that is, in principle, complete up to the Planck scale.

The $\mathbf{Z}_2$ and gauge symmetries guarantee that the singlet-Higgs interactions respect a full U(4) global symmetry, of which gauge and Yukawa interactions preserve an $\mathrm{SU(2)_A} \times \mathrm{U(1)_A} \times \mathrm{SU(2)_B} \times \mathrm{U(1)_B}$ subgroup. To make this explicit, we write the A and B sector Higgs fields in U(4) multiplets as

$$H_u = \begin{pmatrix} h_u^A \\ h_u^B \end{pmatrix}, \quad H_d = \begin{pmatrix} h_d^A \\ h_d^B \end{pmatrix}, \tag{2.1}$$

and the superpotential of the Higgs-singlet sector becomes

$$\begin{aligned} W_{\mathrm{U(4)}} &= \mu(h_u^A h_d^A + h_u^B h_d^B) + \lambda S(h_u^A h_d^A + h_u^B h_d^B) + M_S S S \\ &\equiv \mu H_u H_d + \lambda S H_u H_d + M_S S S. \end{aligned} \tag{2.2}$$

The $\mathbf{Z}_2$ symmetry also guarantees that the quadratic soft breaking terms preserve the full U(4), even after radiative corrections. Assuming the singlet has a large soft mass $m_S^2 \gg \mu, M_S$, it will decouple leaving its F-term quartic intact. The full U(4) preserving scalar potential in the Higgs sector is then given by the sum of supersymmetric and soft contributions,

$$V_{\mathrm{U}(4)} = (m_{H_u}^2 + \mu^2)|H_u|^2 + (m_{H_d}^2 + \mu^2)|H_d|^2 - b(H_u H_d + \mathrm{h.c.}) + \lambda^2 |H_u H_d|^2 \quad (2.3)$$

Crucially, the $\mathbf{Z}_2$ symmetry automatically leads to a potential for the Higgs with both quadratic terms *and a potentially large quartic term* respecting the larger U(4) symmetry. This can be contrasted with composite twin Higgs models, where the $\mathbf{Z}_2$ on its own does not guarantee that the strong sector will respect the necessary U(4) symmetry.

The gauge and Yukawa couplings of the A and B sectors give rise to explicit breaking of the U(4) at both tree and loop level. When the U(4)-symmetric quartic dominates over the U(4)-breaking quartic terms (and other higher order terms), this model provides a perturbative realization of the twin Higgs mechanism. In particular, in the limit that the H_u and H_d vevs lie completely in the B-sector direction, the pseudo-goldstones of the broken U(4) correspond to a light A-sector Higgs doublet with a scalar mass protected by the twin mechanism against large radiative corrections from the top and gauge sectors.

In the absence of supersymmetry, electroweak gauge and Yukawa interactions would only give rise to U(4) breaking quartics at one loop, the most important of which is the quartic $\delta\lambda_u$ generated by the top sector. However, with the introduction of supersymmetry, the D-terms of the A and B sector gauge groups necessarily generate U(4)-breaking quartic terms at tree level. For the neutral components of the Higgs field these contributions are

$$V_{\cancel{U(4)}} = \frac{g^2 + g'^2}{8}\left[(|h_u^{0\,A}|^2 - |h_d^{0\,A}|^2)^2 + (|h_u^{0\,B}|^2 - |h_d^{0\,B}|^2)^2\right] + \delta\lambda_u(|h_u^{0\,A}|^4 + |h_u^{0\,B}|^4) + \ldots . \quad (2.4)$$

The U(4)-breaking terms are important to generate a mass for the light pseudo-goldstone Higgs, but unfortunately their form necessarily leads to symmetric vevs between the A and B sector, $v_A = v_B$, which we find to be phenomenologically unviable. To rectify this problem, we assume there is a small source of soft breaking of the $\mathbf{Z}_2$ symmetry which we take to be of the simple form

$$V_{\not{\mathbf{Z}}_2} = \Delta m^2_{H_u}(|h_u^A|^2 - |h_u^B|^2) + \Delta m^2_{H_d}(|h_d^A|^2 - |h_d^B|^2). \tag{2.5}$$

2.2.2 The pseudo-goldstone limit

The Higgs sector of the SUSY twin model can be most easily understood in the limit that all of the non-goldstone directions have decoupled. This condition is satisfied at tree-level when $b \sin 2\beta \gg (\frac{g^2+g'^2}{4}\cos^2 2\beta) f^2$ and $\lambda^2 \gg \frac{g^2+g'^2}{2}\cot^2 2\beta$, where $f^2 \equiv \langle h_A\rangle^2 + \langle h_B\rangle^2 \equiv v_A^2 + v_B^2$ is the total magnitude of the U(4) breaking vev.

In this limit, f and $\tan\beta_A = \tan\beta_B$ can be determined from the U(4) symmetric potential (Eq. 2.3),

$$\tan\beta = \frac{\mu^2 + m^2_{H_d}}{\mu^2 + m^2_{H_u}} \tag{2.6}$$

$$f^2 = \frac{1}{\lambda^2}\left(m_A^2 - 2\mu^2 - m^2_{H_u} - m^2_{H_d}\right) \tag{2.7}$$

where $m_A = \frac{2b}{\sin 2\beta}$ is the tree-level mass of one of the physical pseudoscalar Higgses. To study the light Higgs state, it is convenient to work in terms of the nonlinear realization of the uneaten goldstone direction

$$H_u = f\sin\beta \begin{pmatrix} 0 \\ \sin\frac{\phi}{\sqrt{2}f} \\ 0 \\ \cos\frac{\phi}{\sqrt{2}f} \end{pmatrix}, \quad H_d = f\cos\beta \begin{pmatrix} 0 \\ \sin\frac{\phi}{\sqrt{2}f} \\ 0 \\ \cos\frac{\phi}{\sqrt{2}f} \end{pmatrix} \tag{2.8}$$

where ϕ is the pseudo-goldstone Higgs. A potential for ϕ is generated by the U(4) breaking terms Eqs. 2.4 and 2.5. The minimization conditions yield the vev in terms

of the $\mathbf{Z}_2$ breaking masses

$$\sin^2 \frac{\phi}{\sqrt{2}f} = \frac{v^2}{f^2} = \frac{1}{2}\left(1 - \frac{\Delta m^2}{\left(\frac{g^2+g'^2}{8}\cos^2 2\beta + \delta\lambda_u \sin^2\beta\right) f^2}\right) \tag{2.9}$$

where we now take the canonical observed vev in the A sector $v_A = v \approx 174\text{GeV}$ and define $\Delta m^2 \equiv \Delta m^2_{H_u} \sin^2\beta + \Delta m^2_{H_d} \cos^2\beta$. The mass of the light state ϕ at the minimum is given by

$$m^2_\phi = (m^2_Z \cos^2 2\beta + 4\delta\lambda_u v^2 \sin^4\beta)\left(2 - \frac{2v^2}{f^2}\right). \tag{2.10}$$

Eqs. 2.9 and 2.10 illustrate several important points for the following more detailed discussion. First, it is clear that to obtain a hierarchy in vevs $v^2 < f^2/2$, the $\mathbf{Z}_2$ breaking mass terms must be tuned against the potential generated by the U(4) breaking quartic terms. This leads to an intrinsic tuning of the weak scale of order $f^2/2v^2$. Ref. [69] sought to remedy this tuning in a similar SUSY twin model by removing the B-sector D-term quartics. This additional $\mathbf{Z}_2$ breaking modifies Eq. 2.9 to give a small hierarchy $v^2 < f^2/2$ even in the absence of a $\mathbf{Z}_2$ beaking mass, but we see immediately that the remaining symmetric radiative contributions $\delta\lambda_u$ will remain important, and we find numerically that there is in fact very little to be gained by this modification. Likewise ref. [70] sought in a left-right twin SUSY model to introduce a natural hierarchy $v^2 < f^2/2$ through removing the D-term contributions by forcing $\tan\beta = 1$ and including soft $\mathbf{Z}_2$ breaking quartics from a non-minimal singlet sector. This mechanism can be adapted to the mirror model, but again we find that after including the radiatively generated quartic terms there is little benefit. In this respect, the added model-building complications of [69, 70] can be sidestepped without substantially worsening the tuning of the theory.

Another important point is that the mass of the light Higgs state is generated by the same quartic terms that give mass to the light MSSM Higgs, with no contributions from the U(4) symmetric coupling λ. However, for large hierarchies of v^2/f^2 there can be up to a factor of two enhancement in the squared mass compared to the

MSSM formula, as is evident in Eq. 2.10. Physically, in this limit the ϕ potential receives contributions from both the A- and B-sector quartics. This enhancement brings the tree-level Higgs mass prediction tantalizingly close to the observed value, and is critical to obtain the observed mass of the SM-like Higgs in regions of small $\tan\beta$. Note also that the MSSM-like limit *cannot* be obtained simply by taking the $f \to \infty$ limit of Eq. 2.10, since there are large trilinear couplings of $\mathcal{O}(f)$ in the Higgs sector. The MSSM-like limit is instead obtained by taking $\lambda \to 0$ and $M_S \to \infty$, which introduces appropriate corrections to Eq. 2.10 that are not apparent in the pseudo-goldstone limit.

2.2.3 Full effective potential and Higgs mass

Perturbativity limits the range of allowed singlet couplings λ, and the observed light Higgs mass $m_h \approx 125\text{GeV}$ limits the range of allowed $\tan\beta$. We therefore find that over most of the parameter space of interest there are important non-decoupling effects in the potential and a treatment beyond the pseudo-goldstone limit is necessary.

The structure of the radiative corrections is also very important to understanding the light Higgs mass and the minimum of the U(4) breaking potential, and we find it is necessary to carefully include the large U(4) breaking contributions to the effective potential. In particular, we evaluate the effective potential at the SUSY breaking scale m_{soft} including the full leading log plus one-loop finite contributions from both the A and B top/stop sectors (see e.g. [71, 72]), as well as the one-loop leading log contributions from the A and B electroweak gauge sectors. The leading contributions of the singlet to the effective potential are U(4) symmetric and not included in our analysis. A qualitatively important aspect of the effective potential is that it is $\mathbf{Z}_2$ symmetric and has a minimum at the symmetric vev $v_A = v_B$, as can easily be seen from inspecting the one-loop contributions. Therefore the $\mathbf{Z}_2$ breaking masses remain necessary to obtain a hierarchy in vevs.

After including the effective potential contributions to the full tree-level potential of Eqs. 2.3, 2.4, and 2.5, we numerically determine the minimum and spectrum of Higgs states, including the wave-function renormalization of the lightest Higgs state.

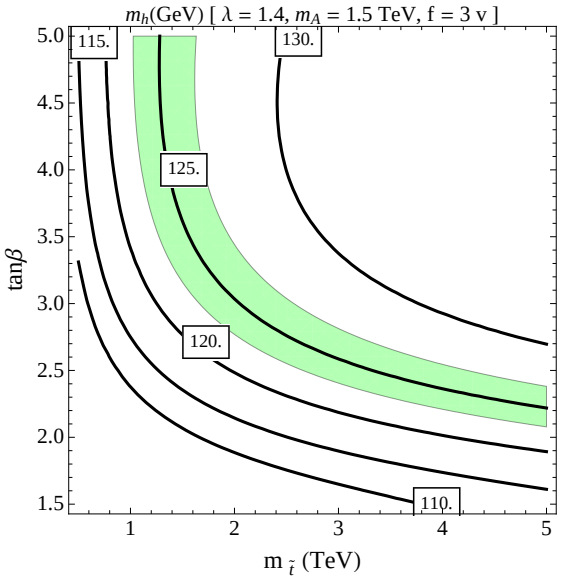

Figure 2.1: The lightest Higgs mass in the SUSY twin Higgs model as a function of a common stop mass $m_{\tilde{t}_1} = m_{\tilde{t}_2} \equiv m_{\tilde{t}}$ and $\tan\beta$ with $\lambda = 1.4$, $f = 3v$, and $m_A = 1.5$TeV. The green shaded region denotes $123\text{GeV} < m_h < 127\text{GeV}$.

Away from the pseudo-goldstone limit $\tan\beta_A = \tan\beta_B$ no longer necessarily holds. We fix the relative values of the $\mathbf{Z}_2$ breaking masses by requiring $\tan\beta_B = \tan\beta_A - 0.1$, which leads typically to a similar magnitude for $\Delta m^2_{H_u}$ and $\Delta m^2_{H_d}$.

The light Higgs mass for $f = 3v$, $\lambda = 1.4$, and $m_A = 1.5$TeV is shown in Fig. 2.1 as a function of $\tan\beta$ and a common stop mass $m_{\tilde{t}_1} = m_{\tilde{t}_2}$ with no mixing. We find that the non-decoupling effects decrease the mass by $5 - 10\%$ below the pseudo-goldstone expectation of Eq. 2.10 in the region of interest. For large $\tan\beta$, the radiative corrections from $m_{\tilde{t}} \approx 1.3$TeV stops are necessary to obtain the observed Higgs mass, while for a heavy stop $m_{\tilde{t}} \approx 5$TeV, $\tan\beta$ can be as small as 2.4.

2.2.4 Fine-tuning

The supersymmetric UV completion of the mirror twin Higgs model provides the crucial advantage of allowing a meaningful calculation of fine-tuning in terms of soft SUSY-breaking parameters. There are two independent sources of tuning in the twin SUSY model. The first comes from creating a hierarchy between the A and B sector

vevs. According to Eq. 2.9, this introduces a tuning of Δm^2 against the quartic U(4) breaking terms,

$$\Delta_{v/f} \approx \frac{\partial \ln(v^2/f^2)}{\partial \Delta m^2} = \left(\frac{f^2}{2v^2} - 1\right). \tag{2.11}$$

Numerically we find this relationship to be quite accurate even away from the pseudo-goldstone limit and in the presence of additional contributions to the effective potential. This tuning is present in any twin Higgs model in which a soft $\mathbf{Z}_2$ breaking mass leads to the hierarchy in vevs [68]. An important aspect of the twin mechanism is that the $\mathbf{Z}_2$ breaking is soft and therefore the Δm^2 terms do not have any additive sensitivity to other soft masses.

The second source of tuning in the twin SUSY model is the tuning of the total U(4) breaking vev f against the quadratic contributions to the U(4) symmetric Higgs masses. This is analogous to the tuning of the normal electroweak vev in non-twinned SUSY models. At one loop the most important radiative corrections to the U(4) symmetric Higgs masses arise from the stop and singlet soft masses

$$\delta m_{H_u}^2 \approx \frac{3y_t^2}{8\pi}(m_{\tilde{t}_L}^2 + m_{\tilde{t}_R}^2)\log\frac{\Lambda_{\rm mess}}{m_{\rm soft}} + \frac{\lambda^2}{8\pi^2}m_S^2\log\frac{\Lambda_{\rm mess}}{m_{\rm soft}} + \ldots \tag{2.12}$$

$$\delta m_{H_d}^2 \approx \frac{\lambda^2}{8\pi^2}m_S^2\log\frac{\Lambda_{\rm mess}}{m_{\rm soft}} + \ldots \tag{2.13}$$

where $\Lambda_{\rm mess}$ is the scale of mediation of SUSY breaking. In the full RG there are also important contributions from the effect of the gluino on the running of the stop mass and from the running of λ if it approaches its Landau pole near the messenger scale.

In the limit $m_A^2 \gg \lambda^2 f^2$, the f tuning takes a simple form. When the dominant tuning is due to the stop contributions to the up-type Higgs mass for example,

$$\Delta_f \approx \frac{\partial \ln f^2}{\partial \ln \delta m_{H_u}^2} = \frac{\delta m_{H_u}^2}{2\lambda^2 f^2 \cos^2\beta}. \tag{2.14}$$

The total tuning of the the SUSY twin model is the product of the two independent tunings:

$$\Delta_{\rm twin} = \Delta_f \times \Delta_{v/f} \underset{v^2 \ll f^2}{\approx} \frac{\delta m_{H_u}^2}{4\lambda^2 v^2 \cos^2\beta} \tag{2.15}$$

where we have taken the approximate expressions Eqs. 2.11 and 2.14 in the limit $v^2 \ll f^2$.

It is interesting to measure the relative improvement in tuning of the SUSY twin model compared to a more minimal alternative. A convenient benchmark is the NMSSM, which can likewise accommodate the observed Higgs mass with tree-level contributions from the singlet quartic and has been shown to compare favorably with a number of alternative models for reducing the tuning of SUSY models in light of recent LHC results [73]. The NMSSM tuning equation has nearly identical form to the tuning of the SUSY twin model in the same decoupling limit,

$$\Delta_{\rm NMSSM} \approx \frac{\delta m_{H_u}^2}{2\lambda_{\rm NMSSM}^2 v^2 \cos^2\beta} \approx \frac{\delta m_{H_u}^2}{m_h^2/(2\sin^2\beta)}. \tag{2.16}$$

The key difference is that in the NMSSM, the value of the quartic coupling in the denominator is fixed by the observed light Higgs mass, $m_h \approx 125$GeV. In the SUSY twin model, the twin mechanism protects the light A-sector pseudo-goldstone Higgs mass from the large U(4) invariant quartic coupling λ in the denominator. The tuning can therefore be substantially reduced while maintaining a light Higgs. For example, for $\tan\beta = 2$ and $\lambda = 1.4$, Eqs. 2.15 and 2.16 imply that the NMSSM is roughly five times more tuned than the SUSY twin model for the same stop mass. Similar relationships holds for the relative tuning with respect to the singlet soft mass and the tree level μ-term.

This discussion also brings up an important difference between the SUSY twin model and composite twin Higgs models. In composite twin Higgs models, the connection between the tuning and the light Higgs mass re-enters only through the logarithmic dependence on the cut-off scale for the radiative U(4) breaking quartic terms. On the other hand in the SUSY twin model, the simultaneous requirement of a perturbative singlet coupling λ and the observed light Higgs mass introduces an indirect constraint on the size of the effective quartic coupling setting the f tuning. In detail, the structure of the D-term and radiative contributions to the U(4) breaking quartic terms fixes $\tan\beta$ for a given Higgs mass and set of soft parameters. However, the effective size of the tree-level U(4) preserving quartic coupling is dependent on $\tan\beta$

and enters the tuning formulae in the decoupling limit as $\lambda^2 \left(\frac{\sin 2\beta}{2}\right)^2$. For perturbative couplings $\lambda \lesssim 2$, it's critical that the correct Higgs mass can arise at small values of $\tan\beta$ to obtain a large effective quartic.

To improve upon these rough estimates of tuning, we perform a numerical study of the parameter space using the full one-loop RG equations and the complete Higgs effective potential as described in Sec. 2.2.3. In particular, we define a point in the low energy parameter space with a choice of the parameters λ, f, $m_{\tilde{t}}^2$, $m_{\tilde{S}}^2$, m_A, μ, and $\tan\beta$ defined at the scale $m_{\rm soft}^2 = m_{\tilde{t}}^2$. For simplicity, at the soft scale we take the limit of no stop mixing and degenerate stop masses $m_{\tilde{t_L}} = m_{\tilde{t_R}} \equiv m_{\tilde{t}}$ and set the gluino degenerate with the stops, $M_3 = m_{\tilde{t}}$. We then determine the $\mathbf{Z}_2$ preserving Higgs soft masses $m_{H_u}^2$ and $m_{H_d}^2$ and the $\mathbf{Z}_2$ breaking soft masses $\Delta m_{H_d}^2$ and $\Delta m_{H_d}^2$ by minimizing the effective potential. The tunings of the f and $\frac{v}{f}$ parameters are evaluated by independently varying the soft masses at $\Lambda_{\rm mess}$, running them back down to the soft scale, and numerically evaluating the shift in the vevs,

$$\Delta_f = \left[\sum_{x=\{m_{\tilde{t_L}}^2, m_{\tilde{t_R}}^2, M_3, m_{H_u}^2, m_{H_d}^2, \mu, m_{\tilde{S}}^2\}} \left(\frac{\partial \ln f^2|_{m_{\rm soft}}}{\partial \ln x|_{\Lambda_{\rm mess}}} \right)^2 \right]^{\frac{1}{2}} \tag{2.17}$$

$$\Delta_{\frac{v}{f}} = \left[\sum_{x=\{\Delta m_{H_u}^2, \Delta m_{H_d}^2\}} \left(\frac{\partial \ln v^2/f^2|_{m_{\rm soft}}}{\partial \ln x|_{\Lambda_{\rm mess}}} \right)^2 \right]^{\frac{1}{2}} \tag{2.18}$$

Note that the twin mechanism protects the running of the $\mathbf{Z}_2$ breaking masses from additive contributions from the stop and singlet sectors above the soft scale, and the running of the $\mathbf{Z}_2$ breaking masses is a small effect on the tuning. Again the combined tuning of the twin model is the product $\Delta_{\rm twin} = \Delta_f \times \Delta_{\frac{v}{f}}$.

For comparison we also define a benchmark NMSSM model with the same field content, superpotential, and soft terms as the A-sector plus singlet of the twin model. We use the same framework to determine the low energy parameters of this model

and to calculate the tuning, which we define as

$$\Delta^{\rm NMSSM} = \left[\sum_{x=\{m^2_{\tilde{t}_L}, m^2_{\tilde{t}_R}, M_3, m^2_{H_u}, m^2_{H_d}, \mu, m^2_{\tilde{S}}\}} \left(\frac{\partial \ln v^2|_{m_{\rm soft}}}{\partial \ln x|_{\Lambda_{\rm mess}}} \right)^2 \right]^{\frac{1}{2}} . \tag{2.19}$$

In all plots we choose a reference value of the messenger scale of $\Lambda_{\rm mess} = 100 m_{\tilde{t}}$, so that for each choice of $m_{\tilde{t}}$ and λ at the soft scale, the value of λ at the messenger scale is roughly the same.

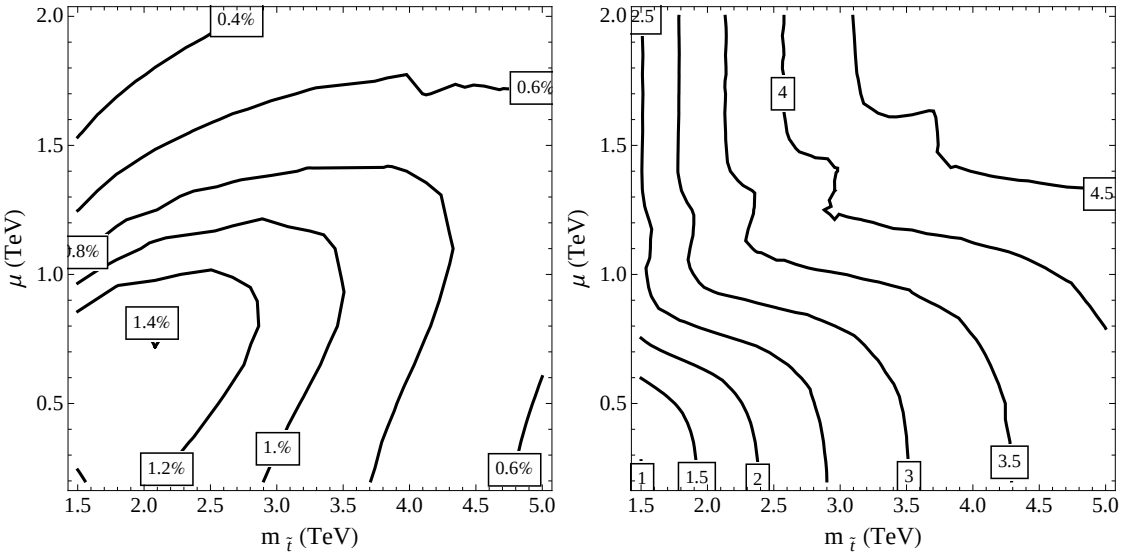

Figure 2.2: Tuning in the twin SUSY model with $\lambda = 1.4$, $f = 3v$, $m_A = 1.5$TeV, and $m_S^2 = (1\text{TeV})^2$. The left is the absolute tuning, and the right is the relative tuning compared to the NMSSM, $\Delta^{\rm NMSSM}/\Delta^{\rm twin}$, with the NMSSM parameters $\lambda = 0.6$, $m_A = 0.8$TeV, and $m_S^2 = (1\text{TeV})^2$. At each point, $\tan\beta$ is determined independently for the twin and NMSSM models to obtain $m_h = 125$GeV.

The dominant LHC limits on SUSY models come from constraints on the production of colored particles. The mass of the (N)LSP is also important both for direct searches and to determine the sensitivity to the decays of colored particles[2]. Direct constraints on stops as well as constraints on other colored sparticles[3] therefore enter

[2]For low-scale mediation models with a light gravitino LSP, the effect of the NLSP mass on limits for colored particles is much less decisive.

[3]In the simplest models of SUSY breaking the mass scale for the other colored sparticles must

the tuning through $m_{\tilde{t}}$, while limits on the LSP mass enter the fine-tuning through the tree-level contributions from μ, which must be at least as large as the (N)LSP mass. In Fig. 2.2 we study the tuning of the twin SUSY model as a function of μ and $m_{\tilde{t}}$, both in absolute terms and compared to the NMSSM. For each value of $m_{\tilde{t}}$ and μ, $\tan\beta$ is determined independently for the twin and NMSSM benchmark models to obtain $m_h = 125\text{GeV}$. For the twin model, the parameter choices of $\lambda = 1.4$, $f = 3v$, $m_A = 1.5\text{TeV}$, and $m_S^2 = (1\text{TeV})^2$ were chosen as an approximate best-case scenario for tuning given the perturbativity and Higgs coupling constraints, which will be discussed respectively in the Sec. 2.3 and Sec. 2.4.2. For the NMSSM we chose also a roughly optimal parameter point of $\lambda = 0.6$, $m_A = 0.8\text{TeV}$, and $m_S^2 = (1\text{TeV})^2$.

As discussed above, the improvement in tuning compared to the NMSSM at low stop masses is small due to the large value of $\tan\beta$ necessary to obtain the correct Higgs mass. However, at large stop masses the effective SUSY twin quartic becomes large and the degree of tuning remains better than 1% out to $m_{\tilde{t}} \approx 3.5\text{TeV}$ and $\mu \approx 1\text{TeV}$. At this point the degree of tuning for the twin model is better by a factor of ~ 3.5 than the NMSSM. There is also an unintuitive mild increase in tuning at small values of μ in the SUSY twin model due to the structure of the RG equations for the singlet and Higgs soft masses.

The consequences of the measured value $m_h \approx 125\text{GeV}$ on the tuning of the SUSY twin Higgs model are emphasized in Fig. 2.3. For this value of the Higgs mass, *additional* U(4) breaking quartic couplings actually *decrease* the tuning of the model by allowing the light Higgs mass to be obtained at smaller values of $\tan\beta$. An important consequence is that the SUSY twin model is much more effective at reducing the tuning for stop masses of a few TeV, where the radiative contributions to the Higgs mass allow a small value of $\tan\beta$. This also raises the interesting possibility of decreasing the tuning at low stop masses by including extra tree-level U(4) breaking quartics. A simple example would be to expand the singlet sector to include independent singlets S_A and S_B coupling separately to the A and B sector Higgses to introduce NMSSM-like quartics. A modest value for the new singlet couplings $\lambda_{\not{\text{U}}(4)} \sim 0.2 - 0.4$ could

be similar to the stop mass, and searches for these particles set the most stringent constraints. In general at least the gluino mass must be within a factor of ~ 2 of the lightest stop mass to avoid introducing additional fine-tuning to obtain a separation after RG flow [74].

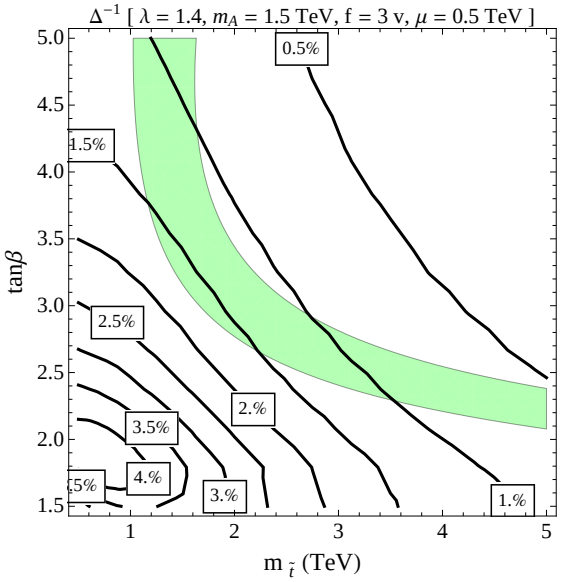

Figure 2.3: Tuning in the twin SUSY model with $\lambda = 1.4$, $f = 3v$, $m_A = 1.5$TeV, $m_S^2 = (1\text{TeV})^2$, $\mu = 0.5$TeV. The green shaded region is $123\text{GeV} < m_h < 127\text{GeV}$.

lift the Higgs mass to the measured value at low $\tan\beta$. For example, for $m_{\tilde{t}} = 1$TeV, $\tan\beta = 1.7$, and $\lambda = 1.4$, we find that a tuning of better than 10% can be obtained (a factor of ~ 3 improvement over the NMSSM) and the Higgs mass can be accomodated with $\lambda_{\cancel{\text{U}(4)}} \sim 0.4$. For simplicity we do not include this non-minimal contribution to the Higgs mass in any of the following results unless otherwise noted.

The soft mass of the singlet plays two important roles in determining the tuning of the twin SUSY model. First, it makes a contribution to the running of the Higgs masses which is important especially for large values of λ. The sensitivity of the tuning to this effect is depicted in Fig. 2.4. For $\lambda \gtrsim 1.5$, the Landau pole becomes too close to the messenger scale and the contributions to the running from the singlet become large (see section 2.3 for further discussion of the Landau poles and UV completion of the singlet). For smaller values $\lambda \sim 1.2 - 1.5$, a 1TeV singlet starts to make contributions to the tuning comparable to a 2TeV stop. As small as possible value for the singlet soft mass is therefore desirable.

On the other hand, as discussed in Sec. 2.2.1 the singlet soft mass must be considerably larger than μ and the supersymmetric singlet mass M_S to obtain a large tree

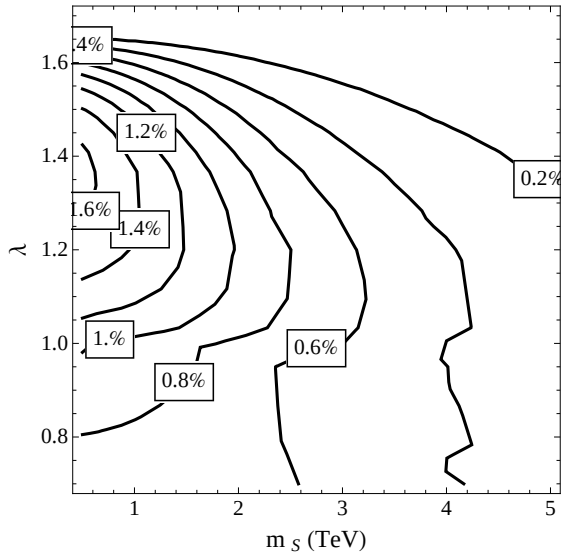

Figure 2.4: Tuning in the twin SUSY model as a function of λ and m_S^2 with $f = 3v$, $m_A = 1.5\text{TeV}$, $m_{\tilde{t}} = 2.0\text{TeV}$, and $\mu = 0.5\text{TeV}$. At each point, $\tan\beta$ is determined to obtain $m_h = 125\text{GeV}$.

level quartic from the singlet sector. We have therefore chosen a benchmark value of $m_S^2 = (1\text{TeV})^2$, allowing moderately sized μ and M_S terms while still generating a large quartic and not generating too large of a contribution to the Higgs soft masses. An interesting possiblity to circumvent this tension between radiative tuning and generating a tree-level quartic is to modify the singlet-Higgs sector to take the form of the Dirac NMSSM of Ref. [75], but we do not study this possibility in detail.

While we have allowed values of λ and $\tan\beta$ such that the singlet requires a UV completion above the SUSY breaking scale, we have assumed large enough values for $\tan\beta$ that the top Yukawa remains perturbative up to the GUT scale (see section 2.3). It is interesting to sacrifice MSSM-like gauge coupling unification and consider how natural the SUSY twin Higgs model can be made if low scale Landau poles in both the singlet and top Yukawa couplings are permitted, with the assumption that a suitable fat-Higgs-like [76] composite Higgs sector can provide a UV completion. The point $m_{\tilde{t}} \approx 3.5\text{TeV}$ and $\mu \approx 1\text{TeV}$ provides a useful benchmark. For $\lambda = 1.4$ and $\tan\beta = 2.6$, the correct Higgs mass is obtained with a tuning of 1% and a Landau pole for the singlet near $\sim 500\text{TeV}$ that can be UV-completed consistent with gauge

coupling unification. The tuning can be improved tenfold to 10% for $\lambda = 2$ and $\tan\beta = 1.1$, which is a factor of 30 less tuned than the NMSSM benchmark for the same point. The cost of this decrease in tuning is that the singlet Landau pole is brought down to ~ 50TeV, and likewise the top Yukawa must be completed before the GUT scale. A version of the fat Higgs [76] could provide the necessary UV completion but appears incompatible with precision gauge coupling unification. The extra U(4) breaking quartics $\lambda_{\cancel{\mathrm{U}(4)}} \sim 0.2$ must also be allowed to obtain the correct Higgs mass. Although this is an interesting possibility for dramatically reducing the fine-tuning in a (semi-)perturbative SUSY model, our primary interest in what follows will remain on the case where $\tan\beta$ is large enough that only the singlet requires UV completion and MSSM-like grand unification can occur.

In section 2.4.2 we will discuss the limits on $\frac{v^2}{f^2}$ from the observed couplings of the light Higgs state at the LHC. From Eq. 2.15 we expect the total tuning to become roughly independent of v/f in the limit of large μ or $m_{\tilde{t}}$ and $f^2 \gg v^2$. In fact, because smaller v^2/f^2 allows the Higgs mass to be obtained at smaller values of $\tan\beta$, the tuning can be slightly reduced in this limit. Fig. 2.5 demonstrates this behavior comparing the tuning at $f = 3v$ to $f = 5v$. For $m_t \lesssim 3$TeV the $f = 5v$ model is more tuned because the stop masses are not yet saturating the f-tuning, but for larger stop masses the $f = 5v$ model accommodates the Higgs mass at smaller $\tan\beta$ and is slightly less tuned.

2.2.5 An emergent $\mathbf{Z}_2$

The crucial aspect of the twin Higgs mechanism is that the $\mathbf{Z}_2$ symmetry is realized in the gauge couplings, the large Yukawa couplings in the Higgs-top-singlet sector, and the soft SUSY breaking terms. On the other hand, sources of $\mathbf{Z}_2$ breaking in the Higgs potential are important to obtain a hierarchy in the A- and B-sector vevs, and $\mathbf{Z}_2$ breaking in the small Yukawa couplings is necessary to address cosmological complications as will be discussed in Sec. 2.5.2. An interesting possibility is that the necessary $\mathbf{Z}_2$ symmetries of the large couplings are emergent in the IR while the smaller couplings reflect an $\mathcal{O}(1)$ breaking of the $\mathbf{Z}_2$ in the UV superpotential.

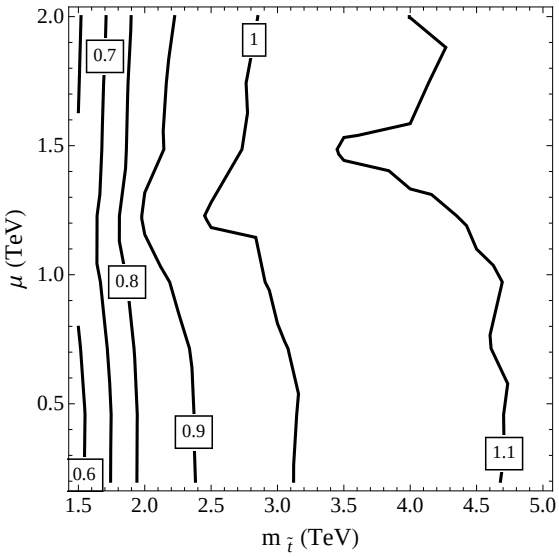

Figure 2.5: Ratio of tuning for twin SUSY models with ($f = 3v$, $m_A = 1.5$TeV) versus ($f = 5v$, $m_A = 2.0$TeV). For both models $\lambda = 1.4$ and $m_S^2 = (1\text{TeV})^2$. At each point, $\tan\beta$ is determined independently for each of the models to obtain $m_h = 125$GeV.

To be concrete, consider a UV model where the $\mathbf{Z}_2$ symmetry of the field content and gauge couplings is exact at Λ_{GUT}, but the $\mathbf{Z}_2$ is broken by $\mathcal{O}(1)$ differences in couplings in the Higgs-Yukawa and Higgs-singlet sector. The singlet must be UV completed to a composite state to allow large values of the IR coupling λ, as will be discussed in detail in section 2.3. The important detail for this discussion is that the IR couplings of both the A and B sectors Higgs to the composite singlet sector are governed by the same interacting fixed point with scaling dimensions set by the common strong sector. Therefore the low energy $\mathbf{Z}_2$ in the Higgs singlet couplings will emerge as long as sufficient time is spent in the interacting fixed point regime. In models where the Higgses themselves are composite, the $\mathbf{Z}_2$ of the top Yukawa couplings can also emerge from the interacting fixed point. Even with an elementary Higgs-top sector, the low values of $\tan\beta$ preferred in the SUSY twin model put the top Yukawa near the IR attractor value, making it insensitive to the value at Λ_{GUT} [77]. For example, for $\tan\beta \sim 2.0$, $y_t(100\text{TeV})$ varies by only 5% for $y_t(\Lambda_{\text{GUT}}) = 0.5 - 2.0$ (disregarding the contributions to the running from the singlet sector, which will move the fixed point to a larger value of $\tan\beta$). This

corresponds to $\lesssim 10\%$ $\mathbf{Z}_2$ breaking in the stop contribution to the Higgs soft masses, which is consistent with the $\mathbf{Z}_2$ breaking necessary to create a hierarchy in vevs. The two-loop contributions of the top Yukawa to the gauge couplings leads to a negligible $\mathbf{Z}_2$ breaking in the gauge sector, and in a pure gauge mediation model the $\mathbf{Z}_2$ symmetry of the gauge couplings automatically leads to $\mathbf{Z}_2$ preserving SUSY breaking masses. If direct messenger-Higgs couplings are necessary, the $\mathbf{Z}_2$ symmetry in these coupling can emerge in the IR from similar attractor behavior.

The SUSY twin Higgs model therefore has the appealing property that the entire U(4) symmetry protecting the light Higgs state results from an IR $\mathbf{Z}_2$ symmetry of the Higgs-top-singlet-gauge sector which can itself emerge from a UV theory with $\mathcal{O}(1)$ breaking of the $\mathbf{Z}_2$ in the superpotential.

2.3 UV completion and λ

The naturalness of the SUSY twin Higgs model is improved for larger values of λ, which raises the prospect of hitting a Landau pole in λ beneath the unification scale. A complete model that preserves the suggestive IR indications of gauge coupling unification should therefore include a suitable UV completion for λ.

Although we are already accustomed to UV completions in the NMSSM for $\lambda(\text{TeV}) \gtrsim 0.7$, the twin Higgs λ coupling hits a Landau pole faster than its NMSSM counterpart due to a larger β function,

$$\beta_\lambda(\text{Twin}) = \frac{6\lambda^3}{16\pi^2} + \dots \tag{2.20}$$

$$\beta_\lambda(\text{NMSSM}) = \frac{4\lambda^3}{16\pi^2} + \dots \tag{2.21}$$

which causes λ to increase faster in the UV. At one loop, the scale of the Landau pole depends on the weak-scale value of λ and on $\tan\beta$ (via dependence on the top Yukawa). In Fig. 2.6 we show the approximate location of the Landau pole in λ for the SUSY twin Higgs as a function of $\lambda(\text{TeV})$ and $\tan\beta$. From Fig. 2.6 it's clear that there is generically a Landau pole well below the GUT scale for the values of $\lambda(\text{TeV}) \gtrsim 1$ favored by naturalness.

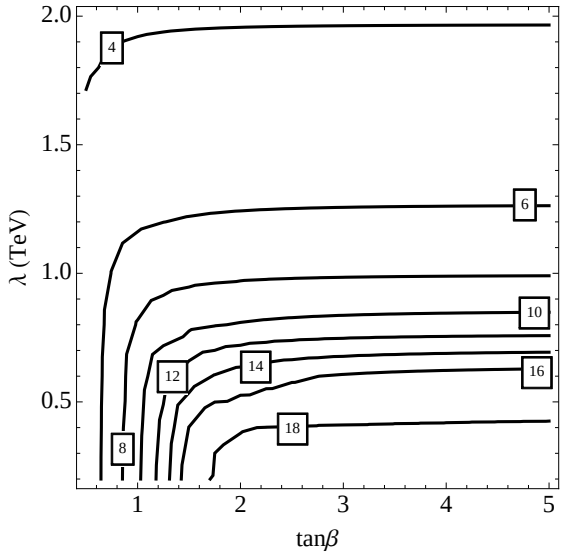

Figure 2.6: The approximate scale Λ of the Landau pole in λ, defined by $\lambda(\Lambda) = \sqrt{4\pi}$, as a function of $\lambda(1\text{ TeV})$ and $\tan\beta$. Contours denote $\log_{10}(\Lambda/\text{GeV})$.

Although there are various possible approaches to UV completing the Landau pole in λ, the Slim Fat Higgs [78] provides an attractive candidate insofar as it does not require a large amount of additional matter charged under the A- and B-sector gauge groups. The essential idea of the Slim Fat Higgs is that the singlet S emerges as a meson of an $SU(N_c)$ gauge group that is deflected from an interacting fixed point to an s-confining fixed point by a mass term for some number of flavors. Concretely, in the UV we introduce an $SU(N_c)$ gauge group with $SU(N_c)$ (anti)fundamentals $\phi(\phi^c)$ that are SM singlets; $SU(N_c)$ (anti)fundamentals $X(X^c)$ that are both A- and B-sector electroweak doublets with a Dirac mass M_D; $SU(N_c)$ (anti)fundamentals $\tilde{X}(\tilde{X}^c)$ with a Dirac mass M_T that partner with X, X^c to fill out complete A- and B-sector $SU(5)$ unified multiplets; and a number of additional $SU(N_c)$ (anti)fundamentals neutral under both A- and B-sector groups. In the twin version of the Slim Fat Higgs, the $X, \tilde{X}$ collectively account for $\delta N_f = 10$ flavors (i.e., a fundamental + antifundamental pair of both A-sector and B-sector $SU(5)$). The UV theory also includes superpotential couplings of the form $W \supset \lambda_1 \phi H_u X^c + \lambda_2 \phi^c H_d X$. At the scale M_D, the fields

X, X^c are integrated out to generate the effective operator

$$W \to -\frac{\lambda_1 \lambda_2}{M_D} \phi \phi^c H_u H_d \tag{2.22}$$

At a scale Λ at or beneath the scale M_D, the theory flows to an s-confining fixed point where $S \sim (\phi \phi_c)$, and we identify $\lambda(\Lambda) \equiv \lambda_1 \lambda_2 \frac{\Lambda}{M_D}$. The challenge is to construct a theory that is at an interacting fixed point at high energies (to retain UV completeness, and to guarantee that $\lambda_{1,2}$ are sufficiently large) and flows to an s-confining fixed point when $X, X^c, \tilde{X}, \tilde{X}^c$ are integrated out, while keeping N_c small enough to avoid introducing too much matter charged under the Standard Model gauge groups. In the conventional Slim Fat Higgs model, the unique solution to these constraints was $N_c = 4$. In the twin Slim Fat Higgs model, the doubling of Standard Model gauge groups means that the $X, \tilde{X}$ account for twice the number of flavors under $SU(N_c)$, and the requirements of asymptotic freedom in the UV, s-confinement in the IR, and the avoidance of SM Landau poles cannot be simultaneously satisfied. However, there is a small modification of the Slim Fat Higgs model that suffices.

A cartoon of the UV completion is shown in Fig. 2.7. We begin with an $SU(N_c+3)$ theory at high energy with $N_f = N_c+14$ flavors, which is asymptotically free for small ($N_c = 3, 4, 5$) values of N_c. This ensures that the theory remains under control in the UV. At the scale M, this theory is Higgsed to $SU(N_c)$ when three flavors acquire vevs and masses of order M. The remaining light flavors now transform as $\mathbf{N_c} + 3 \times \mathbf{1}$, i.e., fundamental flavors plus singlets. These singlets can be given masses of order $\sim M$ by pairing with elementary singlets Σ via superpotential interactions $W \supset \Sigma Q \tilde{Q}$. Thus the theory below M now consists of an $SU(N_c)$ gauge theory with $N_f = N_c + 11$ fundamental flavors, which in general is in a free electric phase. This pattern of Higgsing ensures that the theory is asymptotically free in the UV, but also that there are only N_c additional fundamental + antifundamentals charged under the Standard Model gauge group beneath the scale M. The rest of the story proceeds as with the usual Slim Fat Higgs; at the scale M_T, the triplets $\tilde{X}, \tilde{X}^c$ are integrated out, the theory has $N_f = N_c + 5$ flavors and is generally back in an interacting Coulomb phase down to M_D, the scale where the doublets are integrated out and the theory

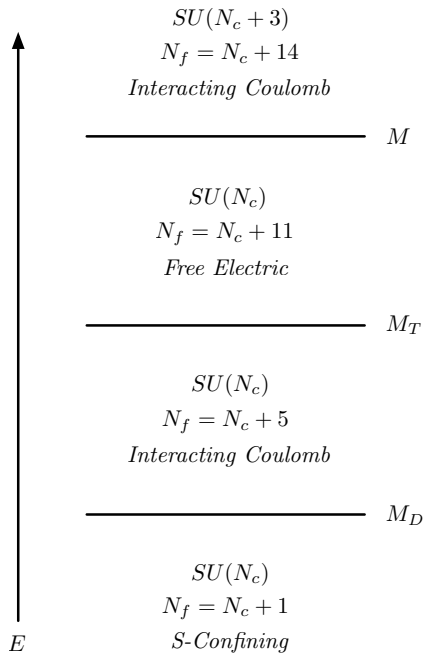

Figure 2.7: Cartoon of the scales and mass flow for the Slim Fat twin Higgs UV completion of λ.

s-confines. Since the theory is in an interacting phase above the scale M and between M_T and M_D, this generally ensures $\lambda_{1,2}$ are sufficiently large to offer a plausible UV completion for λ.

The primary constraint on N_c arises from Landau poles in the A- and B-sector gauge couplings, since the $X, \tilde{X}$ fields collectively account for N_c fundamental + antifundamental pairs under $SU(5)_A$ and $SU(5)_B$. In order to avoid A- and B-sector Landau poles, we would like N_c to be as small as possible, but it should also be large enough that the theory is deep in the interacting Coulomb phase between M_T and M_D, where the fixed point anomalous dimension γ_* of ϕ, ϕ^c controls the size of $\lambda_{1,2}$. We may estimate the fixed point value of $\lambda_{1,2}$ in the weak coupling limit as in [78]. The perturbative RGEs for $\lambda_{1,2}$ are

$$\frac{d\lambda_{1,2}}{dt} = (N_c + 3)\frac{\lambda_{1,2}^3}{16\pi^2} + \gamma_* \lambda_{1,2} + \dots \tag{2.23}$$

and so in the weak coupling approximation the fixed point value of the couplings above the scale M_D is $\lambda_{1,2*} \approx 4\pi\sqrt{|\gamma_*|/(N_c+3)}$. Thus the NDA estimate for λ at the confinement scale Λ is

$$\lambda(\Lambda) \approx \sqrt{N_c}\frac{\lambda_1\lambda_2}{4\pi}\frac{\Lambda}{M_D} \approx 4\pi\frac{\sqrt{N_c}}{N_c+3}|\gamma_*| \tag{2.24}$$

assuming $\Lambda \sim M_D$. For $N_c = 3, 4, 5$, we have $\gamma_* = -1/8, -1/3, -1/2$ and so $\lambda(\Lambda) \approx 0.45, 1.20, 1.76$. Needless to say, this is only an estimate due to the presence of additional incalculable $\mathcal{O}(1)$ factors, but it suggests that $N_c = 4, 5$ both provide suitable UV completions for the values of λ(TeV) under consideration.

The UV completion of the singlet sector can also have an important effect on the running of the top Yukawa coupling through potentially large contributions to the Higgs coupling, especially in the interacting Coulomb phase [79]. The one-loop beta function for y_t at the naive fixed point of the IR interacting Coulomb phase is

$$\frac{dy_t}{dt} \sim \begin{cases} 0.2y_t & N_c = 4 \\ 0.3y_t & N_c = 5 \end{cases}. \tag{2.25}$$

With the low values of $\tan\beta$ preferred by the Higgs mass and tuning, Eq. 2.25 suggests that the theory can not remain near the interacting fixed point very long without increasing y_t sufficiently to run non-perturbative before the GUT scale. Although this introduces some tension with the notion of natural MSSM-like gauge coupling unification in this model, we note that a value near the perturbativity bound is a natural expectation in models where the low energy Z_2 symmetry is partially emergent as discussed in Sec. 2.2.5.

2.4 Phenomenology

The low-energy phenomenology of the SUSY twin Higgs differs radically from conventional supersymmetric scenarios. Although the details of the sparticle spectrum require a complete model for supersymmetry breaking and mediation, it is clear that

the stops and higgsinos can be significantly decoupled in the SUSY twin Higgs without increasing the tuning of the weak scale. Percent-level naturalness is consistent with stops at 3.5 TeV and higgsinos at 1 TeV, well beyond the reach of the 13/14 TeV LHC [80]. In general, radiative corrections tie the mass of the gluino to within a factor of 2 of the stop mass, and gluinos in the range of 3.5-7 TeV likewise lie well beyond the reach of the 13/14 TeV LHC, although such heavy spectra would likely be accessible at an LHC energy upgrade [81]. The avatars of double protection are likewise inaccessible at the LHC, since the fermionic top partner – in the guise of the B-sector top quark – is neutral under the Standard Model gauge groups and only pair-produced with minuscule cross section through the Higgs portal.

In the absence of conventional supersymmetric signals, the primary experimental indications of the SUSY twin Higgs come from the Higgs sector – both in modifications of the couplings of the Standard Model-like Higgs, and in the multitude of additional states in the extended electroweak symmetry breaking sector.

2.4.1 Higgs couplings

The principal constraints on the SUSY twin Higgs arise from tree-level modifications to the couplings of the Standard Model-like Higgs, which we identify with the lighter CP-even neutral Higgs of the A-sector. The couplings of the SM-like Higgs are modified by both the usual SUSY mixing within the two A-sector Higgs doublets, as well as the mixing with B-sector Higgs doublets.[4]

To the extent that we would like to constrain the SUSY twin Higgs parameter space with coupling measurements of the SM-like Higgs, the most interesting properties are those of the lightest CP even Higgs. In general, the matrix of mixings in the CP even Higgs sector is unenlightening, but we may capture the important parametrics by carrying out a perturbative expansion in the U(4) limit, $g^2 + g'^2 \ll \lambda^2$. Since we are interested in a relatively high scale of sparticles, we will also focus on the "SUSY twin decoupling limit" $\lambda^2 f^2 \ll m_A^2$, akin to the usual SUSY decoupling limit, $m_Z^2 \ll m_A^2$. Here $m_A^2 \equiv \frac{2b}{\sin(2\beta)}$ is a mass parameter that corresponds to the

[4]One could also look for NLO effects coming from loops of B-sector top quarks as in [29], but these are typically subdominant to the tree-level coupling deviations.

usual MSSM definition, as well as the mass of one physical pseudoscalar; it provides a convenient means of packaging results, and preserves the customary intuition that certain additional Higgs states decouple in the limit $m_Z^2 \ll m_A^2$.

To leading nontrivial order in the expansion $g/\lambda, m_Z/m_A, \lambda f/m_A \ll 1$, the four CP-even masses are $m_Z^2 \cos(2\beta)^2 \left(2 - \frac{2v^2}{f^2}\right)$, $m_A^2 - \lambda^2 f^2$, $\lambda^2 f^2 \sin(2\beta)^2$, and $m_A^2 - \lambda^2 f^2 \sin(2\beta)^2$. The first corresponds to the Goldstone mode, primarily identified with the A-sector light CP-even Higgs, while the remaining states are primarily identified with the A-sector heavy CP-even Higgs, B-sector light CP-even Higgs, and the B-sector heavy CP-even Higgs, up to inter-sector mixings of order v/f. With this in mind, in what follows we label the corresponding mass eigenstates $h_1(\equiv h), H_1, h_2$, and H_2, respectively, with h identified with the recently-discovered SM-like Higgs. We adopt a similar nomenclature for the pseudoscalars A_1, A_2 and the charged Higgs pairs $H_1^\pm, H_2^\pm$.

The composition of h in terms of the gauge eigenstates is very nearly what one would expect from the direct product of a supersymmetric 2HDM and the twin Higgs mechanism, viz.

$$\begin{aligned}
h \;\approx\; & \left[\left(1 - \frac{v^2}{2f^2}\right)\sin\beta + \frac{m_Z^2}{4\lambda^2 f^2}\cos^2(2\beta)\csc\beta\sec^2\beta + 2\frac{m_Z^2}{m_A^2}\cos^2\beta\sin\beta\cos(2\beta)\right] h_u^{0\,A} \\
+ \; & \left[\left(1 - \frac{v^2}{2f^2}\right)\cos\beta + \frac{m_Z^2}{4\lambda^2 f^2}\cos^2(2\beta)\csc^2\beta\sec\beta - 2\frac{m_Z^2}{m_A^2}\cos\beta\sin^2\beta\cos(2\beta)\right] h_d^{0\,A} \\
+ \; & \left[\frac{v}{f}\sin\beta + \frac{m_Z^2}{4\lambda^2 v f}\cos^2(2\beta)\csc\beta\sec^2\beta\right] h_u^{0\,B} \\
+ \; & + \left[\frac{v}{f}\sin\beta + \frac{m_Z^2}{4\lambda^2 v f}\cos^2(2\beta)\csc^2\beta\sec\beta\right] h_d^{0\,B}
\end{aligned}$$

Indeed, in the limit $g/\lambda \to 0$ the mixing contributions from the SUSY 2HDM and the twin Higgs factorize such that the couplings of the Standard Model-like Higgs to

vectors, top quarks, bottom quarks, and leptons are modified by an amount

$$\begin{aligned} c_V &\approx 1 - \frac{v^2}{2f^2} - \frac{m_Z^4}{8m_A^4}\sin^2(4\beta) + \dots \\ c_t &\approx 1 - \frac{v^2}{2f^2} + \frac{2m_Z^2}{m_A^2}\cos^2\beta\cos(2\beta) + \dots \\ c_b = c_\tau &\approx 1 - \frac{v^2}{2f^2} - \frac{2m_Z^2}{m_A^2}\sin^2\beta\cos(2\beta) + \dots \end{aligned} \tag{2.26}$$

where $c_i \equiv g_{hii}/g_{h_{SM}ii}$.

In addition to modifications of the Higgs couplings to Standard Model states, there is also generically an invisible width coming from decays of the Higgs to B-sector fermions, predominantly $h \to b_B\bar{b}_B$, due to the $\mathcal{O}(v^2/f^2)$ mixing of h with the B-sector CP-even Higgses. The B-sector bottom quark mass and couplings are fixed by the Z_2 symmetry, and so the partial width for $h \to b_B\bar{b}_B$ at leading order is

$$\Gamma(h \to b_B\bar{b}_B) \approx \Gamma(h \to invis.) \approx \Gamma(h \to b\bar{b})\tan^2(v/f)\left(\frac{1 - 4\frac{m_b^2}{m_h^2}\frac{f^2}{v^2}}{1 - 4\frac{m_b^2}{m_h^2}}\right)^{3/2} \tag{2.27}$$

The modified Higgs couplings and invisible width have two novel implications. The first is that the intrinsic $\mathcal{O}(v^2/f^2)$ tuning of the theory is set by measurements of Higgs couplings, much as in composite Higgs models. Since the precision of current Higgs coupling measurements in combination approaches $\mathcal{O}(10\%)$, this suggests $f \gtrsim 3v$; we will make this statement more precise in the next subsection.

The second novel implication is that the invisible Higgs width is also of order v^2/f^2, so that the invisible width of the Higgs directly probes the tree-level naturalness of the theory. Whereas the mass scale of higgsinos and top partners in the SUSY twin Higgs provides little concrete information regarding the naturalness of the weak scale, the invisible width provides an unambiguous indication.

2.4.2 Coupling Fits

To establish the allowed range of both v/f and the 2HDM mass scale m_A, we construct a combined fit to Higgs couplings using available data from both ATLAS and CMS searches at 7 and 8 TeV.[5] To do so, we adopt the methods of [87]. We construct a likelihood for each individual exclusive channel in [87] using a two-sided gaussian whose mean is given by the experimental value of the signal strength modifier μ and whose width is given by the 1σ errors on μ. Where two-sided measurements are unavailable, we use an approximate gaussian likelihood constructed from the observed and expected limits.[6]

To determine the dependence of the signal strength on the relevant SUSY twin Higgs parameters f, m_A, and $\tan\beta$, we use the techniques of [91] with the tree-level coupling modifiers in Eq. 2.26 plus the invisible width in Eq. 2.27. For simplicity, we take the limit $(g^2+g'^2)/\lambda^2 \to 0$, for which the effects due to the SUSY 2HDM and twin Higgs sector approximately factorize. We have checked that this approximation to the Higgs couplings always agrees with full numerical results to within a few percent in the parameter regions of interest. We do not include any contributions from loops of superpartners, since the mass scale of superpartners is sufficiently high that these contributions are negligible.

Given these single-channel likelihoods, we construct a combined likelihood from the product of the single-channel likelihoods. To perform the fit, we fix the representative value $\tan\beta = 2.5$ and compute $-2\Delta\ln\mathcal{L}$ in the f, m_A plane relative to the best-fit point of $f, m_A \to \infty$. We denote the 95% CL region by $-2\Delta\ln\mathcal{L} < 5.99$ in this 2D plane.

[5] For fits to the related left-right twin Higgs model [82, 83] using various stages of LHC Higgs data, see [84, 85, 86].

[6] Note that the channels in [87] do not include direct limits on the Higgs invisible branching ratio from e.g. [88, 89, 90]. To check the effects of the direct invisible branching ratio limit on the fit, we construct a single-channel likelihood using the numerical values of $-2\log\mathcal{L}$ for the invisible branching ratio measurement in [88]. The effects of invisible branching ratio limits [89, 90] are very similar. The inclusion of this likelihood leads to an insignificant change in the best-fit region since the direct limit of $\mathrm{Br}(h \to \text{invis.}) < 0.65$ is much weaker than the implicit limit in the SUSY twin Higgs framework coming from measured branching ratios. We do not include this invisible branching ratio likelihood in our final fit due to uncertainties in the shape of the likelihood in [88] for low values of the invisible branching ratio.

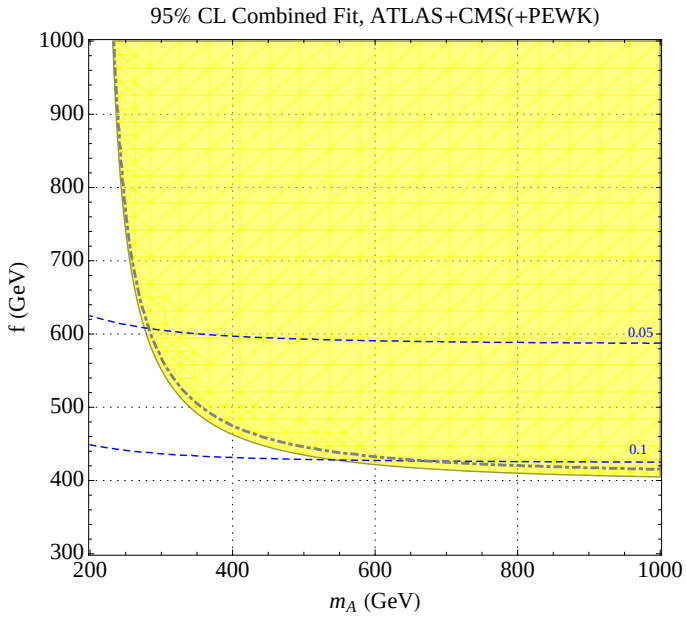

Figure 2.8: Coupling fit in the SUSY twin Higgs model as a function of m_A and f for the representative value of $\tan\beta = 2.5$ in the limit $(g^2+g'^2)/\lambda^2 \to 0$. The fit procedure is described in the text. The yellow shaded region denotes the 95% CL allowed parameter space defined by $-2\Delta \ln \mathcal{L} < 5.99$, not including precision electroweak constraints. The gray dot-dashed line denotes the edge of the 95% CL allowed region including IR contributions to the S- and T-parameters, marginalizing over the U-parameter. The blue dashed lines indicate the contours of $\mathrm{Br}(h \to \text{invis.}) = 0.05, 0.10$, respectively.

It is well known in the case of composite Higgs models that the strongest constraint comes from the combination of Higgs coupling measurements and precision electroweak data, including the IR contribution to the S- and T-parameters from the modification of the SM-like Higgs couplings to vectors [92, 93]. As we will discuss in the next section, the situation is substantially improved in the SUSY twin Higgs model. For the sake of illustration, we also show the 95% best fit region including precision electroweak limits on the IR contribution to the S- and T-parameters (Eq. 2.28) for $\lambda = 1.5$, marginalizing over the U-parameter. This includes the leading constraints from electroweak precision tests on modified couplings of the SM-like Higgs. We do not include UV contributions to the S- and T-parameters, which depend on the details of the heavy Higgs spectrum but are numerically of the same

order as the IR contributions and decouple as $m_A \to \infty$.

The coupling fit is shown in Fig. 2.8, which illustrates that $f \gtrsim 3v$ is comfortably allowed by current coupling measurements (recall we work in units where $v \approx 174$ GeV and f is similarly normalized), with a modest invisible branching ratio of up to $\sim 10\%$. The invisible branching ratio in the SUSY twin Higgs consistent with current coupling measurements is smaller than the allowed values found in e.g. [94] because the invisible width scales similarly to the modifications of tree-level couplings, leading to a tighter constraint.

2.4.3 Extended Higgs sector

The extended twin Higgs sector offers a plethora of additional states in the Higgs sector, including three additional CP-even neutral scalars, two pseudoscalars, and two pairs of charged Higgses. For the most part, these additional degrees of freedom are kinematically decoupled. As discussed above, the masses of the the "heavy" CP-even scalars H_1, H_2 are $m_{H_1}^2 \sim m_A^2 - \lambda^2 f^2, m_{H_2}^2 \sim m_A^2 - \lambda^2 f^2 \sin^2(2\beta)$. Both charged Higgs pairs have masses of order $m_{H_{1,2}^\pm}^2 \sim m_A^2 - \lambda^2 f^2$ with subleading splittings of order $\mathcal{O}(m_W^2, m_{W_B}^2)$. The pseudoscalars have masses $m_{A_1}^2 \sim m_A^2 - \lambda^2 f^2, m_{A_2}^2 \sim m_A^2$. Consequently, all of these states are typically $\gtrsim$ TeV with correspondingly low production cross sections at the LHC. Moreover, the additional Higgs states coming predominantly from the A-sector enjoy the usual decoupling properties of a SUSY 2HDM, with correspondingly small couplings to Standard Model gauge bosons and the SM-like Higgs h. Given the limited reach for narrow Higgs scalars $\gtrsim$ TeV, it seems unlikely that these degrees of freedom can be meaningfully probed at the LHC.

However, the second-lightest CP-even neutral scalar h_2 may remain relatively light, with $m_{h_2} \approx \lambda f \sin(2\beta)$. It possesses a coupling to top quarks of $\mathcal{O}(v/f)$, so that it is produced at the LHC via gluon fusion with a cross section $\sigma(gg \to h_2) \approx (v/f)^2 \sigma(gg \to h_{SM})$, where h_{SM} is a Standard Model Higgs of equivalent mass. Consequently, the gluon fusion cross section can remain relatively large, $\mathcal{O}(1$ pb) at $\sqrt{s} = 14$ TeV for $m_{h_2} \sim 500$ GeV.

The decay of h_2 is likewise promising. Although in general h_2 couples to degrees of freedom in the B-sector, it possesses a relatively large trilinear coupling with the SM-like Higgs h, $\lambda_{h_2hh} \approx \frac{m_{h_2}^2}{2\sqrt{2}f}$. Consequently, the partial width $\Gamma(h_2 \to hh)$ grows as $\sim m_{h_2}^3/f^2$ with no small numerical suppression, and indeed parametrically competes with the partial width into B-sector gauge bosons. For the range of λ of interest, the two-body decays of $h_2 \to Z_BZ_B, W_BW_B$ are kinematically accessible, so that $\Gamma(h_2 \to Z_BZ_B, W_BW_B)$ and $\Gamma(h_2 \to hh)$ differ only by kinematic factors and degree-of-freedom counting. Both decays dominate over decays to B-sector top quarks – which are kinematically inaccessible for $\lambda \lesssim 2$ – and decays to lighter B-sector fermions and gauge bosons. Note that h_2 is not exceptionally wide for $m_{h_2} \lesssim$ TeV, since $\Gamma_{\rm tot}/m_{h_2} \sim \lambda^2/16\pi^2 \ll 1$.

Thus $\mathrm{Br}(h_2 \to hh) \sim \mathcal{O}(0.1 - 0.4)$ over a wide range of masses with no strong suppression from decoupling, in stark contrast to the heavy Higgs of the MSSM.[7] This raises the tantalizing prospect of a resonant di-Higgs signal at the LHC [68, 95, 96, **?**] with cross sections of order $\sigma \cdot \mathrm{Br}(pp \to h_2 \to hh) \sim 10 - 500$ fb at $\sqrt{s} = 14$ TeV for $m_{h_2} \sim 500 - 1000$ GeV. This should be compared to the Standard Model Higgs pair production rate, ~ 34 fb at $\sqrt{s} = 14$ TeV, and will be easier to distinguish from background due to the boosted kinematics and resonant production mode. Unlike conventional 2HDMs (SUSY or otherwise), there is no competitive signal from $h_2 \to WW, ZZ$ (i.e., the massive A-sector gauge bosons), due to the suppressed coupling of h_2 to Standard Model gauge bosons. This strongly motivates searches for resonant di-Higgs production over a wide range of heavy Higgs masses.

Alternately (or perhaps in conjunction with the $h_2 \to hh$ signal), one may look for vector boson fusion production or Z-associated production of h_2 followed by invisible decay into B-sector states (primarily W_B, Z_B). The production cross section times invisible branching ratio for e.g. $\sigma \cdot \mathrm{Br}(pp \to qqh_2 \to jj + invis.)$ should be of order 10-100 fb at $\sqrt{s} = 14$ TeV for $m_{h_2} \sim 500 - 1000$ GeV, and could provide strong validation of a signal in $h_2 \to hh$ or serve as an independent detection mode in its

[7] The violation of conventional 2HDM decoupling intuition here stems from the fact that there are two separate vacuum expectation values in the extended Higgs sector and genuine decoupling also requires $\lambda \to 0$. The trilinear coupling still exhibits the necessary property that $\lambda_{h_2hh}v \to 0$ in the appropriate alignment limit $v/f \to 0$.

own right. Similar sensitivity to an invisibly-decaying heavy Higgs scalar should be available in associated production with a Z boson. At present, the ATLAS invisible Higgs search [88] and the CMS invisible Higgs search [89] present limits for heavy Higgs masses up to $m_H = 300, 400$ GeV, respectively, but could be meaningfully extended to higher masses. Clearly, if the remaining SUSY states lie above 1 TeV, these novel Higgs signatures may be the most promising direct signal of the SUSY twin Higgs at the LHC.

2.4.4 LHC search strategy

As we have seen, the most promising signals of the SUSY twin Higgs include $\mathcal{O}(v^2/f^2)$ deviations in the tree-level couplings of the SM-like Higgs; a modest $\mathcal{O}(v^2/f^2)$ invisible branching ratio; resonant pair production of the SM-like Higgs from a heavier CP-even Higgs with a large trilinear coupling and $\mathcal{O}(v^2/f^2)$-suppressed gluon fusion production; and vector boson fusion and/or Z associated production of the heavier CP-even Higgs followed by decay to invisible final states. To the extent that measurements of Higgs couplings and invisible width will attain at best $\mathcal{O}(10\%)$ precision at the LHC, this motivates searching for resonant pair production of the SM-like Higgs and extending Higgs invisible width searches beyond $m_H = 300 - 400$ GeV. Discovery of either process would strongly motivate construction of a Higgs factory to further test for tree-level coupling deviations and a modest Higgs invisible width.

2.5 Ancillary constraints

2.5.1 Precision electroweak and flavor

In contrast to composite Higgs models, the precision electroweak corrections in the SUSY twin Higgs are all calculable and, by construction, quite small. A key advantage, even with respect to other natural models in which the Higgs is a goldstone boson, is the inertness of the heavy B-sector gauge bosons with respect to A-sector gauge bosons and fermions. There are therefore no tree-level contributions to the

S and T parameters. This avoids the largest corrections to precision electroweak observables present in, e.g., little Higgs models.

Unsurprisingly, here the extended Higgs sector is the principal source of new contributions to precision electroweak observables. In general these contributions are completely consistent with current limits on S and T. For the sake of simplicity and clarity, we'll restrict ourselves to a brief discussion of precision electroweak contributions in the limit $v \ll f \lesssim m_A$, in which case the Higgs sector consists of the light SM-like Higgs, a second CP-even Higgs h_2 around $m_{h_2} \sim \lambda f$, and the remaining Higgs scalars $H_{1,2}, A_{1,2}, H^{\pm}_{1,2}$ clustered around a common mass $m_A \gtrsim$ TeV. In this limit, we can simply treat the largest corrections to Standard Model expectations from the coupling deviations of h and additional contributions of h_2. In the m_h, m_{h_2} sector, the additional contributions to the S and T parameters – *beyond* the usual contribution from a Standard Model Higgs of mass m_h – are given by

$$\Delta S \approx \frac{1}{6\pi}\left(\frac{v}{f}\right)^2 \log\left(\frac{m_{h_2}}{m_h}\right) \qquad \Delta T \approx -\frac{3}{16\pi \cos^2\theta_W}\left(\frac{v}{f}\right)^2 \log\left(\frac{m_{h_2}}{m_h}\right) \tag{2.28}$$

This captures the leading correction to the S and T parameters from variations in the couplings of the SM-like Higgs in the limit $m_A \to \infty$ and is quite small for the parameter range of interest. Additional corrections arise from the remaining Higgs scalars $H_{1,2}, A_{1,2}, H^{\pm}_{1,2}$ at the scale $m_A \gtrsim$ TeV. However, as in the MSSM, the these additional states decouple with increasing m_A; in particular the sectors $(H_1, A_1, H_1^{\pm})$ and $(H_2, A_2, H_2^{\pm})$ are approximately degenerate so that electroweak corrections are small. In the limit $g, g' \to 0$, the $(H_1, A_1, H_1^{\pm})$ sector is exactly degenerate, and corrections from this sector to S and T vanish; for nonzero g, g' this leads instead to the customary MSSM-like contributions that are strongly suppressed by $\mathcal{O}(m_Z^2/m_A^2)$ in the regime of interest. Corrections from the $(H_2, A_2, H_2^{\pm})$ sector are additionally suppressed by a factor of v^2/f^2 due to the smallness of mixing with the A sector, but in the $g, g' \to 0$ limit nonzero splitting between H_2, A_2, and $H_2^{\pm}$ persists. Expanding the appropriate loop functions (e.g., [97]), in the limit $m_A^2 \gg \lambda^2 f^2$, the leading

contributions to S and T from the $(H_2, A_2, H_2^{\pm})$ sector are parametrically of order

$$\Delta S \approx \frac{1}{16\pi}\frac{\lambda^2 v^2}{m_A^2} \qquad \Delta T \approx \frac{1}{48\pi}\frac{\lambda^2}{g^2 s_W^2}\frac{\lambda^2 f^2}{m_A^2}. \tag{2.29}$$

There are also contributions from loops involving one scalar from each sector, but these share an overall suppression factor of $\mathcal{O}(v^2/f^2)$ due to mixing, as well as a similar magnitude of mass splitting between states, leading to corrections of the same order as Eq. 2.29. Taken together, the corrections to S are insignificant, while the corrections to T are typically numerically of the same magnitude as those in Eq. 2.28, and both show the expected decoupling as $m_A \to \infty$. However, the corrections to T have the potential to generate (mild) tension with precision electroweak limits if $m_A \sim \lambda f \lesssim$ TeV, though this depends in detail on the extended Higgs sector and is readily susceptible to cancellations. Finally, corrections from the remainder of the sparticle spectrum are parametrically small unless there is substantial mixing in the squark sector.

There are no pernicious new sources of flavor violation in the SUSY twin Higgs beyond those usually encountered at one loop. In particular, the extended Higgs sector automatically satisfies the Glashow-Weinberg condition [98] due to a combination of holomorphy and gauge invariance, guaranteeing the absence of new tree-level contributions to flavor-changing neutral currents. At one loop, the decoupling of charged Higgs states protects against prohibitive contributions to, e.g., $b \to s\gamma$. Although sfermions may all be in the multi-TeV range, this alone is insufficient to suppress one-loop FCNC in the presence of large flavor-violating soft masses, and so the usual solutions to the supersymmetric flavor problem are still required.

2.5.2 Cosmology

The cosmology of mirror twin Higgs models has been discussed in detail in refs. [35, 68, 69], and for mirror models in general in refs. [99, 100, 101]. Here we review briefly the important constraints from light degrees of freedom and dark matter abundance.

The principal cosmological constraints on mirror twin Higgs models are the CMB and BBN bounds on extra light degrees of freedom, most stringently the recent Planck

result $N_{\rm eff} = 3.30 \pm 0.27$ [102]. The light Higgs state keeps the A and B sector in thermal equilibrium down to temperatures $T_{\rm eq} \sim \mathcal{O}(1{\rm GeV})$ [69]. In the limit of an exact $\mathbf{Z}_2$ symmetry there is an unacceptably large contribution to $N_{\rm eff}$ if the reheating is symmetric or $T_{\rm RH} \gtrsim T_{\rm eq}$.

The possibility of asymmetric reheating is discussed in refs. [99, 100, 101]. An alternative solution in a high-T symmetric reheating scenario is to include $\mathbf{Z}_2$ breaking contributions to the B-sector Yukawas to lift the light quarks and charged leptons above $T_{\rm eq}$ [35, 68, 69]. This can be a hard breaking in the flavor sector or spontaneous breaking from asymmetric vevs of flavon fields; the small Yukawa couplings feed into the RG of the Higgs-top-gauge sector at acceptably small levels and do not modify the tuning. If only the B-sector photons, gluons and neutrinos remain below $T_{\rm eq}$, then in the absence of entropy production in the QCD phase transition $\Delta N_{\rm eff} \sim 1.4$ [68]. This may be reduced to comfortably within bounds if the A-sector QCD phase transition involves entropy production not present in the B-sector transition (due to the presence of light quarks in the A-sector), or if the B-sector QCD phase transition is raised above $T_{\rm eq}$ [35, 68]. The tension may be further ameliorated if B-sector gauge groups are spontaneously broken (via, e.g., tachyonic B-sector soft masses giving rise to charge- and color- breaking minima).

In mirror twin Higgs models, the B-sector baryon and lepton number are independently conserved and can lead to stable relics. If a baryon asymmetry is generated in the B-sector, the lightest B-baryon, which may be charged or neutral, can be the DM and naturally link the DM and SM baryon abundance [68]. The lightest B-sector charged lepton can also make up a component of the DM if its decay to a charged B-pion and neutrino is kinematically forbidden. The phenomenology of charged baryonic or leptonic B-sector DM components depends in detail on whether or not the B-sector U(1) is broken and on the spectrum of hadronic and nuclear states. In the SUSY twin Higgs model, the lightest superpartner can also provide a dark matter candidate. The R-parity of the A and B sectors is shared, and a neutralino LSP can be a mixture of A and B-sector states. The larger B-sector Higgs vev can naturally lead to an LSP with primarily B-sector components, suppressing standard direct and indirect detection signals.

2.6 Conclusions

We have shown that a minimal supersymmetric completion of the mirror twin Higgs model yields MSSM-like gauge coupling unification, a naturally light SM-like Higgs, and small corrections to electroweak precision and flavor observables. The level of tuning of this model is comparable to the NMSSM with a superpartner mass scale half as large, and the observed ~ 125GeV mass of a SM-like Higgs state is consistent with a percent-level tuned spectrum of superpartners likely unobservable at both the 13/14 TeV LHC and a ~ 1TeV linear collider. Provided additional U(4)-breaking quartics, a spectrum with superpartners at current LHC limits is consistent with tuning at the 10% level. Furthermore, if we discard the requirement of perturbative MSSM-like gauge coupling unification, a Higgs compositeness scale of ~ 50TeV allows 10%-level tuning with superpartners entirely out of reach of the LHC.

With the superpartners in these models out of reach, the most promising collider signals come from the Higgs sector. The mixing of the lightest Higgs with the mirror sector is proportional to the hierarchy of vevs $\frac{v}{f}$, and constraints on the Higgs couplings translate into a direct and unambiguous constraint on the fine-tuning of the model, $\Delta^{-1} < \frac{2v^2}{f^2}$. Already the measurements of the couplings of the SM-like Higgs state at the LHC and precision electroweak measurements require a hierarchy in vevs $\frac{v}{f} \lesssim \frac{1}{3}$, and few-percent-level measurements of Higgs couplings at the 13/14 TeV LHC will put more stringent limits on this model. The Higgs coupling limits we derived in the supersymmetric decoupling limit also apply equally well to any low-energy effective twin Higgs theory. While most of the extra Higgs states can easily be decoupled, the next-to-lightest CP-even Higgs state typically remains within reach of the 13/14 TeV LHC and has large branching ratios to both the striking di-Higgs channel and invisible final states. Just as the discovery of the light SM-like Higgs determined the size of the effective quartic self-coupling and made concrete the natural scale for physics cutting off the top quark contribution to the Higgs mass, measuring the mass of the next lightest CP-even Higgs state in the mirror twin model will point to the natural scale for the superpartners in the twin SUSY model. The presence of this light state is also an important signal that the twin mechanism is perturbatively

realized, rather than resulting from compositeness at the scale of a few TeV.

The SUSY twin Higgs, like any model involving a "double-protection" solution to the hierarchy problem, clearly presents a challenge from the point of view of UV model-building and parsimony. Compared to composite models, this issue is somewhat alleviated for the SUSY twin Higgs model; here the full approximate U(4) symmetry emerges accidentally from a smaller $\mathbf{Z}_2$ symmetry which can originate far in the UV and may in fact be partially emergent at low energies. As a minimal supersymmetric extension of the twin Higgs, the model we have presented is also considerably more appealing from this point of view than earlier efforts at supersymmetrizing the twin Higgs [69, 70]. If null results in searches for superpartners persist at the 13/14 TeV LHC, understanding in detail the signatures of models like the SUSY twin Higgs – which trade parsimony for decreased fine-tuning – will become crucial to interpreting the role of naturalness as a predictive principle for the next generation of collider, dark matter, and low-energy precision experiments.

There are many possible avenues for further study. In this chapter we have focused on the low-energy phenomenology without committing to a detailed model for supersymmetry breaking. It would be interesting to investigate mediation mechanisms giving rise to the appropriate combination of U(4)-symmetric and U(4)-breaking soft terms, perhaps via gauge mediation with suitable Higgs-messenger couplings. A SUSY-breaking mechanism that gives rise to tachyonic scalars in the B sector would be attractive from the perspective of cosmology, where spontaneous breaking of B sector gauge symmetries helps to alleviate constraints from N_{eff}. We have also not discussed dark matter candidates in detail, but the super-abundance of dark matter candidates in the SUSY twin Higgs model could give rise to a number of interesting scenarios that merit further study. Finally, while we have presented parametric estimates for the rates of resonant di-Higgs and invisible heavy Higgs production, a detailed study of these signals and their prospects for LHC discovery would be worthwhile.

Chapter 3

Maximally Natural Supersymmetry

3.1 Introduction

The LHC has set stringent limits on the masses of SUSY particles and deviations in Higgs properties, implying a tuning of electroweak symmetry breaking (EWSB) at the percent level or worse for traditional SUSY models [53, 73, 103, 104, 105, 106]. This undermines the motivation for SUSY as the solution to the hierarchy problem and the case for discovery of SUSY at the LHC or proposed future colliders. Given the importance of this issue for current and future searches for new physics we examine the possibility of constructing natural, untuned theories. We find a promising example in theories where some particles propagate in a 5th dimension of physical length $\pi R \sim \text{TeV}^{-1}$ and SUSY is broken by the boundary conditions (bc's) for these bulk fields [107, 108, 109, 110, 111, 112, 113, 114, 115, 116, 117, 118, 119, 120, 121]. This mechanism is known as Scherk-Schwarz SUSY breaking (SSSB), and the key features of these models are:

• The theory is never well approximated by a 4D theory with soft supersymmetry breaking, and many problems of the minimal supersymmetric standard model (MSSM) and its extensions are avoided.

• The higgsinos, gauginos, and the 1st and 2nd family sfermions propagate in the

5th dimension and obtain SSSB masses of size $1/2R$.

• The 3rd family is localized on a 4D brane to protect the 3rd generation squarks from a large tree-level SSSB mass, thus realizing a natural SUSY spectrum [42, 43, 44] and significantly easing collider bounds. The super-softness of SSSB [122, 123, 124, 125, 126, 127, 128] prevents large logs in the loop-level mediation of SUSY breaking, further protecting the weak scale and suppressing the tendency of the gluino to pull up the stop mass [73, 103].

• Only a single Higgs doublet H_u acquires a VEV and has Yukawa couplings. The μ and b terms are not needed, and the physical Higgs is automatically SM-like.

• An additional SUSY breaking sector is necessarily present for radius stabilization with zero cosmological constant (CC), and SUSY breaking in this sector can naturally be driven by SSSB. Higher dimensional couplings of the MSSM fields to this sector play a crucial role in EWSB and collider phenomenology.

The pattern of localization of matter and Higgs multiplets and the mechanism driving EWSB, generating Yukawa couplings, and accommodating the observed physical Higgs mass lead to important differences from previously studied models of near-maximal SSSB near the TeV scale [107, 108, 109, 110, 111, 112, 113, 114, 115, 116, 117, 118, 119, 120, 121] and models obtaining a realistic spectrum from non-maximal SSSB at scales $1/R \gg$ TeV [129, 130, 131].

The structure of the chapter will be as follows. In Section 3.2, we consider a toy model that illustrates the basics of the SSSB mechanism and the role of the different ingredients present in the minimal model. Section 3.3 contains a realistic description of the minimal theory, featuring all necessary ingredients, as well as a discussion of EWSB and the status of the physical Higgs mass. In Section 3.4, we consider several extensions of the model that allow for a physical Higgs mass consistent with observations. The phenomenology of the different versions of the model considered is discussed in Section 3.5. An interesting possibility for decays of brane-localized states to a bulk LSP is motivated by these models, and the associated unusual collider phenomenology of these decays is discussed in Section 3.6.

3.2 The basics of Scherk-Schwarz SUSY breaking

For simplicity of presentation, and after a very brief discussion in Section 3.2.1 of 5D SUSY and the generalities of SSSB, this Section focuses on the physics of a toy model containing just the right-handed top superfield $\overline{U}_3$ (on shell: $\overline{U}_3 = (\tilde{\overline{u}}_3, \overline{u}_3)$, with $\overline{u}_3$ a 2-component Weyl fermion) localized on the orbifold $y = 0$ brane and the $SU(3)$ color gauge group in the bulk, as depicted in Figure 3.1. Although this simplified model is inconsistent in several ways as a stand-alone theory, it forms part of the final and fully consistent picture that will be described in Section 3.3 and contains the minimal ingredients that will help us illustrate some of the most important features of maximal SSSB. Specifically, these include (i) large hierarchies in soft masses generated at tree level by the 5D geography, (ii) the very soft nature of loop communication of SSSB, and (iii) the potential importance of extra SUSY breaking sectors associated with radius stabilisation.

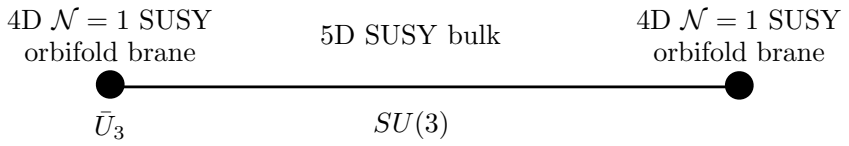

Figure 3.1: Schematic geography of the toy model containing bulk $SU(3)$ interactions and a brane-localized right-handed top superfield $\overline{U}_3$.

3.2.1 5D SUSY with Scherk-Schwarz breaking

For enhanced pedagogy and completeness we start with a short review of the relevant aspects of 5D SUSY and SSSB. Readers already familiar with this material are encouraged to jump to Section 3.2.2.

A realistic description of the world arising from an extra-dimensional theory can be constructed provided the extra dimensions are compactified. From a 4D perspective, fields that propagate along the bulk of the extra dimension are equivalent, upon compactification, to an infinite tower of fields of ever increasing mass—the Kaluza-Klein (KK) excitations—with a mass gap between different modes set by the compactification scale. For example, if an extra spatial dimension is compactified on a circle

S^1 of radius R, KK modes have masses that are multiples of the compactification scale $1/R$. Nevertheless, to obtain chiral fermions in the low energy theory the extra dimension needs to be compactified not on a circle but on an 'orbifold' where discrete identification(s) of the extra-dimensional coordinate, such as $y \sim -y$ with associated fixed points (here $y = 0, \pi R$), imply the presence of 4D branes violating the higher-dimensional bulk Lorentz symmetry. For example, an extra spatial dimension compactified on an orbifold $S^1/\mathbb{Z}_2$ has physical length πR, with the two orbifold fixed-points at $y = 0, \pi R$ corresponding to 4D branes where fields and interactions may be localized. This $\mathbb{Z}_2$ orbifold action is then extended to an action on the bulk fields; e.g. for a bulk scalar the indentification $\phi(x^\mu, y) = \pm\phi(x^\mu, -y)$ can be made, which translates to Neumann (for $+$) or Dirichlet (for $-$) boundary conditions for the bulk field at the fixed points.

It is important for our entire construction that the minimal representation of SUSY in 5D corresponds to $\mathcal{N} = 2$ extended SUSY from a 4D perspective, i.e. the theory has 8 rather than 4 supercharges. After such an extra dimension is compactified on an $S^1/\mathbb{Z}_2$ orbifold just a minimal $\mathcal{N} = 1$ 4D SUSY survives (4 supercharges) as the other supercharges are automatically removed by the action of the orbifold boundary conditions. In addition, on the two 4D orbifold branes, 4D $\mathcal{N} = 1$ supersymmetric field content and interactions may be localized. On the other hand an $S^1/(\mathbb{Z}_2 \times \mathbb{Z}_2')$ orbifold has two inequivalent fixed points (and thus branes) and can, depending on the choice of field parities under the $\mathbb{Z}_2 \times \mathbb{Z}_2'$ actions, break SUSY completely in the IR theory.

To understand this crucial point we briefly review how $\mathcal{N} = 2$ SUSY can be expressed in $\mathcal{N} = 1$ superfield notation. An $\mathcal{N} = 2$ vector superfield $\mathbb{V}^a$ may be written in terms of one $\mathcal{N} = 1$ vector superfield V^a plus one $\mathcal{N} = 1$ chiral superfield χ^a, both transforming under the adjoint representation of the corresponding gauge group (on shell: $\mathbb{V}^a = \{V^a, \chi^a\}$ with $V^a = (V_\mu^a, \lambda^a)$ and $\chi^a = (\overline{\sigma}^a, \overline{\lambda}^a)$ respectively, with the complex adjoint scalar $\overline{\sigma}^a$ containing V_5^a). On the other hand, a hypermultiplet $\mathbb{H}$, the $\mathcal{N} = 2$ generalization of the familiar $\mathcal{N} = 1$ chiral multiplet, can be described in terms of two $\mathcal{N} = 1$ chiral superfields with on shell content $\mathbb{H} = \{H, H^c\}$ with $H = (h, \tilde{h})$ and $H^c = (h^c, \tilde{h}^c)$. Notice λ^a and $\overline{\lambda}^a$, as well as $\tilde{h}$ and $\tilde{h}^c$, denote two

different 2-component Weyl fermions. Additionally the bulk $\mathcal{N} = 2$ SUSY theory possesses an enhanced R-symmetry, $SU(2)_R$, which is broken to the usual $U(1)_R$ of minimal 4D $\mathcal{N} = 1$ SUSY upon compactification on $S^1/\mathbb{Z}_2$.

As explained in detail in e.g. [109], SSSB consists in breaking SUSY *non-locally* by imposing on the 5D fields a non-trivial periodicity condition under translation around the 5th dimension – in fact an $SU(2)_R$ *twist* upon translation – that is different for the bosonic and fermionic components of a given supermultiplet. As it treats fermions and boson components differently the twist breaks the remaining $\mathcal{N} = 1$ 4D SUSY. Crucially, the twist is only defined *globally*, with any local physical observable being unaffected by the twist, and SUSY is unbroken *locally*. In particular, only Feynman diagrams that stretch all the way around the (finite sized) extra dimension are sensitive to SUSY breaking, and such diagrams are finite and free from even logarithmic sensitivity to UV scales above $1/R$. This non-local nature of SSSB is the fundamental reason why SUSY breaking parameters are UV insensitive, for above the scale $1/R$ the theory *is* supersymmetric.

In this work we will exclusively focus on the case where the Scherk-Schwarz twist is maximal, namely with values on component fields ± 1, in which case the spectrum of the theory is equivalent to compactification on an $S^1/(\mathbb{Z}_2 \times \mathbb{Z}_2')$ orbifold with $R \to 2R$, and with a particular choice of $\mathbb{Z}_2 \times \mathbb{Z}_2'$ field parities[1]. In fact, for our purposes, it will be more convenient to refer to the spectrum of the model as arising from such a compactification on $S^1/(\mathbb{Z}_2 \times \mathbb{Z}_2')$, with the circle having radius $2R$. The 5D theory always locally preserves at least $\mathcal{N} = 1$ SUSY (this is true at the fixed points; in the bulk, $\mathcal{N} = 2$ SUSY is locally preserved) but, in this way of formulating SSSB, is broken down to two *inequivalent and incompatible* $\mathcal{N} = 1$ SUSYs on the two orbifold fixed-points. Thus the maximal SSSB mechanism completely breaks the remaining $\mathcal{N} = 1$ SUSYs in the effective 4D theory below the scale $\sim 1/R$, with the transition from the 5D theory to the 4D theory happening at the same scale as that at which SUSY is fully broken. We emphasise that there is *no* regime where the theory is describable as a softly broken 4D SUSY theory. In this respect, as in many others,

[1]Parities under the two $\mathbb{Z}_2$ symmetries given by $(+,+)$, $(+,-)$, $(-,+)$ and $(-,-)$ correspond to a KK spectrum of modes given by $m_n = n/R$, $(2n+1)/2R$, $(2n+1)/2R$ and $(n+1)/R$ respectively

4D theories based upon SSSB radically differ from the MSSM and its variants. The case of SSSB with maximal twist is a symmetry enhanced point, for the IR theory possesses a $U(1)_R$ R-symmetry, the details of which will be discussed in Section 3.3.3.

3.2.2 Bulk States

Going back to our toy model, depicted in Figure 3.1, we now proceed to illustrate the physics of the SSSB mechanism. The field content of this toy model is an $\mathcal{N} = 2$ vector supermultiplet that propagates in the bulk and transforms under the adjoint representation of $SU(3)$ together with a 4D $\mathcal{N} = 1$ chiral superfield $\overline{U}_3$ localized in the $y = 0$ brane. The parities under the two $\mathbb{Z}_2$ symmetries of the bulk field are chosen such that the gauge field has a massless KK 0-mode (to be identified with the 4D gluon), and can be summarized as follows: $(+,+)$ for V_μ^a, $(+,-)$ for λ^a, $(-,+)$ for $\overline{\lambda}^a$ and $(-,-)$ for $\overline{\sigma}^a$. Since these parities lead to the lightest KK mode gluinos being massive, but keep the gluons massless, SUSY is, as advertised, fully broken. From a phenomenological point of view, we will be interested in the lightest KK modes of the 5D states. The gauginos λ^a and $\overline{\lambda}^a$ obtain purely Dirac masses, and their lightest modes form a Dirac gluino with mass $M_3 = 1/2R$. The Dirac nature of the gaugino masses is a consequence of the $U(1)_R$ symmetry preserved by the maximal Scherk-Schwarz twist. The adjoint scalars and KK excitations of the 4D vector fields begin to appear at $1/R$.

In the following, it will be important to recall that a 5D gauge theory is necessarily an effective theory valid up to a scale M_*. The bulk 5D gauge couplings are dimensionful ($1/g_{I,5}^2$ has dimensions of mass; the 4D gauge couplings at the matching scale $\mu \simeq 1/R$ are given by $1/g_{I,4}^2 = \pi R/g_{I,5}^2$ up to small brane-kinetic-term corrections), and 5D perturbative unitarity bounds for g_3 requires $M_*\pi R \lesssim 25$ [132, 133, 134], or $M_* \sim 30-100$ TeV for the TeV-scale radii we consider. We will parameterise potential strong-coupling UV effects by HDOs with coefficients evaluated by the standard naive dimensional analysis (NDA) treatment of extra-dimensional theories with branes (see e.g. Section 3.2 of [135]).

For example, SUSY-preserving brane-localized kinetic terms are the lowest dimension derivative operators that can be generated, and have no analog in the 4D MSSM. For bulk vector fields they appear in the superpotential in the form

$$W \supset \frac{\tilde{Z}}{M_*} W_\alpha W^\alpha \delta(y), \tag{3.1}$$

where W_α refers to the superfield strength of the $\mathcal{N} = 1$ vector supermultiplet. The choice of bulk boundary conditions guarantees the existence of a zero mode for the gauge bosons and the absence of zero modes for the gauginos and extra $\mathcal{N} = 2$ scalar superpartners, but the spectrum of the bulk superpartners and KK excitations can be perturbed by these operators. NDA estimates for the size of these terms give $\tilde{Z} \sim \frac{3\pi}{2}$ [135] which leads to $\lesssim 10\%$ deviations in the masses of the superpartners and KK modes for $M_*\pi R \sim 25$, and brane-localized operators with transverse derivatives have comparable effects [136]. This perturbation of the spectrum can be important for the phenomenology of the heavy bulk superpartners and KK modes. However, we will mostly be focused on the spectrum and phenomenology of brane-localized superpartners and bulk zero modes, and for these purposes the effects of these perturbations of the bulk KK spectrum can be safely disregarded.

3.2.3 Brane-Localized States

Because the right-handed top is localized on the $y = 0$ brane, it has no KK excitations and need only form part of a supermultiplet, $\overline{U}_3$, consistent with the $\mathcal{N} = 1$ SUSY preserved on the brane (just as in the MSSM). At tree level, locality in 5D protects the $\overline{U}_3$ multiplet from the breaking of this $\mathcal{N} = 1$ SUSY by the incompatible $\mathcal{N} = 1'$ SUSY on the $y = \pi R$ brane, and a SUSY-breaking mass for the scalar will only be generated by SSSB at loop level.

The 1-loop contributions to the scalar mass involve SUSY breaking bulk loops of the gluons and gluinos propagating between the $y = 0$ and $y = \pi R$ brane. The 1-loop

contribution gives a *finite*, and positive, mass squared,

$$\tilde{m}^2_{U_3} = \frac{7\zeta(3)}{16\pi^4}\frac{4g_3^2}{3}\frac{1}{R^2} \approx \left(\frac{1}{10R}\right)^2 \approx \left(\frac{1}{5}M_3\right)^2. \tag{3.2}$$

The gluino is naturally five times heavier than the stop! In MSSM-like models, even a small amount of running from the messenger scale pulls the stop mass to within a factor of two of the gluino mass unless the parameters are specially tuned to give a hierarchy [45], and the comparatively large built-in gluino-stop hierarchy in SSSB is attractive. The softness of SSSB arises because loops communicating SUSY breaking must propagate between both branes and are exponentially suppressed at large 4-momenta $|p_4| > 1/(\pi R)$ [107], giving an effective messenger scale for SUSY breaking of $\sim 1/(\pi R)$.

If only SSSB effects are present, then the spectrum for both the brane-localised superpartners and the bulk superpartners is very predictive, with the dominant effects determined completely by the scale $1/R$ and the choices of boundary conditions. However, there is a generic possibility for additional sources of SUSY breaking from the dynamics of radius stabilisation which we discuss in Section 3.2.4. While this will have a small effect on the spectrum of bulk superpartners like the $SU(3)$ gauginos, we will find it can have an $\mathcal{O}(1)$ effect on the spectrum of brane-localized sfermions.

3.2.4 SUSY Breaking from Radius Stabilisation

A phenomenologically consistent theory requires that the scale of the compactified 5th dimension $\sim 1/R \sim$ TeV $\ll M_*$ must be dynamically stabilised, otherwise a massless radion mode with excluded couplings would exist in the spectrum. In pure SSSB, the only ingredients in the radion potential are supersymmetric brane tensions, a supersymmetric 5D cosmological constant (CC), and SUSY-breaking Casimir energies induced by the Scherk-Schwarz boundary conditions. Although these ingredients can stabilise the radion, they generically do so at a non-vanishing (and negative) value of the 4D CC, and additional sources of SUSY-breaking contributions to the potential are needed to lift the minimum to a vanishing 4D CC.

For example, if the brane tensions, bulk CC, and the Casimir energy of the minimal bulk matter content are the only ingredients in the stabilisation sector, then the brane and bulk tensions must break SUSY to stabilise the radius with vanishing 4D CC [137]. With non-minimal field content the radius can have meta-stable minima with SUSY preserving brane tensions, for example if the theory contains additional quasi-localized states [137], but generic stable minima with vanishing 4D CC require SUSY breaking tensions [138]. If the radius is stabilised by additional tree-level dynamics for bulk fields [139], then the brane dynamics also generically lead to brane-localized F-terms.

While it is not necessary to fully specify the radion stabilisation dynamics to study the properties of the SM fields and their superpartners in SSSB models, we find it is important to parameterise the effects of the additional sources of SUSY breaking which may be present to cancel the 4D CC. We thus study the effects of a brane-localized SUSY-breaking tension, which we parameterise by a hidden sector field X with F-term F_X. The Casimir energy of the bulk gravitational, gauge, and matter states $V_C \sim -(\pi R)^{-4}$ [137] sets the typical scale for contributions to the radion potential, and therefore sets a typical scale of $F_X \sim 1/(\pi R)^2$ to cancel against other contributions and give a vanishing 4D CC.

Operators coupling the SM superpartners to X can generate additional soft SUSY breaking masses beyond those originating at tree and loop-level from the Scherk-Schwarz boundary conditions. For example, if X is localized on the same brane as $\overline{U}_3$, then there are dimension six Kähler operators coupling these states,

$$\mathcal{K} \supset \delta(y)\frac{c_3}{M_*^2}\left(X^\dagger X \overline{U}_3^\dagger \overline{U}_3\right), \tag{3.3}$$

which gives a SUSY breaking scalar mass of size

$$\Delta\tilde{m}_{U_3}^2 \approx f_X^2\left(\frac{c_3}{16\pi^2}\right)\left(\frac{25}{\pi M_* R}\right)^2 \times \left(\frac{1}{10R}\right)^2. \tag{3.4}$$

where the dimensionless $\mathcal{O}(1)$ quantity f_X is defined as $F_X \equiv f_X/(\pi R)^2$. When this operator saturates the NDA value at the fundamental scale M_*, the contribution to

the SUSY breaking mass of $\tilde{\overline{u}}_3$ is comparable to the 1-loop minimal Scherk-Schwarz contribution Eq.(3.2).

Therefore the on-brane spectrum can be perturbed by contributions from F_X comparable to the 1-loop SSSB masses, leading to a prediction for the overall scale of masses of on-brane states with $\mathcal{O}(1)$ uncertainty. This has important phenomenological consequences for the production and decay of brane-localized superpartners, and we will also find that the extra contribution to the stop mass can be important to radiatively drive EWSB. (SUSY breaking effects from the radius stabilisation sector can also be communicated by anomaly mediation, but these are negligible compared to the direct F_X terms and the loop-level SSSB effects.)

3.3 Minimal Model

The discussion so far of the $SU(3)$ gauge multiplet and right-handed top chiral supermultiplet $\overline{U}_3$ has illustrated some key features of SSSB. The gauge multiplet propagates in the bulk, and its $\mathcal{N} = 2$ superpartners obtain large tree-level SUSY breaking masses from the maximal SUSY breaking boundary conditions, with gluinos obtaining a Dirac mass $M_3 = 1/(2R)$. The $\overline{U}_3$ multiplet is localized on the brane, and the stop squark obtains a mass from SUSY breaking gluino bulk loops $\tilde{m}^2_{U_3} \approx \left(\frac{1}{10R}\right)^2$. The stop can also obtain a comparable contribution to its mass from additional sources of SUSY breaking F_X associated with cancelling the 4D CC. In this section, we extend the previous toy model to a realistic theory that includes the absolute minimal ingredients. (Though, as we will argue, fails to give the correct physical Higgs mass in the parameter regime of low tuning. We discuss ways to correct this deficit in Section 3.4.)

3.3.1 Full matter content and gauge interactions

The results discussed in Section 3.2 can be easily generalized in order to build a model that contains the full SM matter and gauge interactions at low energies – the minimal ingredients of such model are depicted in Figure 3.2. The gauge and Higgs

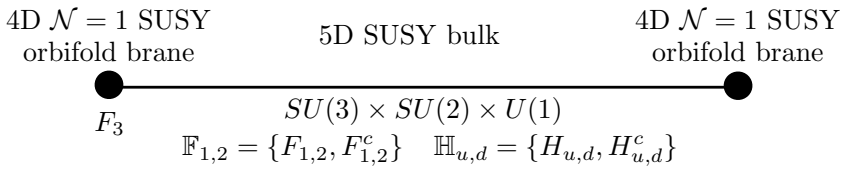

Figure 3.2: Schematic geography of natural spectrum embedded in a 5D Scherk-Schwarz model. Gauge and Higgs sectors, together with the 1st and 2nd generation of matter, propagate in the extra dimensional bulk. Each SM state is accompanied by a full 5D SUSY multiplet and KK excitations, and SUSY breaking is felt by these states at tree level from the Scherk-Schwarz boundary conditions. The 3rd generation states are localized on the brane at $y = 0$ and fill out multiplets of the locally preserved $\mathcal{N} = 1$ SUSY; SUSY breaking is communicated to these states at loop level by their interactions with the 5D gauge and Higgs fields. F_i referes to the usual $\mathcal{N} = 1$ chiral supermultiplets needed for each generation, i.e. $F_i = Q_i, \overline{U}_i, \overline{D}_i, L_i, \overline{E}_i$ $(i = 1, 2, 3)$.

sectors propagate in the bulk, with the former extended to include the full SM gauge group $SU(3) \times SU(2) \times U(1)$. As before, gauginos get Dirac masses at tree-level of size $M_{1,2,3} = 1/(2R)$ from maximal SSSB. Regarding matter content, the 1st and 2nd generations also propagate in the 5D bulk, and therefore five hypermultiplets for each of the two families are present: $\mathbb{F}_i = \{F_i, F_i^c\}$ $(i = 1, 2)$, where F_i refers to the usual $\mathcal{N} = 1$ chiral superfields present in the MSSM ($F_i = Q_i, \overline{U}_i, \overline{D}_i, L_i, \overline{E}_i$). SSSB boundary conditions are such that chiral fermions (the 1st and 2nd generation SM quarks and leptons) remain in the low energy theory whereas sfermions of the 1st and 2nd generation get tree-level masses of size $1/2R$ (degenerate with gauginos, and, as we will soon argue, Higgsinos) and the first conjugate fermion partner appears paired with the first KK excitation of the SM fermion with a Dirac mass of $1/R$. Because the first two generations appear as bulk states, the spectrum of superpartners and KK excitations can be perturbed at the $\lesssim 10\%$ level by brane-localized kinetic terms without significant consequences, just as described for the gauge multiplets.

The Higgs sector includes two hypermultiplets $\mathbb{H}_{u,d} = \{H_{u,d}, H^c_{u,d}\}$, albeit only the scalar component of H_u gets a non-zero vev, which automatically results in a SM-like Higgs sector at low energies[2] and H_d is therefore left as an inert Higgs doublet[3].

[2]This fact will become apparent once we discuss the structure of the Yukawa interactions in Section 3.3.2.

[3]In Section 3.4.3 we argue that one of variant models that accommodates the Higgs mass, $m_h \simeq$

At tree-level, an accidental global $U(1)_{H_d}$ symmetry (or $\mathbb{Z}_k$) acting on $\mathbb{H}_d$ is present, which can be chosen to remain exact. Notice that a μ-term, either in the bulk or brane-localized, can be forbidden by both the IR $U(1)_R$ symmetry (see Section 3.3.3) and the $U(1)_{H_d}$ if chosen to remain unbroken. Despite the absence of μ-terms, Higgsinos, similar to gauginos, get a Dirac tree-level mass of size $1/2R$ due to the SSSB boundary conditions, whereas *the contribution to the mass-squared parameters of the scalar components of the Higgs multiplets is strictly zero at tree-level*. This elegantly solves the μ-problem! Notice that although a few examples of 4D solutions to the μ-problem exist [140, 141, 142], SSSB with maximal twist provides a 5D realisation and in fact the choice of maximal boundary conditions corresponds to an enhanced $U(1)_R$ and $U(1)_{H_d}$ symmetry. On the other hand, as we will see in detail in Section 3.3.4, the radiative part of the tuning is irreducible, and we will of course find that at loop level the Higgs zero modes do obtain SUSY breaking masses.

The boundary conditions for all the fields that propagate in the extra dimensional bulk are summarised in Table 3.1 and are chosen to be consistent with the two inequivalent and incompatible $\mathcal{N} = 1$ SUSYs that are preserved by the gauge multiplet boundary conditions at, respectively, $y = 0$ and $y = \pi R$.

	$(+,+)$	$(+,-)$	$(-,+)$	$(-,-)$
$\mathbb{V}^a = \{V^a, \chi^a\}$	V^a_μ	λ^a	$\overline{\lambda}^a$	$\overline{\sigma}^a$
$\mathbb{H}_{u,d} = \{H_{u,d}, H^c_{u,d}\}$	$h_{u,d}$	$\tilde{h}_{u,d}$	$\tilde{h}^c_{u,d}$	$h^c_{u,d}$
$\mathbb{F}_{1,2} = \{F_{1,2}, F^c_{1,2}\}$	$f_{1,2}$	$\tilde{f}_{1,2}$	$\tilde{f}^c_{1,2}$	$f^c_{1,2}$

Table 3.1: Boundary conditions at $y = (0, \pi R)$ for 5D fields with $\pm$ corresponding to Neumann/Dirichlet. Only the $(+,+)$ fields have a zero mode, and the KK mass spectrum ($n \geqslant 0$) is: $m_n = n/R$ for $(+,+)$ fields; $(2n+1)/2R$ for $(+,-)$ and $(-,+)$; and $(n+1)/R$ for $(-,-)$. $f_{1,2}$ stands for all 1st/2nd generation fermions and $\tilde{f}_{1,2}$ their 4D $\mathcal{N} = 1$ sfermion partners. States in the last two columns correspond to the extra 5D SUSY partners.

On the other hand, the 3rd generation of matter is fully localized on the $y = 0$ brane and therefore 3rd generation sfermions only pick up masses at 1-loop from

125 GeV, involves an NMSSM-like structure with both H_u and H_d acquiring vevs. However, the simplest and most natural models for the physical Higgs mass maintain the feature that only H_u acquires a vev.

radiative corrections involving bulk fields. Notice that due to the different localization of the 1st and 2nd generations compared to the 3rd, a natural hierarchy between sfermions is present in the theory. Due to the $\mathcal{N} = 2$ structure of the bulk, Yukawa interactions between Higgs and matter supermultiplets cannot be written as bulk terms but need to be localized on the $y = 0$ brane – the detailed structure of the Yukawa couplings in MNSUSY will be explored in Section 3.3.2.

The 1-loop contributions to the scalar masses of brane localized fields, as well as to the mass-squared parameters of the scalar components of $H_{u,d}$, are given by similar expressions to Eq.(3.2) but generalized to include extra gauge and Yukawa interactions:

$$\delta\tilde{m}_i^2 \simeq \frac{7\zeta(3)}{16\pi^4 R^2}\left(\sum_{I=1,2,3} C_I(i) g_I^2 + C_t(i) y_t^2\right), \tag{3.5}$$

where $C(\overline{U}_3) = \{4/9, 0, 4/3, 1\}$, $C(\overline{D}_3) = \{1/9, 0, 4/3, 0\}$, $C(\overline{E}_3) = \{1, 0, 0, 0\}$, $C(L_3) = \{1/4, 3/4, 0, 0\}$, $C(Q_3) = \{1/36, 3/4, 4/3, 1/2\}$ and for the 0-mode Higgs scalar components $C(H_{u,d}) = \{1/4, 3/4, 0, 0\}$ [107, 108]. As mentioned in Section 3.2.3, 3rd generation squarks receive the dominant part of their mass from bulk $SU(3)$ loops, giving $\tilde{m}^2_{Q_3,U_3} \approx 1/(10R)^2$, with a splitting between Q_3 and U_3 due to the top-Yukawa and $SU(2)$ contributions. On the other hand, the right-handed stau gets the smallest 1-loop SSSB mass due to its SM gauge quantum numbers and tiny Yukawa interactions,

$$m^2_{\tilde{\tau}_R} \approx \left(\frac{1}{40R}\right)^2 \approx \left(\frac{1}{4} m_{\tilde{t}}\right)^2. \tag{3.6}$$

However, while the pure SSSB limit is an interesting spectrum to study, couplings to F_X of the form of Eq.(3.3) can contribute to the masses of all of the third generation brane-localized sfermions. This sets a scale $\tilde{m}^2_{f_3} \sim \Delta\tilde{m}^2_{U_3}$ for the third generation sfermion masses with a non-predictive ordering of the spectrum.

Although in this work we will only consider the case where the 3rd generation is fully localized on the brane whereas the 1st and 2nd propagate on the bulk, small variations of this localization, motivated for instance by flavor constraints [143], are possible provided the spectrum is *locally* in the 5th dimension free of gravitational anomalies (rather than just globally free once integrated across the extra dimension)

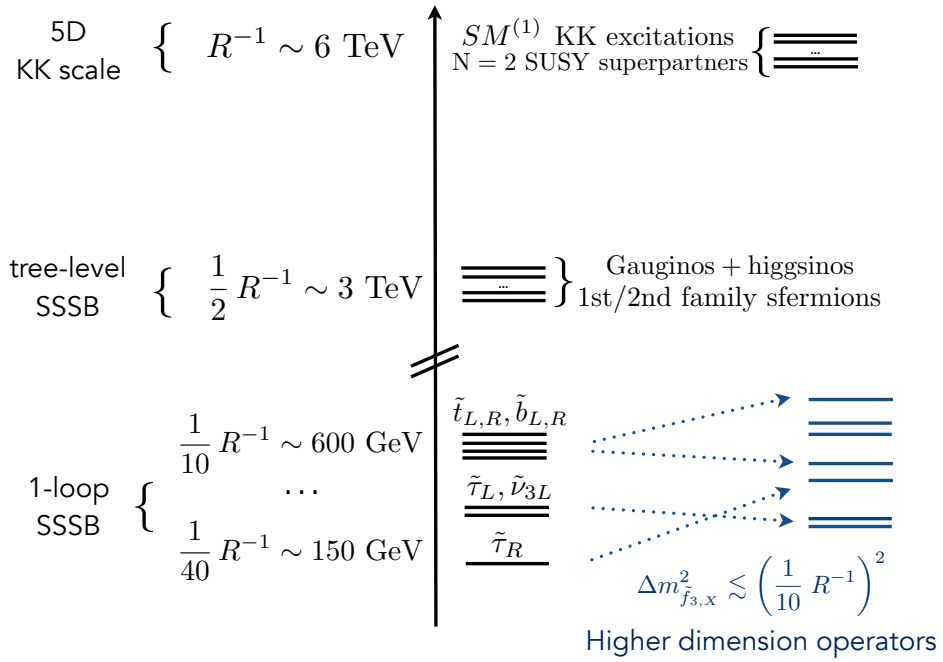

Figure 3.3: The schematic spectrum of new states in the 5D SSSB model with an example KK scale of $1/R \sim 6$ TeV. The MSSM-like gauginos and Higgsinos get tree-level SSSB Dirac masses at the scale $1/(2R)$ by pairing with their 5D conjugates. The lightest modes of the MSSM-like 1st and 2nd generation sfermions also appear at $1/(2R)$, along with their 5D SUSY conjugate scalar partners. The brane-localized 3rd generation sfermions get masses from SSSB at loop level, making the 3rd generation squarks about five time lighter than the gauginos. Although the SSSB tree-level and 1-loop contributions are fixed relative to $1/R$, higher dimensional operators can contribute to the 3rd generation sfermion masses at a similar order of magnitude and with undetermined coefficients, so that only the overall scale of the 3rd generation sfermion spectrum is predicted. At the KK scale $1/R$ the first SM KK excitations and additional 5D SUSY partners appear.

in order to avoid generating brane-localized Fayet-Illiopoulos terms [144, 145, 116], which would lead to power-sensitivity of EWSB to the UV scale. As discussed in [143], some convenient possibilities consist of allowing part of the 3rd generation multiplets to propagate in the bulk, or to make part or all the 1st and 2nd generation content brane-localized. Although the latter possibility would no longer correspond to a strictly 'natural SUSY' spectrum [42], the limits on 1st and 2nd generation squarks can still be rather weak when the gluino is heavy, and this model provides a simple realisation of the 'super-safe' Dirac gluino scenario [146].

Notice that we focus on the case where all states are either exactly localized on one of the branes or are allowed to propagate uniformly in the bulk. However, when bulk masses are allowed for the bulk hypermultiplets, states can be quasi-localized toward the $y = 0$ or $y = \pi R$ brane [147, 113]. Forbidding these masses in our model is technically natural since the bulk parity P_5 [113] (a symmetry that corresponds to a reflection about any point of the bulk in the limit $R \to \infty$) is broken only globally by the inequivalence of the $y = 0$ and $y = \pi R$ branes, but interesting properties arise in models where these mass terms are included and the 3rd generation is only quasi-localized. For example, as studied in Refs. [113, 112], the propagation of quasi-localized 3rd generation sfermions into the bulk allows small tree-level SUSY breaking masses from the Scherk-Schwarz boundary conditions in addition to the loop-level contributions from bulk multiplets. Phenomenologically, such contributions play a very similar role to the F_X shifts in the brane-localized masses we consider in this work, and most of our results apply straightforwardly to the quasi-localized models.

3.3.2 Yukawa Couplings

Up-Type Yukawas

Yukawa interactions for up-like states cannot be written as bulk interactions, since they are forbidden by the extended bulk $\mathcal{N} = 2$ SUSY, and must be generated instead

as HDOs localized on the orbifold branes. For example, Yukawa couplings for the up-like quark sector are given in the superpotential by (here $i, j = 1, 2$)

$$W \supset \delta(y) H_u \left\{ \frac{\tilde{y}_{33}}{M_*^{1/2}} Q_3 \overline{U}_3 + \frac{\tilde{y}_{3i}}{M_*} Q_3 \overline{U}_i + \frac{\tilde{y}_{i3}}{M_*} Q_i \overline{U}_3 + \frac{\tilde{y}_{ij}}{M_*^{3/2}} Q_i \overline{U}_j \right\}. \tag{3.7}$$

These bulk-brane interactions are volume suppressed, as reflected in the dimensionality of the couplings, and the 4D effective top Yukawa will naturally take a parametrically larger value than those involving the 1st and 2nd generation, due to the brane-localization of the top sector. The effective 4D Yukawas of the top, charm and up quarks can be written in terms of the fundamental 5D parameters as $y_t = \tilde{y}_{33}(M_* \pi R)^{-1/2}$ and $y_{c,u} = \tilde{y}_{22,11}(M_* \pi R)^{-3/2}$ respectively, such that

$$\frac{y_{c,u}}{y_t} = \frac{\tilde{y}_{22,11}}{\tilde{y}_{33}} \frac{1}{M_* \pi R} \sim \mathcal{O}(\frac{1}{25}) \tag{3.8}$$

for $\tilde{y}_{33} \sim \tilde{y}_{11,22}$. A natural hierarchy between y_t and $y_{c,u}$ arises due to the 3rd generation being brane-localized. For NDA estimates, $\tilde{y}_{33} \sim 4\pi$, a sufficiently large effective coupling y_t can easily be generated that is consistent with the cutoff $M_* \pi R \sim 25$ of the 5D gauge theory. Of course the extreme lightness of the up quark relative to the charm quark is *not* explained by this geometrical arrangement of multiplets, but extensions to 6D orbifold models [148] (with one dimension having a SSSB twist), or the inclusion of traditional Frogert-Nielsen style broken flavor symmetries [149] acting on the 1st and 2nd generations can accommodate/explain the peculiarities of the up quark and the other 1st generation SM fermion states and their mixings.

Non-Holomorphic Down-Type Yukawas

The fact that the scalar component of H_d does not get a vev implies that down-type quark and lepton masses and mixings cannot arise from interactions with H_d. We instead consider the case where down-type Yukawas are generated via non-holomorphic HDOs in the Kähler potential involving both H_u and the SM-singlet X. For example,

for down-type quarks

$$\mathcal{K} \supset \delta(y)(X^\dagger H_u^\dagger)\left\{\frac{\hat{y}_{33}}{M_*^{5/2}}Q_3\overline{D}_3+\frac{\hat{y}_{3i}}{M_*^3}Q_3\overline{D}_i+\frac{\hat{y}_{i3}}{M_*^3}Q_i\overline{D}_3+\frac{\hat{y}_{ij}}{M_*^{7/2}}Q_i\overline{D}_j\right\}+\text{h.c.} \quad (3.9)$$

$(i,j=1,2)$ and similarly for leptons. As for up-type Yukawa couplings, this structure implies a $1/(M_*\pi R)$ suppression of the down-type couplings of the 1st and 2nd generation compared to that of the 3rd. Moreover, the different structure of the up- and down-type Yukawas implies that the latter are naturally suppressed compared to the former. For example, the ratio of the 4D effective bottom and top couplings is naturally (taking $F_X \sim 1/(\pi R)^2$)

$$\frac{y_b}{y_t} \approx \frac{\tilde{y}_b}{\tilde{y}_t}\frac{1}{(M_*\pi R)^2} \sim 10^{-3}. \quad (3.10)$$

This strong suppression of the down-like and lepton couplings relative the up-like couplings is an interesting generic feature of our model, though $\mathcal{O}(10^{-3})$ is of course somewhat too small, so that either $\tilde{y}_b \sim 10\tilde{y}_t$ or $F_X \sim 1/R^2$, or possibly a combination, is required. Nevertheless we see that there are new opportunities for flavor model building in MNSUSY models, a large topic that is beyond the scope of this work.

Finally we remark that although we do not utilise the possibility here, Yukawa couplings for the 1st and 2nd generations may also be written as brane-localized interactions on the $y=\pi R$ brane, making use of the different $\mathcal{N}=1$ SUSY that is preserved there [115]. This would involve superpotential terms of the form

$$W \supset \delta(y-\pi R)\frac{\hat{y}_{ij}}{M_*^{3/2}}H_u^{c\prime}Q_i'\overline{D}_j' \qquad (i,j=1,2) \quad (3.11)$$

where $H_u^{c\prime}=(h_u^\dagger,\tilde{h}_u^c)$, and $F_i'=(\tilde{f}_i^\dagger,f_i)$ for $F=Q,\overline{D}$ (the unusual combinations of multiplet components being due to the different $\mathcal{N}=1$ SUSY on the $y=\pi R$ brane). A third possibility for flavor arises if exact localization of the 3rd generation is given up and, instead, one assumes it is exponentially localised towards the $y=0$ brane [113] (this may be achieved by writing sufficiently large bulk masses for the 3rd generation states [147]). In this case, down-type Yukawa couplings for the 3rd

generation may also be written as localized in the $y = \pi R$ brane, and the 4D effective couplings would be exponentially suppressed compared to the up-type ones which remain localised to the $y = 0$ brane.

In summary, because the Yukawa couplings can be realised with only a vev for H_u, the structure of the Higgs sector can be substantially different than in the MSSM. We will focus mostly on this limit where H_d does not obtain a vev and behaves as an inert doublet, corresponding to an enhanced $U(1)_{H_d}$ (or $\mathbb{Z}_k$) symmetry of the theory. Note that despite the fact that $\langle H_u^0 \rangle / \langle H_d^0 \rangle \to \infty$ the physics differs substantially from the $\tan\beta \to \infty$ limit of the MSSM. In particular rare flavor processes are *not* enhanced by powers of $\tan\beta$ even though the Higgs sector itself is realising the $\tan\beta \to \infty$ limit.

3.3.3 $U(1)_R$ Symmetry and Dirac Gauginos

The choice of bc's required for maximal SSSB preserves a $U(1)$ subgroup of the $SU(2)_R$ R-symmetry present in $\mathcal{N} = 2$ SUSY so long as gravitational interactions are ignored. The R-charges of the different fields are shown in Table 3.2.

$\mathcal{N} = 1$ superfield	Boson	Fermion
$V^a = (V_\mu^a, \lambda^a)$	0	+1
$\Sigma^a = (\overline{\sigma}^a, \overline{\lambda}^a)$	0	−1
$H_{u,d} = (h_{u,d}, \tilde{h}_{u,d})$	0	−1
$H_{u,d}^c = (h_{u,d}^c, \tilde{h}_{u,d}^c)$	+2	+1
$F_{1,2,3} = (\tilde{f}_{1,2,3}, f_{1,2,3})$	+1	0
$F_{1,2}^c = (\tilde{f}_{1,2}^c, f_{1,2}^c)$	+1	0
$X = (x, \tilde{x})$	+2	+1

Table 3.2: R-charges of relevant fields present in the theory (in $\mathcal{N} = 1$ language). The pairs $(\lambda^a, \overline{\lambda}^a)$ and $(\tilde{h}_{u,d}, \tilde{h}_{u,d}^c)$ have opposite R-charges and partner resulting in Dirac gaugino and Higgsino masses. Note that $R(h_{u,d}) = R(F_X) = 0$.

This $U(1)_R$ symmetry ensures that the two Weyl fermions present in an $\mathcal{N} = 2$ vector supermultiplet (λ^a and $\overline{\lambda}^a$) and in Higgs hypermultiplets ($\tilde{h}_{u,d}$ and $\tilde{h}_{u,d}^c$) pair into Dirac fermions, giving Dirac gauginos and Higgsinos with tree-level masses of

size $1/(2R)$. Moreover, A-terms are forbidden because of the exact R-symmetry in maximal SSSB, in contrast to models with a small R-symmetry twist, which generate large A-terms [130]. Notice that the remaining R-symmetry is not broken by the vev of h_u (or of h_d if it was non-zero), by Yukawa interactions, or by the non-zero vev of the F-term of X.

However, once supergravity (SUGRA) is included into the picture, the hitherto exact R-symmetry can be broken by anomaly mediated contributions to Majorana gaugino masses, sfermion soft masses and A-terms appear, all of them proportional to the vev of the SUGRA conformal compensator F-term, F_ϕ (see e.g. [150, 151]). We expect $F_\phi \sim \frac{1}{R}\frac{1}{(\pi R M_g)^3}$ [138] and therefore the effects of anomaly mediated contributions to SUSY breaking parameters are highly suppressed compared to those from SSSB or from HDOs involving F_X, even for $M_g \sim M_*$. Consequently, in the following we ignore R-symmetry breaking effects arising from SUGRA.

It is worth emphasising the contrast between Dirac gauginos in maximal SSSB and in 4D models that contain partial $\mathcal{N} = 2$ SUSY [152]. In 4D, the adjoint scalars present phenomenological difficulties: their imaginary components can be tachyonic unless protected from certain operators [153] and the real components can remove the D-term contributions to the Higgs quartic unless gauginos obtain Majorana masses, thus breaking the R-symmetry [152, 140]. On the other hand, in 5D maximal SSSB both the real and imaginary components of the scalar are lifted without breaking the R-symmetry—the scalar adjoints obtain a mass through the SUSY Stueckelberg mechanism with the KK gauge bosons [154], which removes the tachyons, introduces pure Dirac masses for the gauginos, and preserves the D-term contributions to the Higgs quartic. The qualitative difference between the 5D and 4D implementations of Dirac gaugino masses arises from the fact that partial breaking of $\mathcal{N} = 2$ to $\mathcal{N} = 1$ is a possibility in the former but forbidden in the latter. In 4D models with Dirac gauginos, the logarithmic sensitivity to the messenger scale can also be removed and similar hierarchies can be attained, but a logarithmic sensitivity to the mass of the adjoints remains [152, 140].

Notice that if the radius stabilisation sector broke the R-symmetry then A-terms would be generated through couplings to F_X, and their sizes would be comparable

to 3rd generation sfermion masses (see Eqs.(3.3) and (3.4)). Similarly, gluino brane-localized Majorana masses would be generated, but they would be volume suppressed (due to the brane-bulk overlap factor $1/(M_*\pi R)$) and would only amount to a small perturbation on the large tree-level gluino Dirac mass $M_3 = 1/(2R)$.

3.3.4 The Scale of EWSB

In the absence of SSSB loop contributions and HDOs, the Higgs scalar zero modes are exactly massless and their quartic interactions are given by the standard tree-level MSSM D-terms. Radiative contributions are therefore crucial both to connect the scale of EWSB to the SSSB scale $1/R$ and to determine the viability of a $m_h \approx$ 125 GeV Higgs.

The structure of the corrections to the Higgs mass-squared parameter in comparison with the standard MSSM results is most easily organized in the framework of matching the 5D theory to an effective 4D theory, and this approach will make incorporating additional contributions to the Higgs potential from extended sectors and other sources of SUSY breaking particularly simple. The 5D SUSY theory valid at scales $\gtrsim 1/R$ can be matched to an effective 4D theory containing only the SM (including the Higgs zero modes) and 3rd generation superpartners at lower energies. The leading contributions to the Higgs potential in this effective theory are similar to those of the MSSM, and the properties of the 5D physics are all encapsulated in the matching. As is well known, there are further important log-enhanced IR corrections to the Higgs potential that can be encapsulated by integrating out the scalars at scale $m_{\tilde{t}}$ and running to match the measured SM couplings at the Z and top poles. In the case where only H_u gets a vev, we find that there is a natural hierarchy between the EWSB and SSSB scales, with $v \sim 1/(20R)$. However, the radiative potential does not favor EWSB and additional contributions from HDOs, as discussed later, are required.

To be concrete, our calculation of the H_u zero-mode mass-squared parameter, $m^2_{H_u}$, in the effective theory includes a 1-loop EW contribution, $m^2_{H_u,EW}$, and a two-loop Yukawa-mediated piece, $m^2_{H_u,y_t}$, of order $\sim y_t^4, g_3^2 y_t^2$ that also includes three-loop

leading log terms $\sim (y_t^6, y_t^4 g_3^2, y_t^2 g_3^4) \times \log(x)^2$ where $\log(x) = \log\left(\frac{\tilde{m}_t}{1/\pi R}, \frac{m_t}{\tilde{m}_t}, \frac{m_t}{1/\pi R}\right)$ are treated as formally of the same order. The 1-loop EW piece can be understood by integrating out the bulk Higgs and gauge KK modes at scale $1/(\pi R)$, which generates the 1-loop positive mass-squared parameters in the effective theory given in Eq.(3.5), and for the Higgs is a positive contribution dominated by the $SU(2)$ sector,

$$m^2_{H_u,EW} = \frac{7\zeta(3)}{16\pi^4 R^2}\left(\frac{1}{4}g_1^2 + \frac{3}{4}g_2^2\right) \approx \frac{7\zeta(3)}{16\pi^4 R^2}\frac{3}{4}g_2^2 \sim \left(\frac{1}{20R}\right)^2 \tag{3.12}$$

Matching to the effective theory at 2-loops using the fixed order results of Ref. [112] generates the non-logarithmically enhanced $(y_t^4, g_3^2 y_t^2)$ contribution to $m^2_{H_u,y_t}$. Running the soft masses down from $1/\pi R$ to the stop threshold, and running and matching the gauge couplings down through the stop threshold to the measured SM couplings at the top pole generates the remaining 2-loop and 3-loop leading log contributions. As the log enhanced contributions are generated from running of the soft masses just as in the MSSM, it is not surprising that loops of stops generate a negative contribution to the Higgs mass of comparable size to that expected from a stop of similar mass in the MSSM with a low mediation scale. The three-loop leading log terms are an important contribution, giving a $\sim 50\%$ shift in the result compared to the fixed order calculation of Ref. [112], which can be understood as due to the significant running of y_t and g_3 between $1/R$ and m_t and the quartic dependence of the fixed-order result on these couplings. To within the theoretical error, we find the full result is numerically well approximated by evaluating the usual 1-loop MSSM formula at scale $\mu = 1/(\pi R)$, using the 1-loop stop mass given by Eq.(3.5) and the Yukawa and gauge couplings all evaluated at the $\overline{\text{DR}}$ value given by SM running to the scale $\mu = 1/(\pi R)$,

$$m^2_{H_u,y_t} \approx -\frac{3y^2_{t,SM}(\mu)}{16\pi^2}\left[\tilde{m}^2_{Q_3}(\mu) + \tilde{m}^2_{U_3}(\mu)\right]\log\left[\frac{\mu^2}{\tilde{m}_{Q_3}(\mu)\tilde{m}_{U_3}(\mu)}\right]\Bigg|_{\mu=1/\pi R}. \tag{3.13}$$

The results of the full numerical evaluation of our calculation of EWSB are summarized in Figure 3.4. As shown in Figure 3.4, these minimal contributions given by the pure SSSB contributions to $m^2_{H_u}$ do *not* lead to EWSB; the positive 1-loop EW contribution Eq.(3.12) is about twice the size of the negative radiative contribution

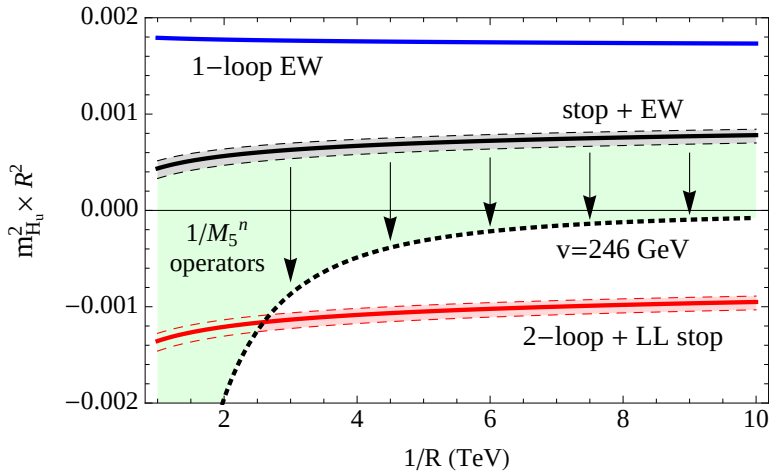

Figure 3.4: Contributions to the Higgs soft mass $m^2_{H_u}$ in units of $1/R^2$. The positive 1-loop EW contribution (blue) and the negative 2-loop + leading log top-stop sector contribution (red) combine to give a positive, but tiny, mass squared (black), implying that the minimal model is close to EWSB. Contributions from HDOs can lead to successful EWSB, indicated by the dotted black curve. The dashed bands show the uncertainty for $\overline{\text{MS}}$ top mass $m_t(M_t) = 160^{+5}_{-4}$ GeV.

from the Yukawa coupling Eq.(3.13).

Nevertheless, the size of the resulting Higgs mass-squared parameter is tiny compared to the basic SUSY-breaking scale, $1/(\pi R)$, of the theory, with $m^2_{H_u} R^2 \sim 5{\cdot}10^{-4}$, and thus the theory is very close to criticality with small perturbations to the basic picture being capable of triggering EWSB with the correct vev. Specifically we find an EWSB vacuum with the observed vev $\langle H_u \rangle = v/\sqrt{2}$ ($v \approx 246$ GeV) is obtained by taking into account HDOs that couple the stop (and to a lesser extent H_u) to SUSY breaking effects in the radius stabilisation sector, as described in Section 3.2.4.

The operators coupling directly to H_u, suppressed by scale M_*, are of the form

$$\mathcal{K} \supset \delta(y) \frac{c_H}{M_*^3} X^\dagger X H_u^\dagger H_u, \tag{3.14}$$

and give a mass-squared of size

$$\Delta m^2_{H_u,X} \approx f_X^2 \left(\frac{c_H}{24\pi^2}\right) \left(\frac{25}{M_* \pi R}\right)^3 \times \left(\frac{1}{25R}\right)^2. \tag{3.15}$$

For NDA values of coefficients, this contribution is of the same order as the radiative piece from the bulk EW sector given in Eq.(3.12). Moreover, F_X can also feed into the Higgs potential radiatively by shifting the stop masses, as can be seen from Eq.(3.3). The shift in $\tilde{m}^2_{Q_3,U_3}$ due to F_X is enhanced by a factor of $M_*\pi R$ because there is no volume suppression, since the stops are brane localised, and this soft mass feeds in to $m^2_{H_u}$ with the usual large 1-loop coefficients, although now including a logarithmic sensitivity to the UV scale M_*,

$$\Delta m^2_{H_u,\tilde{t}} \approx -\frac{3y_t^2}{16\pi^2}\log\left(\frac{M_*^2}{\tilde{m}_{Q_3}\tilde{m}_{U_3}}\right)(\Delta\tilde{m}^2_{Q_3}+\Delta\tilde{m}^2_{U_3}). \tag{3.16}$$

This contribution is enough to drive EWSB when coupling to F_X increases $m^2_{\tilde{t}}$ from the pure SSSB value of $m_{\tilde{t}} \sim 1/(10R)$ to roughly $m_{\tilde{t}} \sim 1/(8R)$. This contribution can also be viewed as a larger than NDA coefficient for c_H in Eq.(3.14) generated from the operator Eq.(3.3) when running to low scales.

Therefore we can use the $\mathcal{O}(1)$ freedom in the coefficients of the F_X contributions to the squark masses to drive EWSB. The natural scale for the soft mass set by SSSB is $m^2_{H_u} \approx 1/(20R)^2$, and the correct value for EWSB is obtained by including the F_X contributions to the Higgs potential. These two cancelling contributions are naturally of comparable size, and it is only when $1/R \gg 4$ TeV that the residual value of $m^2_{H_u}$ is too large and a tuning is introduced to cancel the two contributions to give the observed weak scale. Phenomenologically, this approach has very similar effects to giving the 3rd generation squarks small tree-level SSSB masses by quasi-localization [113, 112].

3.3.5 The SM-like 125 GeV Higgs

The radiative contributions to the Higgs pole mass are IR dominated, and at leading-log match exactly the MSSM radiative corrections. We include the 1-loop leading-log (LL) $g^2_{1,2}\log(x)$ EW contributions to the Higgs potential and up to the two-loop next-to-leading-log (NLL) contributions from the stop sector $(y_t^4, y_t^4 g_3^2, y_t^6) \times \log(x)$. We define an effective Higgs quartic interaction by $m_h^2 = V''_{\text{eff}}(|H_u|^2)v^2 \equiv 2\hat{\lambda}v^2$, with

$\langle H_u \rangle = v/\sqrt{2}$ and the SUSY tree-level value $\hat{\lambda}_0 = \frac{g_1^2+g_2^2}{8}$. The leading 1-loop EW contribution $\delta\hat{\lambda}_{\rm EW}$ has at order $(g_{1,2}^4, g_{1,2}^2 y_t^2) \times \log(m_{\tilde{t}}^2/m_t^2)$ the same form as the MSSM values given in Ref. [155], and because of the structure of the Higgs sector there are no Higgs mixing effects and the y_b-dependent corrections are negligible (unlike the MSSM at large $\tan\beta$). The leading EW piece reads

$$\delta\hat{\lambda}_{\rm EW} = -\frac{3y_t^2}{64\pi^2}(g^2+g'^2)\log\left[\frac{\hat{m}_{\tilde{t}}^2}{m_t^2}\right] \tag{3.17}$$

and the stop contribution is given by the fixed-order calculation in Ref. [112] as

$$\begin{aligned}
\delta\hat{\lambda}_{y_t} \;=\; & \frac{3\hat{y}_t^4}{16\pi^2}\log\left[\frac{\hat{m}_{\tilde{t}}^2}{m_t^2}\right] + \frac{6\hat{y}_t^4}{(16\pi^2)^2}\Bigg\{ y_t^2\left(\frac{3\hat{y}_t^2}{4}\log\left[\frac{\hat{m}_{\tilde{t}}^2}{m_t^2}\right]^2 + \hat{y}_t^2\log\left[\frac{\hat{m}_{\tilde{t}}^2}{1/(\pi R)^2}\right]^2\right) \\
& -\frac{8g_3^2}{3}\left(\frac{1}{2}\log\left[\frac{\hat{m}_{\tilde{t}}^2}{m_t^2}\right]^2 - 2\log\left[\frac{m_t^2}{1/(\pi R)^2}\right]^2 - 2\log\left[\frac{m_t^2}{1/(\pi R)^2}\right]\log\left[\frac{\hat{m}_{\tilde{t}}^2}{1/(\pi R)^2}\right]\right) \\
& +\frac{\hat{y}_t^2}{4}\left(11\log\left[\frac{\hat{m}_{\tilde{t}}^2}{1/(\pi R)^2}\right] + 3\log\left[\frac{m_t^2}{1/(\pi R)^2}\right]\right) \\
& -\frac{8g_3^2}{3}\left((2-12\log(2))\log\left[\frac{\hat{m}_{\tilde{t}}^2}{m_t^2}\right] - 3\log\left[\frac{m_t^2}{1/(\pi R)^2}\right]\right)\Bigg\}
\end{aligned} \tag{3.18}$$

where we have taken equal masses $\tilde{m}_{Q_3}^2 \approx \tilde{m}_{U_3}^2$ for the stops, which holds to a good approximation in the pure SSSB model, and define $\hat{y}_t = \frac{m_t}{v/\sqrt{2}}$ and $\hat{m}_{\tilde{t}}^2 = \tilde{m}_{Q_3,U_3}^2 + m_t^2$, with m_t the pole mass of the top. Here we briefly describe the origin of these terms in the language of matching to the effective 4D theory to illuminate the connection with MSSM results and to clarify how we will incorporate other corrections beyond the minimal SSSB spectrum.

To obtain the two-loop NLL result, the heavy KK modes can be integrated out at 1-loop at the scale $1/(\pi R)$, generating the 1-loop 3rd generation sfermion masses and Higgs soft mass in the effective theory, and non-supersymetric shifts in the Yukawa-like couplings of the top and the stop. These threshold corrections to the Yukawa-like couplings are sensitive to the 5D physics, and are responsible for the deviations from the MSSM result starting at two-loop NLL order. The one and two-loop LL terms are

generated by running through and integrating out the stop thresholds then running to match the SM couplings, and clearly will have the same form as the MSSM with heavy Higgsinos and gauginos. When the stop masses are increased by HDOs involving F_X as given by Eq.(3.4), the effect on the radiatively generated quartic can be completely included at this order by replacing $\tilde{m}^2_{Q_3,U_3} \to \tilde{m}^2_{Q_3,U_3\ (\text{SSSB})} + \Delta m^2_{Q_3,U_3}$ in Eq.(3.18).

Thus we find that the Higgs mass prediction in the pure SSSB model, shown in Figure 3.5, matches well with the large $\tan\beta$ MSSM predictions. Unfortunately this implies that stops $\gtrsim 3$ TeV are necessary to obtain $m_h \approx 125$ GeV, corresponding to a compactification scale $1/R \gtrsim 30$ TeV. At such large stop masses the natural value for the Higgs vev is far above the measured weak scale, and the theory will be tuned to the few percent level. Although this is significantly less tuning than typical MSSM-like theories with comparable stop masses, we will be motivated to consider extensions that can increase the Higgs pole mass without requiring such large contributions from the stop sector. The stops can also be lighter if large A-terms are generated, $A_t^2 \gtrsim m_{\tilde{t}}^2$, which can occur if the X couplings break the R-symmetry. Because the leading radiative contributions to the Higgs pole mass are generated in the effective 4D theory containing the third generation squarks, the effects of including such A-terms can be incorporated using the appropriate 1-loop MSSM formula, and the range of viable parameters is similar to the MSSM. However, when large A-terms are generated by F_X, they feed into the Higgs soft mass with large logarithms sensitive to the fundamental scale M_* and will dominate the tuning for $A_t^2 \gtrsim m_{\tilde{t}}^2$, removing the UV insensitivity that is one of the principle advantages of SSSB and leading to little improvement in the tuning. Instead, we focus in the following sections on extensions to the minimal field content that can increase the Higgs mass for light stops without substantially effecting the tuning or reintroducing further log sensitivity to M_*.

Notice that HDOs coupling H_u to SUSY breaking effects in the radius stabilisation sector, i.e. to F_X, can also contribute to the effective Higgs quartic, with the leading term being a brane-localized Kähler operator of the form

$$\mathcal{K} \supset \delta(y)\frac{c_\lambda}{M_*^6} X^\dagger X (H_u^\dagger H_u)^2 \tag{3.19}$$

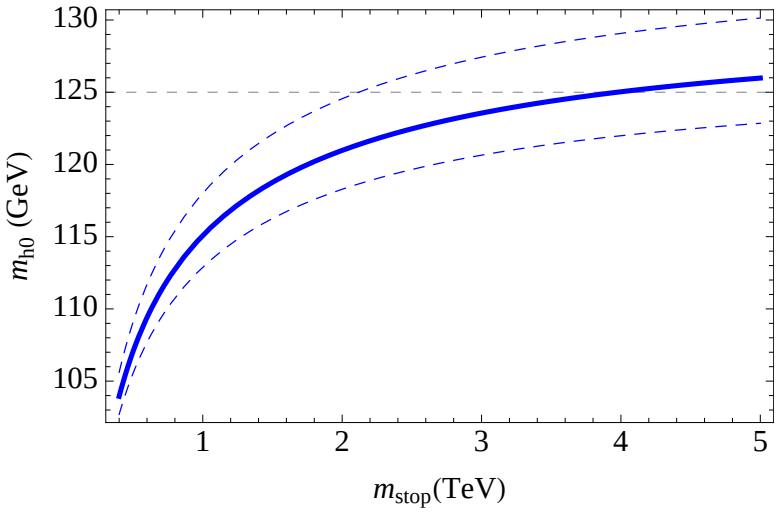

Figure 3.5: Higgs pole mass in pure SSSB with two-loop NLL calculation of Yukawa contributions and 1-loop EW contributions. The horizontal axis is the lightest stop soft mass. Here we have taken the F_X contribution to the stop masses to vanish, so the stop mass is related to the compactification radius $1/R$ giving $m_{\tilde{t}} \approx \frac{1}{10}\frac{1}{R}$. The dashed bands show the uncertainty for $\overline{\text{MS}}$ top mass $m_t(M_t) = 160^{+5}_{-4}$ GeV.

that results in a contribution to the quartic

$$\delta\hat{\lambda}_X \sim 10^{-4}\ f_X^2 \frac{c_\lambda}{(24\pi^2)^2}\left(\frac{25}{M_*\pi R}\right)^6, \tag{3.20}$$

which can be related to the F_X contribution to the H_u mass-squared parameter in Eq.(3.14) as (for NDA values of the corresponding coefficients)

$$\delta\hat{\lambda}_X \sim 10^{-4}\left(\frac{25}{M_*\pi R}\right)^3 \frac{\Delta m^2_{H_u,X}}{1/(25R)^2}. \tag{3.21}$$

Thus, even for an NDA value of the coefficient ($c_\lambda \approx (24\pi^2)^2$), the HDO in Eq.(3.19) results in a negligible contribution to the effective Higgs quartic, unless SUSY breaking from F_X is so large that it dominates completely over the SSSB effects in the Higgs potential, leading to a large tuning of the weak scale.

3.4 Extended Sectors

This sections describes extensions to the minimal model which can lift the Higgs pole mass to $m_h \approx 125\text{GeV}$.

3.4.1 Vector-like Fermions Extension

A simple mechanism to raise the physical Higgs mass m_h consists in adding vector-like (VL) pairs of superfields with Yukawa couplings to the Higgs. As noted in [156], a contribution to the Higgs quartic coupling, and therefore to m_h, will be radiatively generated with size depending on the mass gap between the fermion and scalar components and the size of the new Yukawa. We consider the simple case of adding two colorless $SU(2)_L$ doublets and singlets localized on one of the branes. The extra field content, in $\mathcal{N}=1$ superfield notation, with their SM quantum numbers is the following:

$$\begin{aligned} \tilde{L} &: (\mathbf{1},\mathbf{2},-Y) \qquad & \tilde{E} &: (\mathbf{1},\mathbf{1},Y+1/2) \\ \tilde{L}' &: (\mathbf{1},\mathbf{2},Y) \qquad & \tilde{E}' &: (\mathbf{1},\mathbf{1},-Y-1/2)\ . \end{aligned} \tag{3.22}$$

With this field content, we can write a superpotential for the VL sector as follows[4]:

$$W \supset \delta(y)\left\{\frac{\tilde{k}_u}{M_*^{1/2}} H_u \tilde{L}'\tilde{E}' - \mu_L \tilde{L}'\tilde{L} - \mu_E \tilde{E}'\tilde{E}\right\}\ , \tag{3.23}$$

where we have chosen to localise the new states on the $y=0$ brane (albeit the following discussion applies equally to the case of localization in the $y=\pi R$ brane), and the 4D effective Yukawa coupling k_u is given in terms of the fundamental parameters as $k_u = \tilde{k}_u(\pi R M_*)^{-1/2}$.

The new field content consists of two Dirac fermions with electric charge $\pm(Y+1/2)$ that couple to the Higgs and one Dirac fermion with charge $\pm(Y-1/2)$ that does not, together with their corresponding scalar partners. We will concentrate in the case $Y=1/2$, which means that the mass eigenstates are two fermions with

[4] A Yukawa coupling involving $\tilde{L}$ and $\tilde{E}$ could also be written in the same way as lepton and down-type quark Yukawas. However, as we saw in Section 3.3.2, their size is parametrically suppressed compared to the up-type ones and therefore we neglect it here for simplicity.

charge ± 1 (τ_1', τ_2') and one neutral fermion (ν') whose tree-level mass is equal to μ_L. For $\mathcal{O}(1)$ values of the 4D effective coupling k_u, the masses of the new fermions are such that $m_{\tau_1'} < m_{\nu'} = \mu_L < m_{\tau_2'}$. For simplicity, we impose an extra $\mathbb{Z}_2$ symmetry on these new states to avoid their mixing with SM leptons[5]. For obvious reasons, we will refer to this version of the model as the *VL-lepton* scenario.

A simple way to dynamically generate the VL masses μ_L and μ_E is to introduce a SM singlet in the 5D bulk, K, that couples to the new VL states as follows:

$$W \supset \delta(y)\frac{\tilde{\lambda}_K}{M_*^{1/2}}K(\tilde{L}'\tilde{L} + \tilde{E}'\tilde{E}) \ . \tag{3.24}$$

At 1-loop, this interaction contributes to the soft masses of the scalar partners of the VL states. Including all 1-loop contributions, these are given by the usual expression:

$$\delta\tilde{m}_i^2 \simeq \frac{7\zeta(3)}{16\pi^4 R^2}\left(\sum_{I=1,2,3} C_I(i)g_I^2 + C_{k_u}(i)k_u^2 + C_{\lambda_K}(i)\lambda_K^2\right) \tag{3.25}$$

with $C(\tilde{L}) = \{1/4, 3/4, 0, 0, 1/2\}$, $C(\tilde{L}') = \{1/4, 3/4, 0, 1/2, 1/2\}$,
$C(\tilde{E}) = \{1, 0, 0, 0, 1/2\}$, $C(\tilde{E}') = \{1, 0, 0, 1, 1/2\}$ [107, 108] and where
$\lambda_K = \tilde{\lambda}_K(\pi R M_*)^{-1/2}$ is the 4D effective coupling. In turn, at two-loop order, the VL states generate a scalar potential for the K field, in much the same way as the brane localized top sector does for the Higgs, with a negative soft mass and an $\mathcal{O}(1)$ quartic coupling. This results in the 4D-normalized scalar component of K getting a vev $\langle k\rangle \sim 10^2$ GeV, which leads to VL masses arising from Eq.(3.24) as

$$\mu_L = \mu_E = \frac{\tilde{\lambda}_K}{(\pi R M_*)^{1/2}}\langle k\rangle = \lambda_K\langle k\rangle \equiv \mu_{VL} \ . \tag{3.26}$$

We take $\lambda_K \approx 2.0$ at the scale of the VL masses, which is consistent with a value for λ_K equal to the NDA limit at scale M_*. From now on, we also fix $\mu_{VL} = 350$ GeV for illustration, a reasonable value given the size of λ_K and $\langle k\rangle$. Figure 3.6 shows the extra field content and its location. Notice that this extension of the model that

[5]The $\mathbb{Z}_2$ symmetry can be slightly broken to allow the new states to decay.

includes a bulk SM-singlet K coupling to the VL fermions as specified in Eq.(3.24) is particularly appealing because it generates both VL masses by the above mechanism, and, at 1-loop, SUSY breaking masses for the scalar components. This allows us to localise the VL states in a different brane from the SM-singlet, X, avoiding SUSY breaking contributions to the scalar masses from F_X that would result in the Higgs mass-squared parameter being UV sensitive (*cf*, Section 3.3.4).

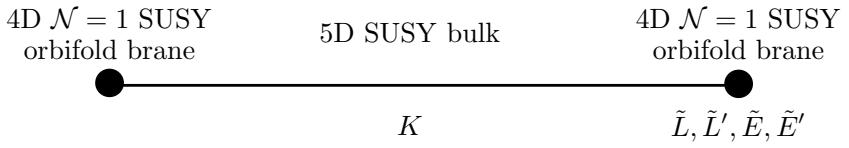

Figure 3.6: Extra field content needed to implement the VL lepton variation. A 5D bulk SM singlet hypermultiplet K and a pair of vector-like $SU(2)_L$ doublets and singlets on the $y = 0$ brane.

In order to compute the contribution from the VL sector to the Higgs mass we use the 1-loop effective potential formalism. The result will depend mostly on the size of the gap between fermion and scalar masses, i.e. on $1/R$, and crucially on the size of the new Yukawa coupling, as $\delta m_h^2 \propto k_u^4$. We add this contribution from the VL sector to the one from the top-stop sector discussed in Section 3.3.5.

As well as a contribution to the Higgs quartic coupling, the new VL states also contribute to the Higgs mass-squared parameter, and therefore somewhat affect the physics of EWSB. Specifically, Figure 3.7 shows the different contributions to the soft mass-squared of the Higgs, showing how the new sector gives a negative contribution to m_H^2 of approximately the same size as that from the top-stop sector, leading to a total contribution closer to the true EWSB value compared to the previous version of the model, *cf*, Figure 3.4. As a rather conservative and intuitive way of measuring the level of fine tuning we adopt the following definition:

$$\Delta = \left\{ \left(\frac{m_{H,\mathrm{EW}}^2 + m_{H,\mathrm{top}}^2}{m_{H,\mathrm{exp}}^2} \right)^2 + \left(\frac{m_{H,\mathrm{VL}}^2}{m_{H,\mathrm{exp}}^2} \right)^2 \right\}^{-1/2} \tag{3.27}$$

where $m_{H,\mathrm{top}}^2$ is the contribution to the Higgs soft mass from the top sector, $m_{H,\mathrm{VL}}^2$

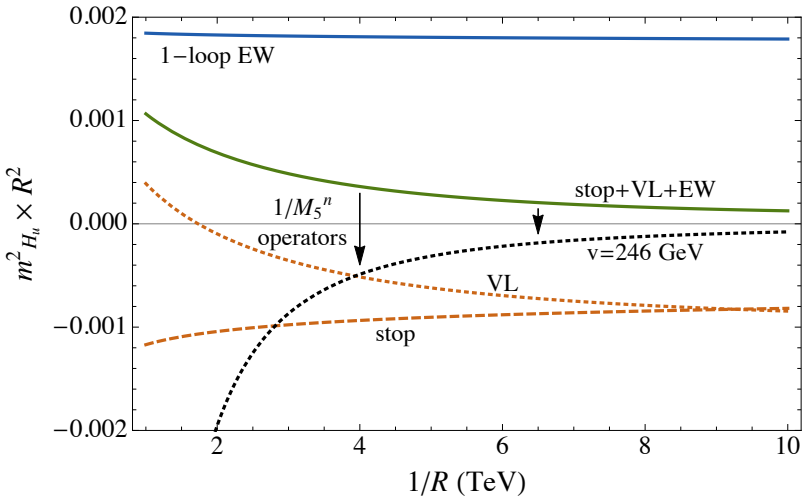

Figure 3.7: Contributions to the Higgs soft mass squared, m_H^2, normalized to $1/R^2$ as a function of $1/R$. The blue line represents the 1-loop contribution from the EW sector, the dashed orange line the contribution from the top-stop sector and the dotted orange line that from the VL sector. The green line is the sum of all three together and the dotted black line represents the correct value of the Higgs soft mass for successful EWSB (as achieved after adding the contributions from HDOs).

the contribution from the VL sector and $m^2_{H,\text{exp}} \approx -(125\text{ GeV})^2/2$ the experimentally measured value.

Finally, Figure 3.8 shows the region of parameter space where one can achieve a 125 GeV Higgs together with the level of fine tuning, quantified as specified in Eq.(3.27). It is apparent that a model with the correct value of the Higgs mass and $\sim 10\%$ tuning is possible in the VL-lepton variation.

3.4.2 $U(1)'$ Extension

If the Higgs is charged under an additional gauge sector, the D-term generates additional contributions to the Higgs quartic that decouple as $\sim m^2_{\text{soft}}/f^2$, where f is the scale of the gauge group breaking and m^2_{soft} is the SUSY breaking mass coupling to the multiplet breaking the gauge group [157, 158, 159]. We will focus on the simple case of a new bulk $U(1)'$ gauge group with gauge coupling $g_{X,5} \equiv g_{X,4}\sqrt{\pi R}$. Collider and precision observables constrain the Z' mass to be $M_V \gtrsim 3$TeV, which means

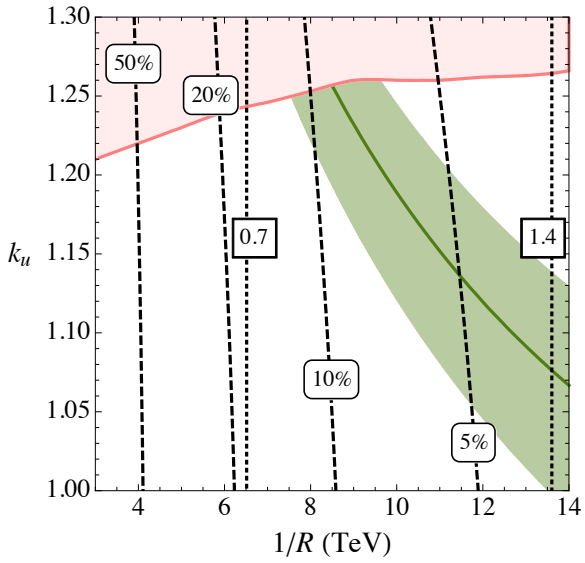

Figure 3.8: The green area represent the region of parameter space where a 125 GeV mass for the Higgs is predicted, within the combined theoretical and experimental (mainly on y_t) uncertainty. The pink area is excluded by precision electroweak constraints, forbiding the region with too large k_u. Dashed lines represent contours of given tuning, as specified in the labels, and dotted lines denote the regions where stop masses are 0.7 TeV (around the current LHC limit) and 1.4 TeV (approximately the maximum stop mass to be probed by LHC14).

SUSY breaking must be felt at scales $\sim 1/R$ for a sizeable non-decoupling effect. A simple model where this occurs has the $U(1)'$ breaking driven by on-brane dynamics for bulk hypermultiplets ϕ_1, ϕ_2 that feel tree-level Scherk-Schwarz SUSY breaking and have charge $Q_\phi = \pm 1$ under the $U(1)'$. To be concrete we identify the $U(1)'$ with T_{3R} normalized to $Q_{H_{u,d}} = \pm 1/2$, introducing sterile neutrinos to cancel anomalies. We find that the Higgs pole mass can be lifted to 125 GeV with $g_{X,4} \approx g_2$ and $M_Z' \sim 1/R$ without substantially increasing the tuning of the weak scale.

In detail, a vev for $\phi_{1,2}$ can be induced by an interaction with a brane-localized singlet,

$$W \supset \frac{\tilde{\lambda}_S}{M_*} S \left(\phi_1 \phi_2 - \frac{f^2}{\pi R} \right) \delta(y) \ . \tag{3.28}$$

If the scalar components of ϕ did not have SUSY-breaking boundary conditions, this potential would introduce a SUSY preserving vev for $\phi_{1,2}$ and the D-term would

decouple. In the presence of the SUSY breaking boundary conditions, the boundary action can induce a SUSY breaking background and the D-term does not decouple. Some intuition for the behavior of $\phi_{1,2}$ can be obtained by truncating to the lightest scalar KK modes. The lightest modes have a SSSB mass $\tilde{m}^2_{\phi^{(0)}} = 1/(2R)^2$ and a potential generated from F_S,

$$\mathcal{L}_4 \supset \left(\frac{\tilde{\lambda}_S}{\pi M_* R}\right)^2 \left|\phi_1^{(0)}\phi_2^{(0)} - f^2\right|^2 . \tag{3.29}$$

For $\frac{\tilde{\lambda}_S f^2}{\pi M_* R} \gtrsim \left(\frac{1}{2R}\right)^2$, a vev in the D-flat direction $\phi_1^{(0)} = \phi_2^{(0)} \sim f$ will be generated. However, in this regime the brane-perturbation is strong and a truncated treatment of the lightest KK modes is no longer justified. Instead a full 5D calculation gives a kinked profile

$$\phi_1(y) = \phi_2(y) = \phi_0 \frac{y - \pi R}{\pi R}, \quad \phi_0^2 = \left(f^2 - \frac{2M_*^2}{\tilde{\lambda}_S^2}\right)\frac{1}{\pi R} \tag{3.30}$$

when $\phi_0^2 > 0$. This results in an F-term for the singlet $F_S = \frac{M_*}{\tilde{\lambda}\pi R}$ and an F-term for the conjugate bulk fields proportional to the gradient $F_{\bar{\phi}_{1,2}} = \frac{\phi_0}{\pi R}$. The surviving D-term for the Higgs zero mode can be determined by integrating out the tree-level fluctuations of ϕ_1 and ϕ_2 on this y-dependent background. Defining a dimensionless $\omega = g_{X,5}\phi_0 \pi R = g_{X,4}\phi_0(\pi R)^{3/2}$ this contribution to the Higgs quartic has the form

$$\Delta\lambda = \frac{g_{X,4}^2}{8}\left(\frac{4}{9} - \frac{8}{2835}\omega^2 + ...\right). \tag{3.31}$$

An interesting feature of this model is that because the SUSY-breaking background $F_{\bar{\phi}_{1,2}}$ never parametrically exceeds the vev $\phi(y)$ breaking the gauge group, there is no regime where the D-term is completely re-coupled.

The parameter ω can be related directly to the mass of the lightest mode of the Z' gauge boson in this background. For $\omega \ll 1$, the mass approaches the 4D result, $M^2_{Z'} = \frac{4}{3}\frac{\omega^2}{(\pi R)^2}$, while for $\omega \gg 1$ the lightest Z' state becomes localized away from the $y = 0$ brane and asymptotically has mass $m^2_{Z'} \to \frac{\omega}{(\pi R)^2}$. In the parameter range of

interest $\omega \sim 1$ and we evaluate $\Delta\lambda$ and $M_{Z'}$ numerically.

In addition to the tree-level contribution to the Higgs pole mass from the non-decoupling D-terms, there will be new contributions to the Higgs soft mass from couplings to the $U(1)'$ gauge sector. If the gauge group were not broken, the contribution would have the same form as the SSSB loop contribution from the SM gauge groups, $\Delta m^2_{H_u,\ U(1)'} = \frac{7\zeta(3) g^2_{X,4}}{64\pi^4 R^2}$. When the gauge group is broken, the gauge states become localized toward the $y = \pi R$ brane, and the pure SSSB contribution is partially screened. However, new sources of radiative SUSY breaking are introduced with $\phi_{1,2}$ acting as messengers to communicate F_S and $F_{\overline{\phi}_{1,2}}$ to the Higgs sector. These contributions are cut-off at the scale of the $\phi_{1,2}$ masses $\sim \phi_0\sqrt{\pi R} \sim 1/R$ and do not introduce any logarithmic sensitivity to M_*. We evaluate the 5D propagators numerically in the $\phi(y)$ background to obtain the loop contributions to the Higgs mass, and find, in the parameter range of interest,

$$\Delta m^2_{H_u,\ U(1)'} \simeq 10^{-3} \times g^2_{X,4} M'^2_Z \ . \tag{3.32}$$

We evaluate the tuning of this model with respect to the shifts in the stop mass through HDOs and shifts in the parameters of the $U(1)'$ sector as

$$\Delta = \sqrt{\left(\frac{\partial \ln v^2}{\partial \ln \Delta m^2_{\tilde{t}}}\right)^2 + \left(\frac{\partial \ln v^2}{\partial \ln m^2_{\tilde{Z}'}}\right)^2} \tag{3.33}$$

The result is shown in Figure 3.9. The tuning is driven by limits on direct production of stops, and the model is tuned at a level of $\sim 25\%$ (for rough LHC8 limits of ~ 700 GeV stops and ~ 3 TeV gluinos).

So far we have discussed how the extended gauge sector can lift the Higgs pole mass to the observed value. In fact, in the model described the extra states can play all the roles of the extra source of SUSY breaking so far parameterised by F_X. When $\tilde{\lambda}_S$ has its NDA value $\sim \sqrt{24\pi^3}$, $F_S \sim 1/(\pi R)^2$ is a brane-localized F-term that can communicate soft masses through additional HDOs in addition to the predictive loop level IR communication we have discussed. The tree-level potential due to $F_{\overline{\phi}_{1,2}}$ and F_S will generate a contribution to the radion potential of the Goldberger-Wise

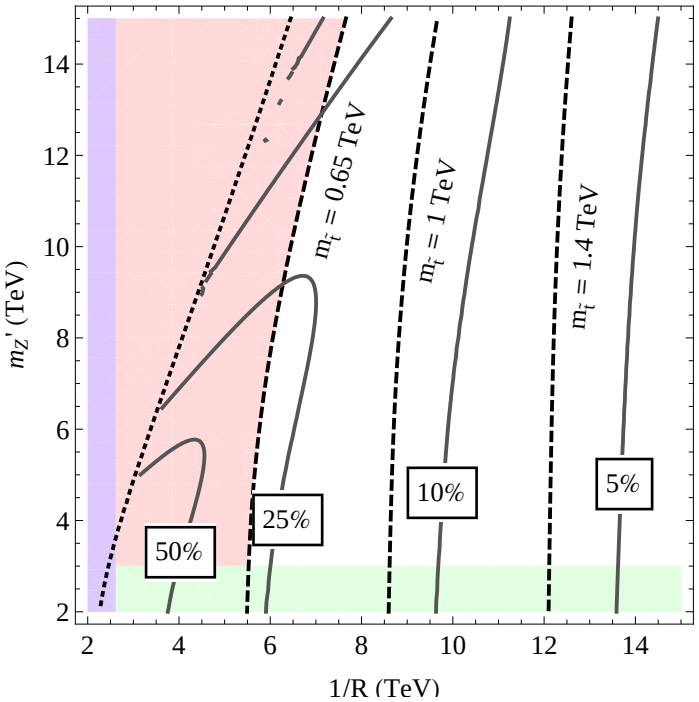

Figure 3.9: Fine-tuning Δ^{-1} (solid lines) as function of $1/R$ and the Z' mass. Iso-contours of stop mass are dashed. Limits from LHC8 searches for $\tilde{t} \to t + \text{MET}$[1, 2] (red) and Z' resonance searches [3, 4] (green) are shaded. Subdominant limits $m_{\tilde{g}} \approx 1/(2R) \gtrsim 1.3\text{TeV}$ from $\tilde{g} \to t\bar{t}/b\bar{b} + \text{MET}$ searches (blue) are also shaded [5, 6].

form [139], which can allow the radion to be stabilised at vanishing CC. A hierarchy between f and M_* is technically natural, and the role of the tree-level potential in stabilising the radius may allow the relationship between scales $f \sim 1/R \ll M_*$ to be dynamically realised. Thus we see that the $U(1)'$ extension is both minimally tuned, and possesses attractive features from a theoretical persepctive.

3.4.3 Singlet Extension

It is well known that when the MSSM is extended to include a SM singlet coupling to both H_u and H_d, and when both Higgs doublets get a non-zero vev, an additional tree-level contribution to the Higgs mass is present. In view of the simplicity of this idea, one could try to implement a similar mechanism in the current 5D framework. The reason why such possibility has not been explored yet is that in the context of

the original MNSUSY theory [55] the doublet H_d was assumed not to get a vev and, since there is no need for a μ or B_μ term, an accidental $U(1)_{H_d}$ (or $\mathbb{Z}_k$) symmetry acting on H_d exists which can remain unbroken, as discussed in Section 3.3.1.

However, once the $U(1)_{H_d}$ symmetry acting on H_d is given up, an NMSSM-like solution to the Higgs mass problem can be implemented. A simple option adds a bulk hypermultiplet $\mathcal{S} = (S, S^c)$, which is a SM singlet, with bc's $(+,-)/(+,+)$ for the scalar/fermion components of the chiral multiplet S and $(-,+)/(-,-)$ for those of S^c. In this case, it is possible to write a brane-localized term in the superpotential:

$$W \supset \delta(y)\frac{\tilde{\lambda}_S}{M_*^{3/2}} S H_u H_d \ , \tag{3.34}$$

and one might naively expect that this gives a tree-level contribution to the lightest Higgs mass proportional to λ_S^2, with $\lambda_S = \tilde{\lambda}_S(\pi R M_*)^{-3/2}$ being the 4D effective coupling. However, the effective theory below the scale $\sim 1/(2R)$ does *not* contain a contribution to the Higgs quartic and therefore to its physical mass. This surprising result does not match the intuition obtained from truncating to the 4D case but can be computed explicitly and is intrinsic to the 5D setup[6].

On the other hand, one can consider the case where the chiral multiplet S is localized on one of the branes[7]. In this situation, both its scalar and fermion components are massless at tree-level but at 1-loop the scalar gets a mass due to its interaction with the Higgs doublets given by $m_{\tilde{s}}^2 \approx 7\zeta(3)\lambda_S^2/(16\pi^4 R^2)$ [107, 108]. In addition there is now a contribution to the physical Higgs mass given by

$$\delta m_h^2 = \frac{v^2}{2}\lambda_S^2 \sin(2\beta)^2 \ . \tag{3.35}$$

A 125 GeV physical Higgs mass is then achievable for moderately light stop masses. For example, when the compactification scale is $1/R \approx 4$ TeV, a coupling $\lambda_S \approx 0.7$

[6] In particular, integrating out the scalar component of S^c, with a mass of $\sim 1/(2R)$ is crucial for the λ_S^2 contribution to the Higgs quartic to vanish. Notice that an analogous situation does not happen in 4D, where we only add a chiral multiplet S but no 5D SUSY partners.

[7] The superpotential term would be as in Eq.(3.34) but with a suppression of M_*^{-1} rather than $M_*^{-3/2}$.

and a value of $\tan\beta \approx 2$ lifts the Higgs to its observed mass.

This lifting, however, has a consequence for EWSB and tuning, as both soft masses $m^2_{H_u}$ and $m^2_{H_d}$ receive a positive 1-loop contribution proportional to λ_S^2, on top of the EW and top sector contributions previously discussed . Whereas the latter is negative and only contributes to $m^2_{H_u}$, the other two are positive and are of the same size for both H_u and H_d. Despite this, we find that both Higgs doublets can achieve a non-zero vev thanks to the effect of HDOs

$$\mathcal{K} \supset \delta(y)\frac{c_{H_a}}{M_*^3} X^\dagger X H_a^\dagger H_a \qquad (a = u, d) \ . \tag{3.36}$$

In order to estimate the tuning of this version of the model, we assume the decoupling limit is realised, such that only a light Higgs boson remains in the low energy theory. In such a case, the condition for successful EWSB can be written as

$$m^2_{H_u}\sin^2\beta + m^2_{H_d}\cos^2\beta = m^2_{H(\text{exp})} \ , \tag{3.37}$$

and the λ_S^2 contribution to $m^2_{H_{u,d}}$ can be estimated, compared to the EW piece, as

$$\frac{m^2_{H(S)}}{m^2_{H(\text{EW})}} \approx \frac{2\lambda_S^2}{3g^2} \tag{3.38}$$

which for $\lambda_S \approx 0.7$ results in $m^2_{H(S)} \approx 0.8\ m^2_{H(\text{EW})}$. In the spirit of the previous section, we then estimate the tuning as

$$\Delta \simeq \left\{ \left(\frac{m^2_{H,\text{EW}} + \sin^2\beta\ m^2_{H,\text{top}}}{m^2_{H,\text{exp}}} \right)^2 + \left(\frac{m^2_{H,S}}{m^2_{H,\text{exp}}} \right)^2 \right\}^{-1/2} \tag{3.39}$$

which is a mild $\Delta \sim 25\%$ tuning for $1/R \sim 4$ TeV.

3.5 Basic Phenomenology

In this Section we briefly discuss the most interesting phenomenological consequences of MNSUSY theories.

The main phenomenological signature of MNSUSY theories is production of sparticles at LHC and future hadron colliders. In particular, stops should be discovered at LHC for the theory to have its best possible level of fine-tuning. The hierarchy between stops and gluinos means the latter will *not* be probed in the near future: observation of a stop well below a gluino at LHC is a prediction of MNSUSY theories with low tuning. Moreover, the fact that Higgsinos are much heavier than 3rd generation sfermions means that usual $\tilde{t}$ and $\tilde{b}$ decays (to Higgsino plus SM fermion) characteristic of 4D SUSY theories are absent in our case. Alternatively, the most likely decay channels for $\tilde{t}$ and $\tilde{b}$ are 3-body decays to the lightest 3rd generation sfermion (likely to be either $\tilde{\tau}_R$ or $\tilde{\nu}_{\tau_L}$, as discussed in Section 3.3.1). However, details of the exact decay channels for 3rd generation sfermions depend on both how the theory is extended to include gravitational interactions and on the physics of SUSY breaking in the radius stabilization sector, as explained in [55].

Needless to say, the discovery of resonances of SM particles, or the presence of 1st and 2nd generation sfermions that are degenerate with gauginos and Higgsinos, would be strong evidence in favor of an MNSUSY setup. The minimum value of the compactification scale required for a model consistent with current constraints ($1/R \gtrsim 4\text{TeV}$) means that while the first and second generation squarks and gluinos may be in reach of the 14 TeV LHC, the KK excitations of SM states, which have a suppressed single production cross section due to the approximate KK parity, are likely out of reach.

Another phenomenological feature of interest in the simplest version of the model is the presence of contributions to flavor changing neutral currents (FCNC) at tree-level due to exchange of gauge boson KK modes, which has its root in the fact that the 3rd generation of matter is localized on one of the branes whereas the first two propagate in the bulk. As a result, deviations of experimental measurements from SM predictions regarding flavor violation are expected [143], in particular concerning

processes that involve 3rd generation fermions (e.g. B-meson mixing) or flavor violation in the lepton sector, unless one of the versions of the model with an enhanced flavor symmetry is implemented. As discussed in [143], some of those variations require allowing part of the 3rd generation to propagate in the bulk or localize on the brane part (or all) the 1st and 2nd generations.

Finally, another feature of the model is the presence of a nearly massless fermion $\tilde{x}$, the fermion component of the SM-singlet X. Given the extremely weak coupling between this state and normal matter (remember it only couples to matter via HDOs, of the form of those in Eq(3.3)), a vanishing value for its mass seems to be perfectly allowed by LEP and LHC data [160] [8]. Similarly, bounds from anomalous cooling of supernovae seem consistent with a massless $\tilde{x}$ [161]. Moreover, given the weakness of its coupling to normal matter, we expect $\tilde{x}$ to decouple from the thermal plasma in the early Universe at high temperatures, of around a few GeV (so well above the QCD phase transition temperature). This results in a small contribution to the number of effective neutrino species, $\Delta N_{\rm eff} \approx 0.01$, that lies well within the uncertainty of the current experimental measurement by Planck [162].

3.6 Phenomenology of Decays to Bulk

The maximally natural SUSY models are embedded in a 5D theory with a low fundamental scale $M_* \lesssim 100$TeV. One possibility for accomodating $M_{\rm pl} \gg M_*$ is the presence of large gravitational extra dimensions, with the 5D SUSY theory localized in the gravitational bulk. If SUSY breaking is localized or partially localized to the 5D brane in the gravitational bulk, there are interesting new candidates for LSPs from states that propagate in the full supersymmetric gravitational bulk. In this section, we analyze this possibility in more detail, focusing on the phenomenological consequences of decays to such states.

For as much generality as possible, we consider a framework in which the SM

[8] Comparing with the case of a massless bino-like neutralino, whose coupling to matter is already much larger than the effective coupling of $\tilde{x}$, lower bounds on sfermion masses are only a few hundreds of GeV.

particles and their SUSY-partners live on a brane that is embedded in a (flat) $4+d$-dimensional supersymmetric bulk whose dimensions are bigger than $\sim 10^{-14}$cm $\sim$ 1/(few GeV). SUSY breaking is felt softly on the brane, and the MSSM superpartners may be produced at colliders[9]. As we will show, many realizations of this scenario have additional light bulk states that are associated with SUSY breaking or additional sequestered sectors. In such cases, the lightest R-parity odd sparticle, the 'bulk LSP', will propagate in the $4+d$ extra dimensions, and the lightest ordinary-sector SUSY particle (LOSP) will decay to this state – in the case of maximally natural SUSY, the lightest third generation state localized on the brane can decay to the gravitational bulk LSP.

Couplings between bulk and brane states are necessarily higher dimensional operators, and if the fundamental scale, M_*, is not too high, decays of the LOSP can occur on collider timescales. From a 4d perspective, the LOSP decays to a distribution of KK modes of the bulk LSP of mass m_n with bulk phase space factor $\sim m_n^{d-1}$. This favors decays to the heaviest KK states, thus suppressing both visible energy and $E_T^{\rm miss}$ in the decay, and so, as we will argue in detail, severely weakening LHC limits on SUSY for certain classes of visible sparticle spectra. The basic mechanism is illustrated in Figure 3.10.

Specifically, we show that two-body decays of the brane-localized LOSP of mass M to a SM state and a bulk LSP are typically dominated by decays to bulk KK modes with masses $m_n \gtrsim 0.4M \div 0.8M$ depending on the nature of the coupling and the dimension of the bulk. This leads automatically to signatures similar to a compressed spectrum, where super-partners with large production cross sections are concealed if they decay to a nearly degenerate invisible LSP[10] [172, 173, 62, 41, 174, 175, 176, 177]. In this work, we focus primarily on limits from searches for prompt decays, which restricts M_* from above depending on the nature of the bulk LSP (modulino, axino, gaugino, gravitino) and the identity of the LOSP. For higher scales of M_*, searches for displaced vertices and out-of-time stopped decays become relevant,

[9] In contrast, studies of brane-worlds with supersymmetric bulks have focused mostly on the case that SUSY is realized only non-linearly on the brane [163, 164, 165, 166, 167, 168, 169, 170].

[10] Ref. [171] provides another example of a theory that dynamically reduces missing and visible energy, reproducing signatures similar to compressed spectra.

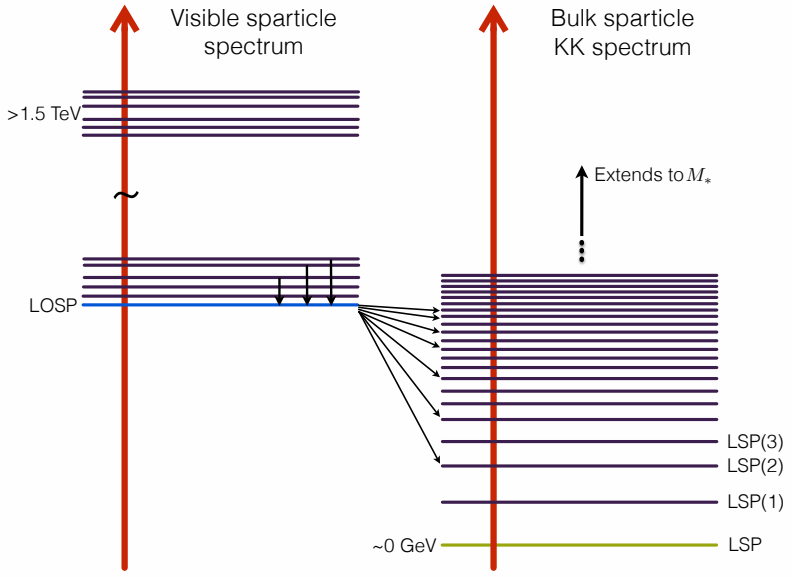

Figure 3.10: Schematic representation of the basic idea behind the auto-concealment mechanism, in which the LSP is a bulk state propagating in $d \geq 1$ extra dimensions. The visible sparticle spectrum has a lightest state, the LOSP, which decays promptly to the full tower of KK excitations of the LSP. As the spectral density of KK excitations behaves as $\sim m_n^{d-1}$ (as a function of the KK mass, m_n), decays to the heavier KK states are favored, dynamically realising the compressed spectrum mechanism of hiding SUSY with reduced E_T^{miss} and visible energy. As the masses of the KK tower of the LSP extend from ~ 0 GeV to the underlying gravitational scale M_* the LOSP mass is automatically within this tower without additional tuning. Transitions from visible sector to the bulk sector are prompt if M_* is not too high depending on the nature of the bulk LSP. In the case that transitions are not prompt, the auto-concealment mechanism no longer functions, but instead the decays of the LOSP can provide a powerful search method for extra dimensions.

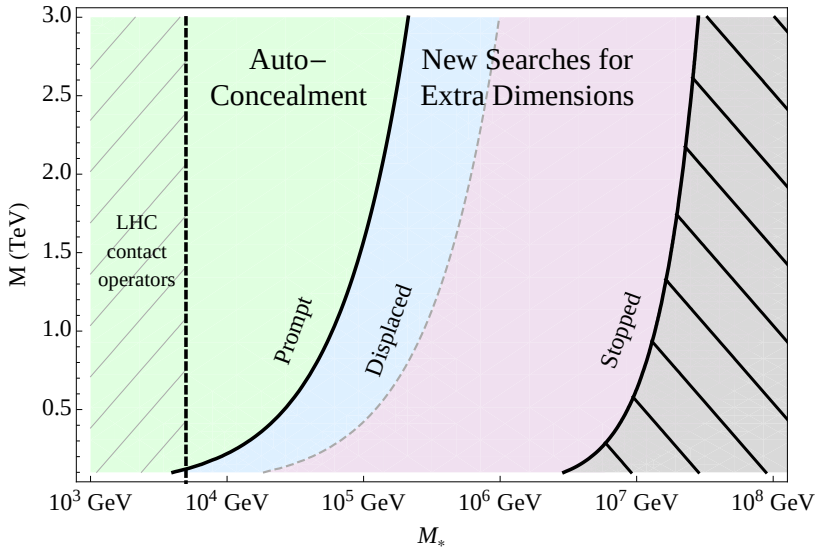

Figure 3.11: Colored regions display the form of LOSP decay as a function of the LOSP mass, M, and the fundamental gravitational scale, M_*. The bulk LSP is taken to be a modulino, the LOSP to be a sfermion, and we show the case $d = 4$. The auto-concealment mechanism applies in the region of prompt decays. In the regions of displaced decays or stopped LOSP out-of-time decays the auto-concealment mechanism no longer functions, but the decays of the LOSP can provide a new search mechanism for extra-dimensions with reach much greater than that provided by contact operators. In the grey hatched region to the far right, the splitting between KK states becomes large compared to the mass of the LOSP, $1/(ML) \gtrsim 0.1$ (all of the decays to the left of this region have lifetimes $\tau \lesssim 1$ yr). The hatched region to the far left shows the range of M_* excluded by current LHC contact operator searches for extra-dimensions.

and their sensitivity is also likely to be affected, though a study of this possibility is beyond the scope of this work.

3.6.1 Decays to the bulk

We now turn to a detailed discussion of the mechanism. The decay of a brane-localised LOSP of mass M into a bulk state propagating in d extra dimensions of size $L \gg 1/M$ can be described by an effective theory for the bulk-brane interactions [178, 179, 180, 154, 181, 182, 183]. The description of the brane states as point-localized objects in the d bulk dimensions is taken to be valid up to a scale $\Lambda_b < M_*$,

where M_* is the fundamental gravitational scale of the theory, and $M < \Lambda_b$ by assumption so that the decay is well described by the effective theory.[11]

To be concrete we start by studying the decays of a brane-localized $\tilde{e}_R$ LOSP to the fermion ψ of a bulk chiral multiplet[12] Φ, and then generalize to other interesting cases. While we now focus on this case as a simple example, there are a variety of other strongly motivated possibilities. In addition to a slepton LOSP, the case of a stop/sbottom LOSP and the case of degenerate first and second generation squark LOSPs provide particularly interesting examples from the point of view of collider phenomenology which we study in detail in the following section. The results derived in this section apply to any sfermion decaying to its massless SM fermion partner and a bulk modulino. In Section 3.6.3 we describe the form of the distribution for a general set of possible LOSPs and a variety of bulk LSP candidates.

Bulk spectrum and profiles

We study the bulk states by expanding in KK modes in the extra dimensions,

$$\psi = \sum_n \frac{1}{\sqrt{V}} f_n(y_i)\psi_n(x),$$

where x are the (3+1) coordinates, y_i are the extra bulk coordinates, V is the volume of the bulk, and each KK mode has mass m_n. In flat extra dimensions and in the absence of any bulk mass terms for the state, there is a zero mode, $m_0 = 0$ and the splittings between KK modes are of order the size of the bulk $\Delta m_n \approx 1/L$. We will be interested in cases where the decays from the brane states are highly-localized compared to the size of the bulk; in this case, the decays are insensitive to the exact

[11] At distances shorter than $1/\Lambda_b$, the embedding of the brane in the d bulk dimensions may be non-trivial; these effects could be taken into account by the presence of higher dimensional operators including terms with bulk derivatives. The scale Λ_b could correspond to the fundamental gravitational scale M_* or to an intermediate scale related to the extension of the brane embedding in the transverse directions.

[12] The bulk theory has at least $N = 2$ extended SUSY from the 4d perspective, and this N=1 'chiral multiplet' must in fact have bulk partners that fill out a full higher dimensional hyper-multiplet or vector multiplet, although these states need not couple to the brane. We use the N=1 superfield field notation of Ref. [180].

form of the boundary conditions for bulk fields far away from the MSSM brane and can be well described in the continuum approximation, $\Delta m_n \to 0$.

The spectrum of KK masses and profiles of a bulk multiplet will be perturbed by the presence of mass terms, which may be spread along the entire $4+d$ dimensional space occupied by the bulk state or be localized in some of the extra dimensions (for example localized on the MSSM brane). A mass term m_{4+d} spread along the full $(4+d)$ dimensional space lifts the start of the KK tower to m_{4+d}. We assume such terms are negligible compared to the mass scale of the decays, and will describe scenarios where this occurs in Section 3.6.3. Mass terms that are localized in some of the d dimensions have their effects suppressed by the volume of the remaining space, and are generally only relevant if they are localized near the MSSM brane, in which case they can affect the wavefunction profiles near the brane $f_n(0)$.

For example, a mass term for the fermion components of Φ localized on the MSSM brane has the form

$$\mathcal{L} = \delta^d(y)\frac{(\mu\psi\psi)}{\Lambda_b^d} + h.c. \tag{3.40}$$

where the fermion ψ is normalized as a bulk field with mass dimension $(3+d)/2$. The effect of the on-brane mass is to suppress the profile $f_n(0)$ of the KK states near the brane, which suppresses the coupling to brane-localized states. For KK masses $m_n \ll \Lambda_b$ and co-dimension $d \geq 3$, the perturbation of the wave function at the brane $f_n(0)$ is independent of m_n: for small perturbations $\mu \lesssim \Lambda_b$, $f_n(0)$ is unsuppressed, while for large perturbations $\mu \gg \Lambda_b$, $f_n(0) \to 0$ and the leading operators coupling brane fields to the bulk field will be those containing bulk derivatives $\sim \frac{\nabla_y \psi}{\Lambda_b}$ (this latter case is the correct description for instance when orbifold conditions in the fundamental theory force the wavefunction to vanish on the brane). For co-dimension $d = 1$, $f_n(0) \sim \frac{m_n}{\mu}$ for $m_n \lesssim \mu$, and for $d = 2$ there is a logarithmic dependence on m_n. Overall, the localized mass terms typically increases the efficiency of auto-concealment by decreasing the relative coupling of lighter KK modes to the MSSM brane states. As the sizes of the localized mass terms μ are only weakly constrained, to be conservative we assume they are negligible for the rest of this work.

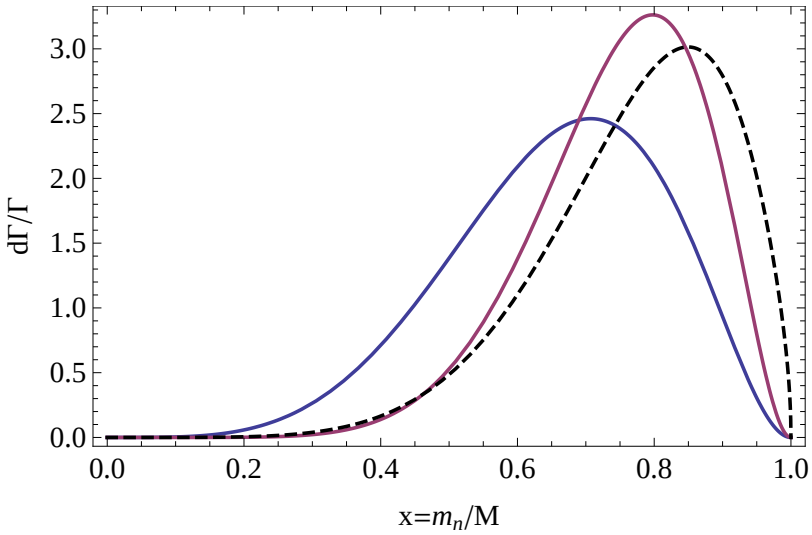

Figure 3.12: Differential distribution of KK masses for the decay $\tilde{e}_R \to e + \psi$ for $d = (3, 6)$ (solid curves with peaks from left to right, respectively). Also shown dashed is the distribution for a 500 GeV stop decaying in $d = 6$ as $\tilde{t}_R \to t + \psi$, with the definition $x \equiv m_n/(m_{\tilde{t}_R} - m_t)$.

Brane couplings and decays

For a simple and well-motivated example, we take Φ to couple to the MSSM states as a modulus in the Kahler potential with a gravitationally suppressed coupling

$$\mathcal{L} = \delta^d(y)\,\frac{1}{2}\left[\frac{(\Phi + \Phi^*){e_R}^* e_R}{M_*^{(d+2)/2}}\right]\Bigg|_{\theta^4}. \tag{3.41}$$

After making the KK expansion, the decay rate of a selectron with mass M to each individual mode of mass $m_n < M$ that follows from Eq.(3.41) is

$$\Gamma_n = \frac{M^3}{8\pi M_*^{2+d} V}\frac{m_n^2}{M^2}\left(1 - \frac{m_n^2}{M^2}\right)^2. \tag{3.42}$$

For co-dimension d, the number of states with mass $\sim m_n$ grows as $\sim m_n^{d-1}$ (this assumes the extra d-dimensions are flat—we later comment on the more general case [184]). For this particular example, the rate to heavier KK states is further enhanced by a factor m_n^2/M^2 due to a helicity suppression of decays to lighter modes. Therefore

even in $d = 1$ the distribution will be peaked towards higher KK masses– the extra-dimensional nature of the LSP is still crucial to provide the continuum of accessible states, but the enhancement of decays to heavier states is due completely to the matrix element. Going to the continuum limit, the total decay rate is

$$\Gamma_{\rm tot} = \sum_{n}^{m_n<M} \Gamma_n = \frac{M^{3+d}}{8\pi M_*^{2+d}} \frac{\Omega_d}{(2\pi)^d} \int_0^1 x^{d+1}(1-x^2)^2 dx, \tag{3.43}$$

where Ω_d is the surface area of a $(d-1)$-sphere and $x \equiv m_n/M$. The resulting differential decay rate with respect to the KK mass of the modulino is shown in Figure 3.12. The most likely KK mass is $\sim (0.6 \div 0.8)M$, and this can have striking observable consequences for collider phenomenology. (For the case of a stop LOSP with decay $\tilde{t} \to t + \psi$, the non-negligible top mass modifies the distribution as shown in Figure 3.12.)

3.6.2 SUSY limits and auto-concealment

To understand the effect of auto-concealment on collider searches, it is useful to consider the limit that the LOSP decays to a very narrow distribution of bulk LSP KK states peaked at $m_n \approx M$. In this case there is no visible energy from the LOSP decay[13], and events involving only direct pair production of the LOSP are invisible at colliders. This is identical to the case of exactly degenerate compressed spectra [41]. In this kinematic limit, missing and visible transverse energy arise only when the system recoils against a radiated jet or photon–dominantly initial state radiation (ISR)–and SUSY searches are significantly weakened.

A realistic distribution of KK masses as shown in Figure 3.12 does not completely realize this limit; the distributions peak below M and they have a non-negligible width. Nonetheless, they remain in the regime where most LOSP decays produce little visible energy and pair production events with large missing and visible energy are still dominantly due to hard ISR. The effect on experimental limits remains substantial.

[13]Decays of the bulk KK states among themselves producing visible energy on the brane are possible, but they are irrelevant on collider time scales due to the volume suppression of couplings to the brane.

To illustrate this, we re-interpret existing 8 TeV LHC sparticle searches for three interesting cases of LOSP pair production followed by decays to a bulk modulino LSP: a right-handed slepton LOSP $\tilde{e}_R/\tilde{\mu}_R \to e/\mu + \psi$, a right-handed stop LOSP $\tilde{t}_R \to t + \psi$, and degenerate first and second generation squarks $\tilde{q}_{u,d,c,s} \to q + \psi$. We simulate sfermion pair production processes with MadGraph5 [185] with shower and decays[14] in Pythia6 [186] and MLM matching of up to one additional jet. With one exception,[15] experimental limits were recast using validated analyses in CheckMATE [187, 188, 189, 190, 191, 192]. While we expect the results of these simulations to broadly characterize how auto-concealment affects current supersymmetry search limits, it is up to the experimental collaborations to set definitive bounds.

The first process we consider is pair production of degenerate right-handed sleptons decaying to a bulk modulino $\tilde{e}_R/\tilde{\mu}_R \to e/\mu + \psi$. The dominant limit is from a 20.3 fb^{-1} ATLAS $l^+l^- + E_T^{\rm miss}$ search [7] based on the kinematic variable m_{T2} [193, 194, 195]. The effect of auto-concealment on missing energy-related observables is dramatic, as illustrated in Figure 3.13, which shows the signal m_{T2} distribution after typical cuts used to reduce backgrounds. For the case of $d = 3$, the number of events satisfying the signal region cuts is very significantly reduced, while for $d = 6$ essentially no events pass cuts for the illustrated case of $M_{\tilde{l}_R} = 150$ GeV and 20.3 fb^{-1}. The effect on exclusion limits is predictable. Figure 3.14 shows the strongest cross section exclusion limit (at 95% CL$_{\rm S}$) from the ATLAS searches [7, 8]. A monojet search [9] was also considered to pick up ISR but the analysis had no effect on limits as it vetoed events with isolated leptons. The existing LHC8 limits of $M_{\tilde{l}_R} \gtrsim 225$ GeV for direct production of right handed sleptons decaying to a massless LSP are completely eliminated, with only the much weaker LEPII limit of $M_{\tilde{l}_R} \gtrsim 95$ GeV for very compressed slepton decays still applying [196, 197, 198, 199, 200].[16]

[14]To implement LOSP decays to a KK tower of fermion LSPs we introduced $N \sim 20$ new gauge neutral spin 1/2 states in Pythia. The masses of these states m_j fell into N evenly spaced bins from 0 to the LOSP mass M. The mass m_j of the $j^{\rm th}$ state was given by the branching ratio-weighted average of masses in the $j^{\rm th}$ bin, and the branching fraction to this state was determined by the integrated width over the bin.

[15]With the exception of [12], all of the analysis used in this paper to recast limits have been validated by CheckMATE. It was felt important to include this unvalidated analysis since it provided the only exclusion limits for stops decaying to a modulino in $d = 6$.

[16]Note that direct production of left-handed sleptons is already concealed independent of the

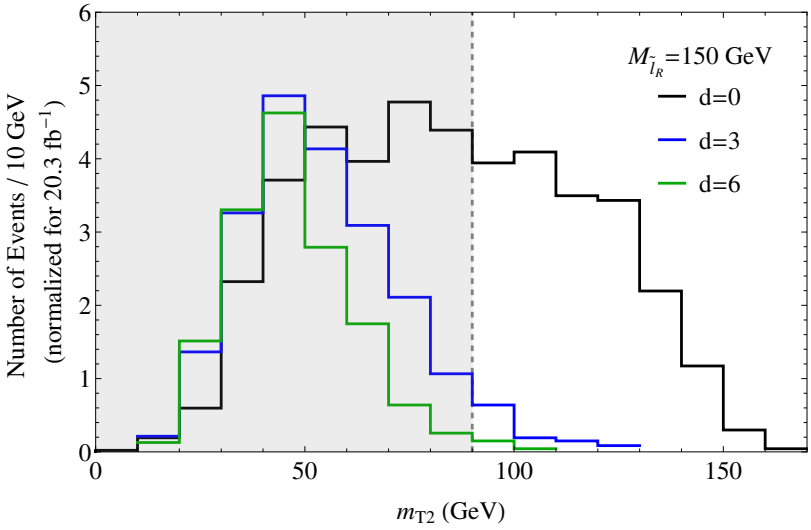

Figure 3.13: Differential distribution in stranverse mass m_{T2} for the decay $\tilde{e}_R \to e + \psi$ for a slepton of mass $M = 150$ GeV to a single massless LSP (black) and a bulk modulino LSP (blue and green) for $d = 3, 6$. The preselections of Ref. [7] have been applied, including a cut on missing energy, $E_T^{\text{miss,rel}} > 40$ GeV, which leads to the different total number of events for each case. Shown by a dashed line is the signal region cut $m_{T2} > 90$ GeV used to reduce backgrounds such as W^+W^- production. Definitions of $E_T^{\text{miss,rel}}$ and m_{T2} can be found within Ref. [7].

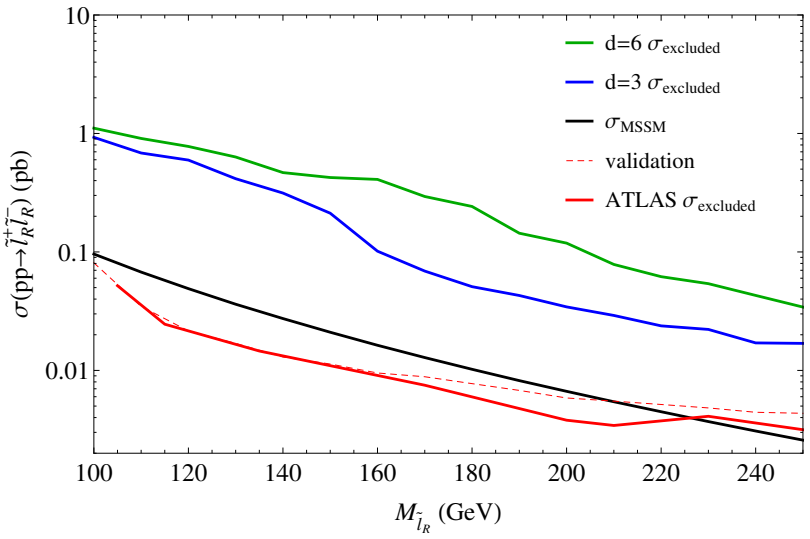

Figure 3.14: Strongest upper bound on degenerate $\tilde{\mu}_R, \tilde{e}_R$ slepton pair production cross sections from ATLAS $l^+l^- + E_T^{\text{miss}}$ m_{T2} [7] and razor analyses [8]. A monojet search was also considered [9] but did not affect limits. The top two curves corresponds to sleptons promptly decaying to the KK tower of a massless modulino in $d = 3$ (blue) and $d = 6$ (green) extra dimensions. The m_{T2} analysis is more effective at higher masses; below 140 GeV (170 GeV) for $d = 3$ ($d = 6$) the razor analysis sets stronger limits. Solid red (lowest) curve gives the observed ATLAS upper bound on the RH slepton production cross section from [7] for decays to a massless LSP. For validation, a dashed red curve gives the same bound using our simulation. Black curve gives the predicted NLO direct production cross section [10] with other superpartners decoupled, illustrating that RH sleptons are excluded up to ~ 225 GeV for decays to a massless LSP. For the searches considered, present limits on direct production of RH sleptons evaporate in the presence of the auto-concealment mechanism.

Limits on 3rd generation squark production can also be dramatically reduced. We studied $\tilde{t}_R$ pair production with $\tilde{t}_R \to t + \psi$. As depicted in Figure 3.12, the distribution of KK states in the decay is slightly modified from the result for a massless SM fermion fermion, Eq.(3.43), due to the non-negligible top mass. The dominant validated analysis in CheckMATE was the ATLAS 20.3 fb^{-1} all hadronic 6 (2 b) jet + $E_T^{\rm miss}$ search [11], while the unvalidated 2 lepton stop search [12] provided the strongest limits below $\sim$ 360 GeV. Figure 3.15 shows cross section limits for these searches. For prompt decays to a massless LSP the limit is $m_{\tilde{t}} \gtrsim 680$GeV, while limits reduce to $\sim 350 \div 410$ GeV for decays to a bulk modulino in $d = 3, 6$. A number of other searches are expected to provide similar limits, for example the ATLAS and CMS semi-leptonic searches [201, 13] and the most recent all-hadronic searches [201, 202] which perform better than [11] at low stop masses in the compressed region.

We finally study pair production of degenerate first and second generation squarks with $\tilde{q}_i \to q_i + \psi$ assuming the gluinos and 3rd generation squarks are decoupled. The dominant limits shown in Figure 3.16 are from the ATLAS 20.3 fb^{-1} $2-6$ jets $+E_T^{\rm miss}$ analysis [17], except for squarks below 200 GeV where limits are driven by the monojet search [9]. These searches have hard cuts on missing and visible energy and are substantially affected by auto-concealment. While for a decay to a single massless LSP the limit is $M \gtrsim 800$ GeV, for decays to a bulk modulino in $d = 3, 6$ the limit is reduced to only ~ 450 GeV. We have assumed no D-term splitting leading to decays between the left handed squarks, but we do not expect that these soft decays would significantly affect the results.

We have seen that auto-concealment significantly reduces bounds on direct production of superpartners, dynamically realizing the signatures of a compressed spectrum where a single LSP is nearly degenerate with the LOSP. This mechanism is particularly effective in models like maximally natural SUSY, where a large hierarchy between the lightest colored sparticles and heavier states gives a highly suppressed cross section for cascade decays of the heavier colored states.

---

existence of a bulk LSP as the EW symmetry breaking mass splitting between the heavier charged and lighter neutral members of the LH slepton doublet is small enough that a compressed spectrum is automatically realised.

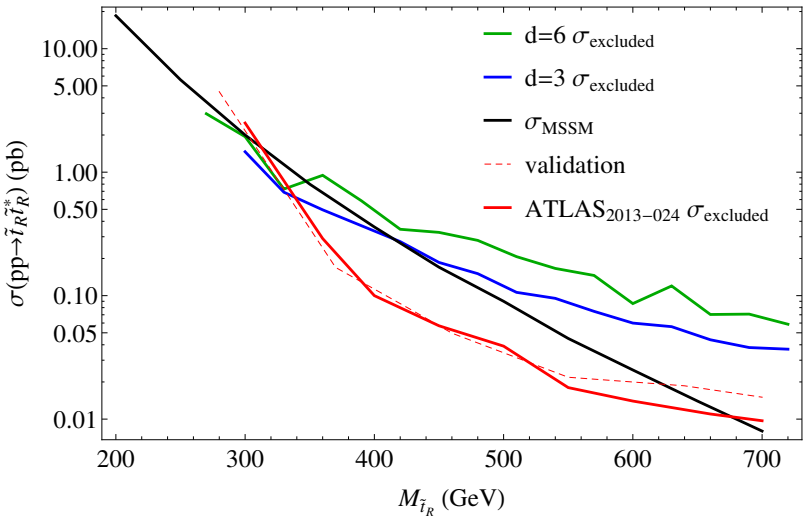

Figure 3.15: Strongest upper bound on stop pair production cross sections from ATLAS 6 (2 b) jet + E_T^{miss} [11] and 2 lepton stop [12] searches. A razor analysis [8], a one lepton stop search [13], and two monojet searches [9, 14] were also considered but did not strengthen the exclusion limits. The upper two curves corresponds to stops promptly decaying to a top + the KK tower of a massless modulino in $d = 3$ (blue) and $d = 6$ (green) extra dimensions. The all hadronic analysis is more effective at higher masses; below ~ 360 GeV the two lepton analysis sets stronger limits, however it should be noted that this analysis is not yet validated by CheckMATE. Solid red (lowest) curve gives the observed ATLAS upper bound on the stop production cross section from [11] assuming prompt decay to a top + a massless LSP. For validation, a dashed red curve gives the same bound using our simulation. Black curve gives the predicted NLO direct production cross section [15, 16], thus illustrating that stops are excluded up to ~ 680 GeV for a single massless LSP. For the search considered, present limits on direct production of stops drop to $\sim 350 \div 410$ GeV in the presence of the auto-concealment mechanism.

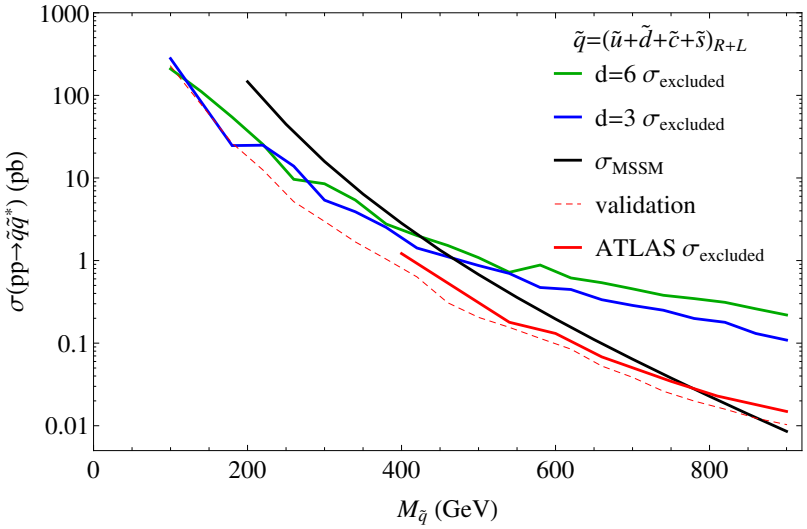

Figure 3.16: Strongest upper bound on pair production cross sections for degenerate first and second generation squarks from ATLAS $2-6$ jets+E_T^{miss} [17] and monojet [9] searches. A razor analysis was also considered [8] but its limits were weaker. The top two curves corresponds to squarks promptly decaying to the KK tower of a modulino in $d=3$ (blue) and $d=6$ (green) extra dimensions. The hadronic search is the more effective of the two analysis except below ~ 200 GeV. Solid red (lowest) curve gives the observed ATLAS upper bound on the squark production cross section from [17] assuming prompt decay to a LSP with mass ~ 40 GeV. Dashed red curve gives our bounds for a single massless LSP for validation. Black curve gives the predicted NLO direct production cross section when gluinos are decoupled [15, 16], thus illustrating that degenerate squarks are excluded up to ~ 775 GeV for a single massless LSP. For the searches considered, present limits on direct production of squarks drops to ~ 450 GeV for $d=3,6$ in the presence of the auto-concealment mechanism.

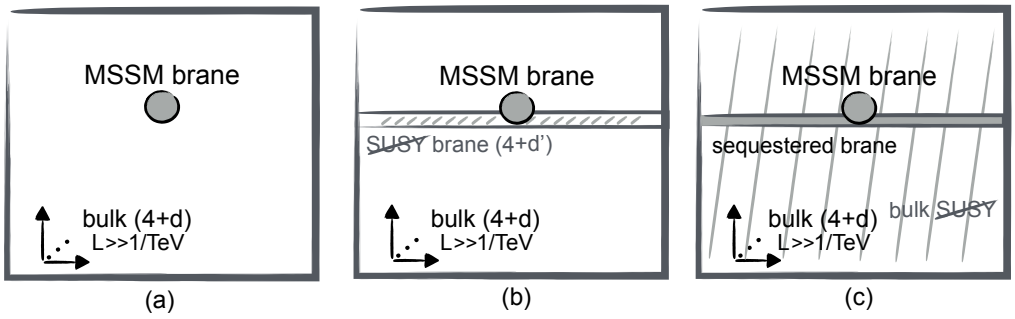

Figure 3.17: (a) The general set-up we consider, with the MSSM brane embedded in a large bulk with d compact dimensions of size $L \gg \text{TeV}^{-1}$. The MSSM brane may have structure at scales smaller than a TeV^{-1}, and possible additional extra dimensions of size $\lesssim \text{TeV}^{-1}$ are not depicted. (b) The same embedding, with the MSSM SUSY breaking shown explicitly to occur on a nearby brane extended in a $(4 + d')$ dimensional subspace of the large bulk. (c) The same embedding of the MSSM, with SUSY breaking extended throughout the entire large bulk. Additional states may live in the bulk or on sequestered branes of lower codimension as shown, and are candidates for light bulk LSPs. Although the SUSY breaking is present everywhere in the large bulk, it may be localized in further dimensions of size $\lesssim \text{TeV}^{-1}$ not shown.

3.6.3 Varieties of bulk LSPs

We are interested in models where the MSSM particles are confined to a brane in a gravitational bulk with d additional compact dimensions of size $L \gg \text{TeV}^{-1}$. At distances $\ll \text{TeV}^{-1}$, the bulk and the MSSM brane are locally supersymmetric, with at least an $N = 1$ subset of the bulk supersymmetries realized on the MSSM brane. While the MSSM brane must be localized within the large compact dimensions, at distances $\lesssim \text{TeV}^{-1}$ some or all of the MSSM states may extend around additional small dimensions or cycles, and other branes of various dimensions may also be present. This set-up is illustrated in Fig. 3.17(a), and allows the realization of a variety of extra-dimensional SUSY breaking mechanisms, sequestered sectors, and string embeddings of the MSSM structure.

The breaking of the supersymmetry remaining on the MSSM brane should be felt softly, giving superpartner masses $m_{\text{soft}} \sim \text{TeV}$. As depicted in Fig. 3.17(b), the MSSM SUSY breaking can occur over any subspace of the bulk with dimension

$4 + d'$ ($d' \leq d$), leaving the SUSY breaking localized in the $d - d'$ transverse large dimensions. The goldstino degrees of freedom from this breaking will also propagate in $4 + d'$ dimensions. After considering the mixing with the gravitino these degrees of freedom are lifted, but as we will show, for low SUSY breaking scales or $d' < d - 2$ they can generically remain lighter than the MSSM states, providing a candidate for a bulk LSP. We discuss this case first, and then discuss other candidates for bulk LSPs which naturally occur in sequestered sectors and are particularly relevant when decays to the goldstino degrees of freedom become suppressed or kinematically inaccessible.

Goldstino Bulk LSP

Take the MSSM SUSY breaking to be parameterized by an F-term for a field localized on a brane in a $4+d'$ subspace of the bulk, $\langle F_{4+d'} \rangle$. In a theory without gravitational degrees of freedom, there is a massless goldstino propagating in $4 + d'$ dimensions. First we study directly the decays of MSSM particles to this degree of freedom, and then we will discuss the effects of mixing the goldstino degree of freedom with the gravitino.

The couplings of the 3-brane localized MSSM states to the bulk goldstino η can be inferred as usual from the soft masses, for example for couplings to a MSSM chiral multiplet $(f, \tilde{f})$,

$$\mathcal{L}_{\text{soft}} = m_f^2 f^\dagger f \ \delta(y) \to\sim \frac{m_f^2}{\langle F_{4+d'} \rangle} f^\dagger \tilde{f} \eta \ \delta(y) + h.c. \tag{3.44}$$

Note we use the canonical normalizations of a $(4 + d')$-dimensional field for η and $\langle F_{4+d'} \rangle$. In comparison to our earlier results for a bulk modulino Eq. 3.43, the decay $\tilde{e}_R \to e + \eta$ has the rate,

$$\Gamma_{\text{tot}} \approx \frac{M^{5+d'}}{8\pi \langle F_{4+d'} \rangle^2} \frac{\Omega_{d'}}{(2\pi)^{d'}} \int_0^1 x^{d'-1} (1 - x^2)^2 dx. \tag{3.45}$$

The distribution of KK masses in these decays is slightly softer than decays to a bulk modulino, and the overall rate depends on a higher power of M. This decay has the usual $1/\langle F \rangle^2$ rate expected for decays to a goldstino in 4d models.

An important consequence is that if SUSY breaking is localized on a 3-brane like the MSSM, then decays to the goldstino will not appear extra dimensional and will often dominate over decays to any bulk LSPs present. For example, even if SUSY breaking is at the fundamental scale, $\langle F_4 \rangle \sim M_*^2$, decays to the 4-dimensional goldstino are parametrically enhanced by powers of $\frac{M}{M_*}$ compared to decays to a modulino living in more than six dimensions. Thus decays to a bulk state with large codimension only occur generically when SUSY breaking is extended in the bulk.

These results for the decays to a goldstino hold exactly in the limit that gravity decouples, $M_* \to \infty$ with $\langle F_{4+d'} \rangle$ held fixed. In the supergravity theory with finite M_*, the goldstino degree of freedom will mix with the gravitino; if there is a single source of SUSY breaking, the goldstino will be completely eaten by the gravitino, while if there is additional SUSY breaking elsewhere in the bulk some combinations will be left as a pseudo-goldstinos with perturbed mass spectra.

The diagonalization of the full gravitino bulk+brane equations of motion and determination of the masses and couplings of gravitino KK modes is beyond the scope of this work, but fortunately the equivalent goldstino approximation provides good intuition, and further we expect it to provide accurate results for many scenarios. We can understand when the equivalent goldstino approximation remains valid by considering the locality of decays from the MSSM brane. A 3-dimensional MSSM state of mass M will couple to gravitino states localized to a distance $\Delta \sim 1/M$ within the full bulk. We can therefore expect qualitatively correct results from considering only the light modes in the $4 + d'$ dimensional theory after compactifying the $d - d'$ bulk dimensions tranverse to the SUSY breaking brane to a size $\sim 1/M$. If the $4 + d'$ dimensions are approximately flat, there is a $4 + d'$ dimensional gravitino mass term related to the mixing with the goldstino,

$$m_{3/2,\ (4+d')} \sim \frac{F_{4+d'}}{\sqrt{M_*^{2+d}/M^{d-d'}}} \tag{3.46}$$

This mass sets the start of the gravitino KK tower in the 4d theory, and the equivalent goldstino approximation holds when $m_{3/2} \ll M$.

For a sufficiently small SUSY breaking scale $\langle F_{4+d'} \rangle$ this can always be satisfied,

but a particularly interesting case is when the breaking is at the fundamental scale, $\langle F_{4+d'} \rangle \sim M_*^{2+d'/2}$. This occurs for example when the MSSM SUSY is broken by the presence of a nearby D-brane extended in $4 + d'$ dimensions, with the $U(1)$ gaugino on the D-brane realizing the goldstino degree of freedom [203, 168, 167, 204]. Then we find

$$\frac{m_{3/2,\ (4+d')}}{M} \sim \left(\frac{M}{M_*}\right)^{\frac{d-d'}{2}-1}. \tag{3.47}$$

For $d' < d-2$, the perturbation is vanishing as $M_* \to \infty$ with brane soft masses M fixed, and we expect the goldstino equivalence theorem to hold. We therefore expect our results for the decays to the goldstino degrees of freedom to be a good description of a wide class of models where the goldstino is the bulk LSP. On the other hand for the cases $d' = d-2$ and $d' = d-1$ the decays to all of the components of the gravitino become important unless the SUSY breaking scale is parametrically below M_*; there may be interesting cases where such a gravitino is the LSP but these cases are subtle and left for future work (the super-higgs mechanism for the $d' = d-1$ case has been studied in 5d models in refs. [205, 206]). In the case $d' = d$, the lightest gravitino KK mode can be heavier than the MSSM LOSP even for $\langle F_{4+d'} \rangle$ well below the fundamental scale. We discuss this case in the following section, focusing on decays to the variety of other motivated light bulk LSPs which may still arise even when the gravitino is heavy.

Heavy Gravitino

In models where SUSY breaking occurs throughout the entire large d-dimensional bulk, as depicted in Fig. 3.17(c), the gravitino can obtain a large bulk mass lifting its lowest KK states to masses $\gtrsim m_{\rm soft}$ if the bulk SUSY breaking is communicated to the MSSM fields via gravitationally coupled operators and states, for instance via radion or dilaton mediation in additional $R \lesssim \text{TeV}^{-1}$ sized extra dimensions. In such models, sequestered sectors with further suppressed soft masses propagating in $\leq d$ large dimensions can naturally occur, providing candidates for bulk LSPs.

As a simple example, we consider the class of models including maximally natural SUSY and those models studied in refs. [107, 108, 109, 112, 113, 114, 115,

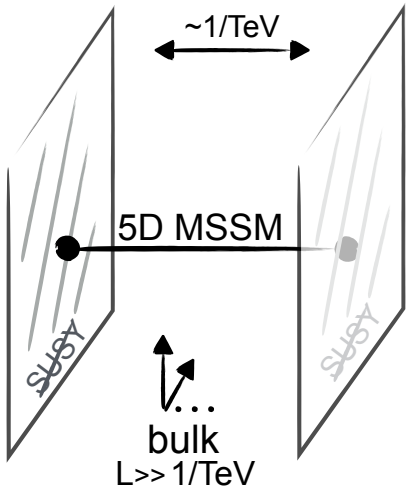

Figure 3.18: Embedding of 5d Scherk-Schwarz model in a $5+d$ dimensional theory as $\mathbb{R}^{3+1} \times (S_1/\mathbb{Z}_{\not 2} \times \mathbb{Z}_2') \times \mathcal{M}_d$. The MSSM states live on 3-branes or 4-branes completely localized within the d large compact bulk dimensions. The boundary conditions on each end of the TeV^{-1}-sized dimension partially break the bulk supersymmetry, leading to a complete breaking of SUSY in the theory at scales below TeV, with the breaking spread through the entire $4+d$ dimensional large bulk and giving large $\sim$ TeV scale masses to the lightest gravitino KK modes. Additional states may live extended in the large bulk but localized at either endpoint of the TeV^{-1}-sized dimension; they will be sequestered from the full SUSY breaking and can lead to a bulk LSP.

116, 117, 118], where some of the MSSM states propagate in a $\sim$ TeV^{-1} sized 5th dimension given by a segment $S_1/\mathbb{Z}_{\not 2} \times \mathbb{Z}_2'$ which breaks SUSY by Scherk-Schwarz boundary conditions [207, 208]. If this is embedded trivially in a large gravitational bulk as $\mathbb{R}^{3+1} \times (S_1/\mathbb{Z}_{\not 2} \times \mathbb{Z}_2') \times \mathcal{M}_d$, as illustrated in Fig. 3.18, then the SUSY breaking boundary conditions on S_1 give a d-dimensional mass $\sim$ TeV to the gravitino uniformly in the large bulk and generates soft masses $\sim$ TeV for the MSSM states. This can equivalently be described as radion mediation with $F_{T,4+d} \sim \text{TeV} \times M_*^{1+d/2}$ [209, 210, 154, 211, 212]. Additional states living on branes localized in the 5th dimension and extended in the bulk dimensions obtain soft masses through the gravitational couplings only at loop level [212], and can naturally arise as the bulk LSP. This scenario is illustrated in Figure 3.18.

The bulk LSP in this scenario can have a variety of forms. We have all ready discussed in detail the coupling to a bulk modulus field, which may arise for example due to branes wrapping additional M_*^{-1} sized dimensions or cycles. Other motivated possibilities for bulk LSPs living on a sequestered brane include a $U(1)'$ gaugino, a bulk axino, or a bulk sneutrino.

Bulk Axino

If the strong CP problem is solved by the axion in a model with a low fundamental scale, then the axion multiplet must propagate in some of the bulk dimensions. A simple possibility for the form of the effective couplings of the axino to the chiral multiplets of the MSSM is

$$\mathcal{L}_{\text{axino}} = \delta(y)\frac{c_{f1}}{f_*^{(d'+2)/2}}\tilde{a}f\tilde{f}^\dagger + \delta(y)\frac{c_{f2}}{f_*^{(d'+2)/2}}\tilde{a}f\tilde{f}^c + h.c. \tag{3.48}$$

where $c_{f1} \sim (10^{-3} - 10^{-4})M_{\tilde{g}}$ is radiatively generated from the anomaly couplings [213] and $c_{f2} \sim m_f$ is generated if the Higges are charged under the PQ symmetry (DFSZ axion) [214, 215]. More general forms of the axion supermultiplet couplings to the visible-sector fields [216, 215] lead to qualitatively similar results. The two-body decays mediated by the interactions of Eq.(3.48) dominate over 3-body decays through off-shell gauginos [213] and can easily dominate over rates into gravitationally coupled

states if scales are chosen to give a (3+1)-dimensional axion scale $f_a \lesssim 10^{16}$ GeV.

Bulk $U(1)'$ gaugino

Another interesting candidate for a bulk LSP is the gaugino of a bulk $U(1)'$ coupling to the MSSM fields through the $B-L$ current or kinetic mixings [217, 218]. In terms of a dimensionless gauge coupling, $\tilde{g}$, the couplings to the chiral brane fields are of the form,

$$\mathcal{L}_{\text{gaugino}} = \delta(y)\frac{\tilde{g}}{M_*^{d'/2}}\tilde{\lambda} f \tilde{f}^\dagger + h.c. \tag{3.49}$$

Note that this coupling is of lower dimension than the decays to gravitational states or an axino, and naturally can dominate over other channels if present. The $U(1)'$ can be broken supersymmetrically on the 3-brane or elsewhere in the bulk to evade constraints on the gauge bosons. Limits on the scale M_* from direct single production of bulk KK gauge bosons will be enhanced compared to the KK graviton limits, while limits from contact operators will not be substantially changed.

Bulk sneutrino

A final well-motivated bulk LSP candidate is a sneutrino superpartner of one of the sterile neutrinos that can exist in the extra-dimensional bulk. Such bulk sterile neutrinos can explain the observed neutrino masses and mixings by way of a volume-enhanced effective (3+1)-dimensional Majorana mass leading to a see-saw like formula [219]. The details of the brane-bulk couplings, and particularly their flavour structure, are potentially interesting in the regime discussed in Section 4 probing extra dimensions, as they may give additional clues to the structure of the underlying neutrino model.

Parameterized Distribution

We have discussed a variety of motivated possibilities for decays to a bulk LSP: a goldstino of SUSY breaking extended in the bulk, a modulino, a $U(1)'$ gaugino, and an axino. We have focused on the case of the decays of a massless sfermion, but we can more generally consider the decay of any MSSM LOSP to a bulk LSP.

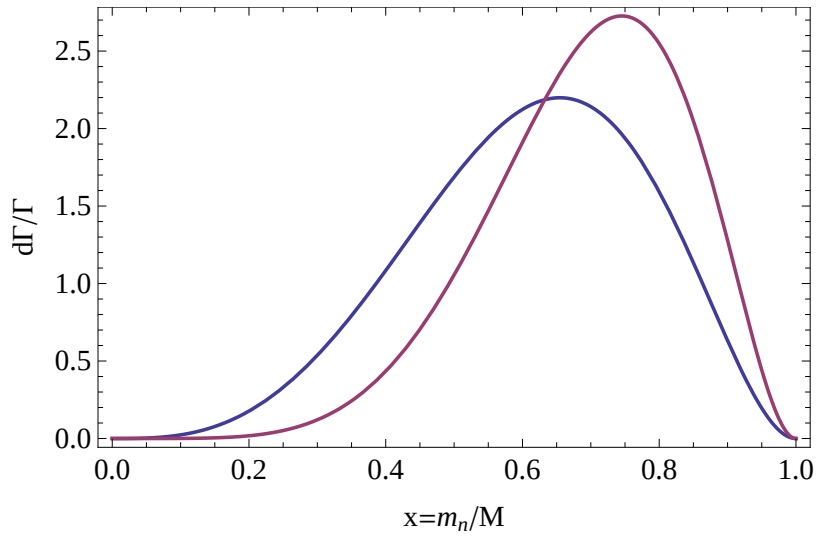

Figure 3.19: Differential distribution of KK masses for the decay $\tilde{e}_R \to e + \tilde{X}$ for differing candidate bulk LSPs, $\tilde{X}$, $\tilde{X} = \eta$, a bulk goldstino (leftmost, blue curve), or, $\tilde{X} = \psi$, a bulk modulino (rightmost, red curve). A bulk $U(1)'$ gaugino or axino has the same distribution as the goldstino. For both cases we fix $d = 6$. This illustrates that auto-concealment is slightly more effective for the modulino coupling than other bulk LSPs.

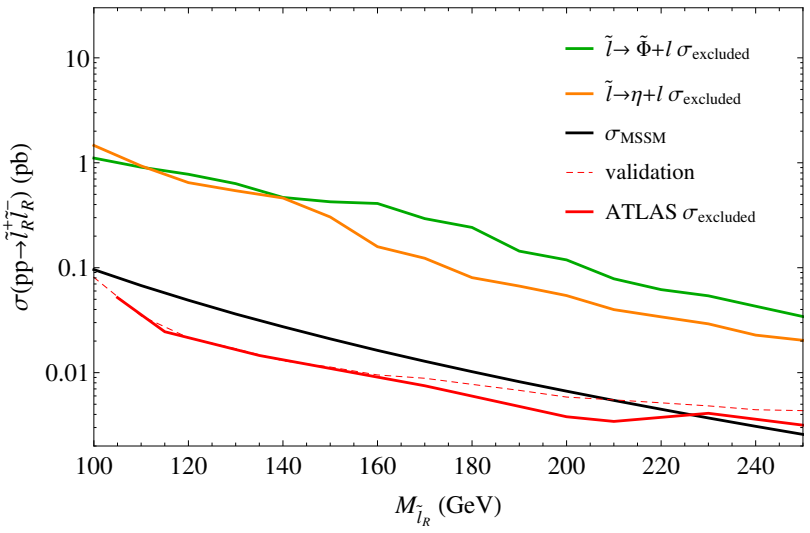

Figure 3.20: Strongest upper bound on degenerate $\tilde{\mu}_R$, $\tilde{e}_R$ pair production cross sections from ATLAS $l^+l^- + E_T^{\text{miss}}$ m_{T2} [7] and razor analyses [8]. A monojet search was also considered [9] but sets weaker limits. The top two curves corresponds to sleptons promptly decaying to the KK tower of a modulino (ψ, green) or goldstino (η, orange), in $d = 6$ extra dimensions. The m_{T2} analysis is the more effective of the two searches except below 170 and 150 GeV for decays to bulk modulinos and goldstino respectively. Solid red (lowest) curve gives the observed ATLAS upper bound on the RH slepton production cross section from [7] for decays to a massless LSP. For validation, the dashed red curve gives the same bound using our simulation. Black curve gives the predicted NLO direct production cross section [10] illustrating that RH sleptons are excluded up to ~ 225 GeV for a single massless LSP. For the searches considered both the modulino and goldstino eliminate present limits on direct RH slepton production.

	ψ (α,β,δ)	$\eta/\tilde{a}$ (α,β,δ)	$\tilde{\lambda}'$ (α,β,δ)
$\tilde{f}_{L/R} \to f + \tilde{X}$	$(2,2,0)$	$(0,2,0)$	$(0,2,0)$
$\tilde{H} \to h/Z + \tilde{X}$	$(0,2,1)$	$(0,2,1)$	$(0,2,1)$
$\tilde{\lambda} \to V/g + \tilde{X}$	$(0,3,0)$	$(0,3,0)$	–

Table 3.3: Possibilities for the kinematic distribution in the decays of sfermion ($\tilde{f}$), higgsino-like ($\tilde{H}$), and wino/bino/gluino-like LOSPs ($\tilde{\lambda}$) to variety of bulk LSPs $\tilde{X}$: a modulino ψ, a goldstino η, an axino $\tilde{a}$, a $U(1)'$ gaugino $\tilde{\lambda}'$. These distributions hold in the massless limit for the SM particle in the decay, $(M - m_n) \gg m_h, m_V, m_t$.

From an observational point of view, these various possibilities for bulk LSPs can be simply summarized. The general form for the differential distribution of KK masses in the decay of a brane-localized LOSP to a bulk LSP and a massless SM particle is a sum of terms of the form

$$\frac{d\Gamma}{dx} \sim x^{d-1+\alpha}(1-x^2)^{\beta}(1+x^2)^{\delta}; \quad x \equiv m_n/M, \tag{3.50}$$

where the $(1-x^2)^{\beta}$ factor captures the 3D phase space dependence, and the $x^{d-1+\alpha}$ factor includes the bulk phase space factor. The remaining freedom in α, β, δ comes from the matrix element for a given process. Typically a single term of the form Eq.(3.50) dominates the distribution; qualitatively, α and β are the most important for determining the shape of the distribution because of their zeros – a large α and a small β corresponds to a distribution of decays peaked at the largest kinematically allowed KK masses. Table 3.3 surveys the forms of the distribution for a variety of combinations of brane LOSP and bulk LSP candidates decaying to an effectively massless SM state. The decays to a goldstino, axino, and $U(1)'$ gaugino have similar matrix elements and all follow the same kinematic form. They do not share the helicity suppression of decays to lighter KK modes found for the modulino-like coupling Eq. 3.41, leading to distributions slightly softer than decays to a modulino.

Figure 3.19 compares the distributions of KK masses for the decays of a RH slepton ($\tilde{\mu}_R, \tilde{e}_R$) to a goldstino or modulino LSP, and Figure 3.20 compares the corresponding effects on experimental limits in slepton searches.

3.6.4 Summary

We have presented a mechanism—auto-concealment in extra dimensions—which significantly weakens present search limits for some SUSY models. Auto-concealment applies to theories like maximally natural SUSY where the LOSP is a brane localized state while the LSP is a bulk state, producing a dense KK tower of LSP excitations with increasing mass, m_n, that automatically brackets the LOSP mass without further tuning. The increased density of states at higher mass due to the bulk phase space factor $\sim m_n^{d-1}$ favours LOSP decays to the heaviest KK states, dynamically generating a quasi-compressed spectra, as discussed in Section 3.6.1 and shown in Figures 3.10 and 3.12. If the scale M_* is such that decays from the LOSP to the LSP are prompt, typical handles used in SUSY searches such as visible energy and $E_T^{\rm miss}$ are then dynamically suppressed as we discussed in Section 3.6.2. This reduces both $E_T^{\rm miss}$ and visible energy in SUSY events (unlike R-parity violation for example, which increases visible energy).

Auto-concealment can occur for a variety of visible-sector LOSP candidates. In particular, we find that LHC limits on right-handed slepton LOSPs evaporate in the case of prompt decays to a bulk modulino (see Figure 3.14), while the LHC limits on stop LOSPs weakens to $\sim 350 \div 410$ GeV (see Figure 3.15). Present LHC limits on direct production of degenerate first and second generation squarks similarly drop to ~ 450 GeV (see Figure 3.16). This can reduce the limits on natural theories like maximally natural supersymmetry for low scales of $1/R$ and light stops, even after bounds on more easily detected decay topologies increase at the 14 TeV LHC.

3.7 Conclusions

The crucial ingredient behind the success of maximally natural SUSY is the Scherk-Schwarz mechanism (with maximal twist) of SUSY breaking in 5D. The non-local nature of this breaking ensures that SUSY breaking parameters are only sensitive to scales up to the compactification scale $1/R$ ($\gtrsim$ 4TeV satisfies all constraints), and are insensitive to the UV cutoff. The 5D geography of fields also plays a major role:

whereas gauge and Higgs sectors propagate in the 5D bulk (often, but not absolutely necessarily, together with the 1st and 2nd matter generations), the 3rd generation remains localized on one of the branes. These two features act together leading to a 4D effective theory where the usual problems of SUSY theories are solved (for example the μ and $B\mu$ problems, and the problem of the radiative sensitivity of EWSB to the gluino mass) with a low level of tuning.

The minimal implementation of the model predicts, however, a Higgs mass $m_h < 125\text{GeV}$ if the theory is restricted to the low fine tuning region. Simple extensions of the minimal theory solve this problem and do not significantly affect the physics of EWSB. We have explicitly discussed three qualitatively different extensions: the addition of extra $U(1)$ gauge structure under which the Higgs is charged; the presence of a family of brane-localized vector-like leptons that couple to the Higgs with an $\mathcal{O}(1)$ Yukawa coupling; and an NMSSM-like extension where both Higgs fields get a non-zero vev and the presence of a brane-localized singlet chiral superfield provides an additional tree-level contribution to the Higgs mass. We have shown that all of them give a successful theory of the weak scale with a level of fine-tuning that is $10\% - 30\%$. At the 13 TeV LHC, limits on third generation squarks may significantly increase the tuning of these models; one novel possibility for evading strengthened constraints that arises naturally in these models is the possibility of decays to an LSP in a large gravitational dimension. These possibilities are by no means a complete set of extensions of the minimal model, but rather illustrate how simple extensions that do not significantly alter the physics of EWSB result in attractive, viable theories.

Bibliography

[1] **ATLAS** Collaboration, G. Aad et al., *Search for direct third-generation squark pair production in final states with missing transverse momentum and two b-jets in $\sqrt{s} = 8$ TeV pp collisions with the ATLAS detector*, *JHEP* **1310** (2013) 189, [arXiv:1308.2631].

[2] **CMS Collaboration** Collaboration, S. Chatrchyan et al., *Search for top-squark pair production in the single-lepton final state in pp collisions at $\sqrt{s} = 8$ TeV*, *Eur.Phys.J.* **C73** (2013) 2677, [arXiv:1308.1586].

[3] **ATLAS Collaboration** Collaboration, *Search for high-mass dilepton resonances in 20 fb^{-1} of pp collisions at $\sqrt{s} = 8$ TeV with the ATLAS experiment*, Tech. Rep. ATLAS-CONF-2013-017, CERN, Geneva, Mar, 2013.

[4] **CMS Collaboration** Collaboration, S. Chatrchyan et al., *Search for heavy narrow dilepton resonances in pp collisions at $\sqrt{s} = 7$ TeV and $\sqrt{s} = 8$ TeV*, *Phys.Lett.* **B720** (2013) 63–82, [arXiv:1212.6175].

[5] *Search for strong production of supersymmetric particles in final states with missing transverse momentum and at least three b-jets using 20.1 fb1 of pp collisions at sqrt(s) = 8 TeV with the ATLAS Detector.*, Tech. Rep. ATLAS-CONF-2013-061, CERN, Geneva, Jun, 2013.

[6] **CMS Collaboration** Collaboration, S. Chatrchyan et al., *Search for supersymmetry in pp collisions at $\sqrt{s} = 8$ TeV in events with a single lepton, large jet multiplicity, and multiple b jets*, arXiv:1311.4937.

[7] **ATLAS** Collaboration, *Search for direct-slepton and direct-chargino production in final states with two opposite-sign leptons, missing transverse momentum and no jets in 20/fb of pp collisions at sqrt(s) = 8 TeV with the ATLAS detector*, Tech. Rep. ATLAS-CONF-2013-049, ATLAS-COM-CONF-2013-050, CERN, Geneva, May, 2013.

[8] **ATLAS** Collaboration, *Search for strongly produced supersymmetric particles in decays with two leptons at $\sqrt{s}$ = 8 TeV*, Tech. Rep. ATLAS-CONF-2013-089, ATLAS-COM-CONF-2013-109, CERN, Geneva, August, 2013.

[9] **ATLAS** Collaboration, *Search for New Phenomena in Monojet plus Missing Transverse Momentum Final States using 10fb-1 of pp Collisions at sqrts=8 TeV with the ATLAS detector at the LHC*, Tech. Rep. ATLAS-CONF-2012-147, ATLAS-COM-CONF-2012-190, CERN, Geneva, May, 2012.

[10] W. Beenakker, M. Klasen, M. Kramer, T. Plehn, M. Spira, et al., *The Production of charginos / neutralinos and sleptons at hadron colliders*, *Phys.Rev.Lett.* **83** (1999) 3780–3783, [hep-ph/9906298].

[11] **ATLAS** Collaboration, *Search for direct production of the top squark in the all-hadronic ttbar + etmiss final state in 21 fb-1 of p-pcollisions at sqrt(s)=8 TeV with the ATLAS detector*, Tech. Rep. ATLAS-CONF-2013-024, ATLAS-COM-CONF-2013-011, CERN, Geneva, March, 2013.

[12] **ATLAS** Collaboration, G. Aad et al., *Search for direct top-squark pair production in final states with two leptons in pp collisions at $\sqrt{s}$ = 8TeV with the ATLAS detector*, *JHEP* **1406** (2014) 124, [arXiv:1403.4853].

[13] **ATLAS** Collaboration, G. Aad et al., *Search for top squark pair production in final states with one isolated lepton, jets, and missing transverse momentum in $\sqrt{s}$ = 8 TeV pp collisions with the ATLAS detector*, arXiv:1407.0583.

[14] **ATLAS** Collaboration, G. Aad et al., *Search for pair-produced third-generation squarks decaying via charm quarks or in compressed supersymmetric scenarios in pp collisions at $\sqrt{s} = 8$ TeV with the ATLAS detector*, *Phys.Rev.* **D90** (2014) 052008, [arXiv:1407.0608].

[15] "LHC SUSY Cross Section Working Group." https://twiki.cern.ch/twiki/bin/view/LHCPhysics/SUSYCrossSections.

[16] M. Kramer, A. Kulesza, R. van der Leeuw, M. Mangano, S. Padhi, et al., *Supersymmetry production cross sections in pp collisions at $\sqrt{s} = 7$ TeV*, arXiv:1206.2892.

[17] **ATLAS** Collaboration, *Search for squarks and gluinos with the ATLAS detector in final states with jets and missing transverse momentum and 20.3 fb^{-1} of $\sqrt{s} = 8$ TeV proton-proton collision data*, Tech. Rep. ATLAS-CONF-2013-047, ATLAS-COM-CONF-2013-049, CERN, Geneva, May, 2013.

[18] **ATLAS Collaboration** Collaboration, G. Aad et al., *Observation of a new particle in the search for the Standard Model Higgs boson with the ATLAS detector at the LHC*, *Phys.Lett.* **B716** (2012) 1–29, [arXiv:1207.7214].

[19] **CMS Collaboration** Collaboration, S. Chatrchyan et al., *Observation of a new boson at a mass of 125 GeV with the CMS experiment at the LHC*, *Phys.Lett.* **B716** (2012) 30–61, [arXiv:1207.7235].

[20] G. 't Hooft, *Naturalness, chiral symmetry, and spontaneous chiral symmetry breaking*, *NATO Sci. Ser. B* **59** (1980) 135.

[21] L. Susskind, *The Anthropic landscape of string theory*, hep-th/0302219.

[22] P. W. Graham, D. E. Kaplan, and S. Rajendran, *Cosmological Relaxation of the Electroweak Scale*, arXiv:1504.07551.

[23] E. Hardy, *Electroweak relaxation from finite temperature*, arXiv:1507.07525.

[24] J. R. Espinosa, C. Grojean, G. Panico, A. Pomarol, O. Pujols, and G. Servant, *Cosmological Higgs-Axion Interplay for a Naturally Small Electroweak Scale*, arXiv:1506.09217.

[25] A. G. Cohen, D. B. Kaplan, and A. E. Nelson, *Effective field theory, black holes, and the cosmological constant*, *Phys. Rev. Lett.* **82** (1999) 4971–4974, [hep-th/9803132].

[26] G. F. Giudice, G. Isidori, A. Salvio, and A. Strumia, *Softened Gravity and the Extension of the Standard Model up to Infinite Energy*, *JHEP* **02** (2015) 137, [arXiv:1412.2769].

[27] M. Farina, D. Pappadopulo, and A. Strumia, *A modified naturalness principle and its experimental tests*, *JHEP* **08** (2013) 022, [arXiv:1303.7244].

[28] M. Papucci, J. T. Ruderman, and A. Weiler, *Natural SUSY Endures*, *JHEP* **09** (2012) 035, [arXiv:1110.6926].

[29] N. Craig, C. Englert, and M. McCullough, *A New Probe of Naturalness*, *Phys.Rev.Lett.* **111** (2013) 121803, [arXiv:1305.5251].

[30] S. El Hedri and A. Hook, *Minimal Signatures of Naturalness*, *JHEP* **10** (2013) 105, [arXiv:1305.6608].

[31] C. Englert, A. Freitas, M. M. Mhlleitner, T. Plehn, M. Rauch, M. Spira, and K. Walz, *Precision Measurements of Higgs Couplings: Implications for New Physics Scales*, *J. Phys.* **G41** (2014) 113001, [arXiv:1403.7191].

[32] J. Barnard and M. White, *Collider constraints on tuning in composite Higgs models*, arXiv:1507.02332.

[33] M. W. Cahill-Rowley, J. L. Hewett, A. Ismail, and T. G. Rizzo, *More energy, more searches, but the phenomenological MSSM lives on*, *Phys. Rev.* **D88** (2013), no. 3 035002, [arXiv:1211.1981].

[34] J. A. Evans and Y. Kats, *LHC Coverage of RPV MSSM with Light Stops*, *JHEP* **04** (2013) 028, [arXiv:1209.0764].

[35] Z. Chacko, H.-S. Goh, and R. Harnik, *The Twin Higgs: Natural electroweak breaking from mirror symmetry*, *Phys.Rev.Lett.* **96** (2006) 231802, [hep-ph/0506256].

[36] N. Craig, S. Knapen, and P. Longhi, *The Orbifold Higgs*, *JHEP* **03** (2015) 106, [arXiv:1411.7393].

[37] G. Burdman, Z. Chacko, H.-S. Goh, and R. Harnik, *Folded supersymmetry and the LEP paradox*, *JHEP* **02** (2007) 009, [hep-ph/0609152].

[38] D. Berenstein, *TeV-Scale strings*, *Ann. Rev. Nucl. Part. Sci.* **64** (2014) 197–219, [arXiv:1401.4491].

[39] S. Dimopoulos and H. Georgi, *Softly Broken Supersymmetry and SU(5)*, *Nucl.Phys.* **B193** (1981) 150.

[40] N. Arkani-Hamed and S. Dimopoulos, *Supersymmetric unification without low energy supersymmetry and signatures for fine-tuning at the LHC*, *JHEP* **06** (2005) 073, [hep-th/0405159].

[41] H. K. Dreiner, M. Kramer, and J. Tattersall, *How low can SUSY go? Matching, monojets and compressed spectra*, *Europhys.Lett.* **99** (2012) 61001, [arXiv:1207.1613].

[42] S. Dimopoulos and G. Giudice, *Naturalness constraints in supersymmetric theories with nonuniversal soft terms*, *Phys.Lett.* **B357** (1995) 573–578, [hep-ph/9507282].

[43] A. Pomarol and D. Tommasini, *Horizontal symmetries for the supersymmetric flavor problem*, *Nucl.Phys.* **B466** (1996) 3–24, [hep-ph/9507462].

[44] A. G. Cohen, D. Kaplan, and A. Nelson, *The More minimal supersymmetric standard model*, *Phys.Lett.* **B388** (1996) 588–598, [hep-ph/9607394].

[45] A. Arvanitaki, M. Baryakhtar, X. Huang, K. van Tilburg, and G. Villadoro, *The Last Vestiges of Naturalness*, *JHEP* **1403** (2014) 022, [arXiv:1309.3568].

[46] T. Gherghetta, B. von Harling, A. D. Medina, and M. A. Schmidt, *The Scale-Invariant NMSSM and the 126 GeV Higgs Boson*, *JHEP* **1302** (2013) 032, [arXiv:1212.5243].

[47] E. Hardy, *Is Natural SUSY Natural?*, *JHEP* **1310** (2013) 133, [arXiv:1306.1534].

[48] J. L. Feng, *Naturalness and the Status of Supersymmetry*, *Ann.Rev.Nucl.Part.Sci.* **63** (2013) 351–382, [arXiv:1302.6587].

[49] T. Gherghetta, B. von Harling, A. D. Medina, and M. A. Schmidt, *The price of being SM-like in SUSY*, *JHEP* **1404** (2014) 180, [arXiv:1401.8291].

[50] J. Fan and M. Reece, *A New Look at Higgs Constraints on Stops*, *JHEP* **1406** (2014) 031, [arXiv:1401.7671].

[51] **ATLAS** Collaboration, G. Aad et al., *Search for direct production of charginos, neutralinos and sleptons in final states with two leptons and missing transverse momentum in pp collisions at $\sqrt{s} = 8$ TeV with the ATLAS detector*, *JHEP* **05** (2014) 071, [arXiv:1403.5294].

[52] A. Arvanitaki and G. Villadoro, *A Non Standard Model Higgs at the LHC as a Sign of Naturalness*, *JHEP* **02** (2012) 144, [arXiv:1112.4835].

[53] T. Gherghetta, B. von Harling, A. D. Medina, and M. A. Schmidt, *The Scale-Invariant NMSSM and the 126 GeV Higgs Boson*, *JHEP* **02** (2013) 032, [arXiv:1212.5243].

[54] N. Craig and K. Howe, *Doubling down on naturalness with a supersymmetric twin Higgs*, *JHEP* **03** (2014) 140, [arXiv:1312.1341].

[55] S. Dimopoulos, K. Howe, and J. March-Russell, *Maximally Natural Supersymmetry*, arXiv:1404.7554.

[56] S. Dimopoulos, K. Howe, J. March-Russell, and J. Scoville, *Auto-Concealment of Supersymmetry in Extra Dimensions*, *JHEP* **06** (2015) 041, [arXiv:1412.0805].

[57] K. Howe and J. Scoville, *Benchmarks of Maximally Natural Supersymmetry*, .

[58] S. Dimopoulos, I. Garcia-Garcia, K. Howe, and J. March-Russell, *Structure of Maximally Natural Supersymmetry*, .

[59] D. B. Kaplan and H. Georgi, *SU(2) x U(1) Breaking by Vacuum Misalignment*, *Phys.Lett.* **B136** (1984) 183.

[60] D. B. Kaplan, H. Georgi, and S. Dimopoulos, *Composite Higgs Scalars*, *Phys.Lett.* **B136** (1984) 187.

[61] O. Matsedonskyi, G. Panico, and A. Wulzer, *Light Top Partners for a Light Composite Higgs*, *JHEP* **1301** (2013) 164, [arXiv:1204.6333].

[62] T. J. LeCompte and S. P. Martin, *Large Hadron Collider reach for supersymmetric models with compressed mass spectra*, *Phys.Rev.* **D84** (2011) 015004, [arXiv:1105.4304].

[63] J. Fan, M. Reece, and J. T. Ruderman, *Stealth Supersymmetry*, *JHEP* **1111** (2011) 012, [arXiv:1105.5135].

[64] A. Birkedal, Z. Chacko, and M. K. Gaillard, *Little supersymmetry and the supersymmetric little hierarchy problem*, *JHEP* **0410** (2004) 036, [hep-ph/0404197].

[65] P. H. Chankowski, A. Falkowski, S. Pokorski, and J. Wagner, *Electroweak symmetry breaking in supersymmetric models with heavy scalar superpartners*, *Phys.Lett.* **B598** (2004) 252–262, [hep-ph/0407242].

[66] B. Bellazzini, C. Csaki, A. Delgado, and A. Weiler, *SUSY without the Little Hierarchy*, *Phys.Rev.* **D79** (2009) 095003, [arXiv:0902.0015].

[67] F. Caracciolo, A. Parolini, and M. Serone, *UV Completions of Composite Higgs Models with Partial Compositeness*, *JHEP* **1302** (2013) 066, [arXiv:1211.7290].

[68] R. Barbieri, T. Gregoire, and L. J. Hall, *Mirror world at the large hadron collider*, hep-ph/0509242.

[69] S. Chang, L. J. Hall, and N. Weiner, *A Supersymmetric twin Higgs*, *Phys.Rev.* **D75** (2007) 035009, [hep-ph/0604076].

[70] A. Falkowski, S. Pokorski, and M. Schmaltz, *Twin SUSY*, *Phys.Rev.* **D74** (2006) 035003, [hep-ph/0604066].

[71] M. S. Carena, J. Espinosa, M. Quiros, and C. Wagner, *Analytical expressions for radiatively corrected Higgs masses and couplings in the MSSM*, *Phys.Lett.* **B355** (1995) 209–221, [hep-ph/9504316].

[72] M. S. Carena, M. Quiros, and C. Wagner, *Effective potential methods and the Higgs mass spectrum in the MSSM*, *Nucl.Phys.* **B461** (1996) 407–436, [hep-ph/9508343].

[73] A. Arvanitaki, M. Baryakhtar, X. Huang, K. Van Tilburg, and G. Villadoro, *The Last Vestiges of Naturalness*, arXiv:1309.3568.

[74] A. Arvanitaki, N. Craig, S. Dimopoulos, and G. Villadoro, *Mini-Split*, *JHEP* **1302** (2013) 126, [arXiv:1210.0555].

[75] X. Lu, H. Murayama, J. T. Ruderman, and K. Tobioka, *A Natural Higgs Mass in Supersymmetry from Non-Decoupling Effects*, arXiv:1308.0792.

[76] R. Harnik, G. D. Kribs, D. T. Larson, and H. Murayama, *The Minimal supersymmetric fat Higgs model*, *Phys.Rev.* **D70** (2004) 015002, [hep-ph/0311349].

[77] B. Schrempp and M. Wimmer, *Top quark and Higgs boson masses: Interplay between infrared and ultraviolet physics*, *Prog.Part.Nucl.Phys.* **37** (1996) 1–90, [hep-ph/9606386].

[78] S. Chang, C. Kilic, and R. Mahbubani, *The New fat Higgs: Slimmer and more attractive*, *Phys.Rev.* **D71** (2005) 015003, [hep-ph/0405267].

[79] E. Hardy, J. March-Russell, and J. Unwin, *Precision Unification in λ SUSY with a 125 GeV Higgs*, *JHEP* **1210** (2012) 072, [arXiv:1207.1435].

[80] Y. Gershtein, M. Luty, M. Narain, L. T. Wang, D. Whiteson, et al., *New Particles Working Group Report of the Snowmass 2013 Community Summer Study*, arXiv:1311.0299.

[81] T. Cohen, T. Golling, M. Hance, A. Henrichs, K. Howe, et al., *SUSY Simplified Models at 14, 33, and 100 TeV Proton Colliders*, arXiv:1311.6480.

[82] Z. Chacko, H.-S. Goh, and R. Harnik, *A Twin Higgs model from left-right symmetry*, *JHEP* **0601** (2006) 108, [hep-ph/0512088].

[83] H.-S. Goh and S. Su, *Phenomenology of The Left-Right Twin Higgs Model*, *Phys.Rev.* **D75** (2007) 075010, [hep-ph/0611015].

[84] D. Carmi, A. Falkowski, E. Kuflik, and T. Volansky, *Interpreting LHC Higgs Results from Natural New Physics Perspective*, *JHEP* **1207** (2012) 136, [arXiv:1202.3144].

[85] D. Carmi, A. Falkowski, E. Kuflik, T. Volansky, and J. Zupan, *Higgs After the Discovery: A Status Report*, *JHEP* **1210** (2012) 196, [arXiv:1207.1718].

[86] Y.-B. Liu, S. Cheng, and Z.-J. Xiao, *The left-right twin Higgs model confronted with the latest LHC Higgs data*, arXiv:1311.0183.

[87] A. Azatov and J. Galloway, *Electroweak Symmetry Breaking and the Higgs Boson: Confronting Theories at Colliders*, *Int.J.Mod.Phys.* **A28** (2013) 1330004, [arXiv:1212.1380].

[88] **ATLAS Collaboration** Collaboration, *Search for invisible decays of a Higgs boson produced in association with a Z boson in ATLAS*, .

[89] **CMS Collaboration** Collaboration, C. Collaboration, *Search for an Invisible Higgs Boson*, .

[90] **CMS Collaboration** Collaboration, C. Collaboration, *Search for invisible Higgs produced in association with a Z boson*, .

[91] N. Craig, J. Galloway, and S. Thomas, *Searching for Signs of the Second Higgs Doublet*, arXiv:1305.2424.

[92] R. Barbieri, B. Bellazzini, V. S. Rychkov, and A. Varagnolo, *The Higgs boson from an extended symmetry*, *Phys.Rev.* **D76** (2007) 115008, [arXiv:0706.0432].

[93] A. Azatov, R. Contino, and J. Galloway, *Model-Independent Bounds on a Light Higgs*, *JHEP* **1204** (2012) 127, [arXiv:1202.3415].

[94] G. Belanger, B. Dumont, U. Ellwanger, J. Gunion, and S. Kraml, *Status of invisible Higgs decays*, *Phys.Lett.* **B723** (2013) 340–347, [arXiv:1302.5694].

[95] M. Bowen, Y. Cui, and J. D. Wells, *Narrow trans-TeV Higgs bosons and H to hh decays: Two LHC search paths for a hidden sector Higgs boson*, *JHEP* **0703** (2007) 036, [hep-ph/0701035].

[96] N. Craig, J. A. Evans, R. Gray, C. Kilic, M. Park, et al., *Multi-Lepton Signals of Multiple Higgs Bosons*, *JHEP* **1302** (2013) 033, [arXiv:1210.0559].

[97] M. Baak, M. Goebel, J. Haller, A. Hoecker, D. Ludwig, et al., *Updated Status of the Global Electroweak Fit and Constraints on New Physics*, *Eur.Phys.J.* **C72** (2012) 2003, [arXiv:1107.0975].

[98] S. L. Glashow and S. Weinberg, *Natural Conservation Laws for Neutral Currents*, *Phys.Rev.* **D15** (1977) 1958.

[99] Z. Berezhiani, A. Dolgov, and R. Mohapatra, *Asymmetric inflationary reheating and the nature of mirror universe*, *Phys.Lett.* **B375** (1996) 26–36, [hep-ph/9511221].

[100] Z. Berezhiani, *Through the looking-glass: Alice's adventures in mirror world*, hep-ph/0508233.

[101] R. Foot, *Mirror matter-type dark matter*, *Int.J.Mod.Phys.* **D13** (2004) 2161–2192, [astro-ph/0407623].

[102] **Planck Collaboration** Collaboration, P. Ade et al., *Planck 2013 results. XVI. Cosmological parameters*, arXiv:1303.5076.

[103] E. Hardy, *Is Natural SUSY Natural?*, *JHEP* **1310** (2013) 133, [arXiv:1306.1534].

[104] J. L. Feng, *Naturalness and the Status of Supersymmetry*, *Ann.Rev.Nucl.Part.Sci.* **63** (2013) 351–382, [arXiv:1302.6587].

[105] T. Gherghetta, B. von Harling, A. D. Medina, and M. A. Schmidt, *The price of being SM-like in SUSY*, arXiv:1401.8291.

[106] J. Fan and M. Reece, *A New Look at Higgs Constraints on Stops*, arXiv:1401.7671.

[107] I. Antoniadis, S. Dimopoulos, A. Pomarol, and M. Quiros, *Soft masses in theories with supersymmetry breaking by TeV compactification*, *Nucl.Phys.* **B544** (1999) 503–519, [hep-ph/9810410].

[108] A. Delgado, A. Pomarol, and M. Quiros, *Supersymmetry and electroweak breaking from extra dimensions at the TeV scale*, *Phys.Rev.* **D60** (1999) 095008, [hep-ph/9812489].

[109] A. Pomarol and M. Quiros, *The Standard model from extra dimensions*, *Phys.Lett.* **B438** (1998) 255–260, [hep-ph/9806263].

[110] A. Delgado and M. Quiros, *Supersymmetry and finite radiative electroweak breaking from an extra dimension*, *Nucl.Phys.* **B607** (2001) 99–116, [hep-ph/0103058].

[111] A. Delgado, G. von Gersdorff, and M. Quiros, *Two loop Higgs mass in supersymmetric Kaluza-Klein theories*, *Nucl.Phys.* **B613** (2001) 49–63, [hep-ph/0107233].

[112] R. Barbieri, G. Marandella, and M. Papucci, *The Higgs mass as a function of the compactification scale*, *Nucl.Phys.* **B668** (2003) 273–292, [hep-ph/0305044].

[113] R. Barbieri, L. J. Hall, G. Marandella, Y. Nomura, T. Okui, et al., *Radiative electroweak symmetry breaking from a quasilocalized top quark*, *Nucl.Phys.* **B663** (2003) 141–162, [hep-ph/0208153].

[114] R. Barbieri, G. Marandella, and M. Papucci, *Breaking the electroweak symmetry and supersymmetry by a compact extra dimension*, *Phys.Rev.* **D66** (2002) 095003, [hep-ph/0205280].

[115] R. Barbieri, L. J. Hall, and Y. Nomura, *A Constrained standard model from a compact extra dimension*, *Phys.Rev.* **D63** (2001) 105007, [hep-ph/0011311].

[116] D. Marti and A. Pomarol, *Fayet-Iliopoulos terms in 5-d theories and their phenomenological implications*, *Phys.Rev.* **D66** (2002) 125005, [hep-ph/0205034].

[117] D. Diego, G. von Gersdorff, and M. Quiros, *Supersymmetry and electroweak breaking in the interval*, *JHEP* **0511** (2005) 008, [hep-ph/0505244].

[118] D. Diego, G. von Gersdorff, and M. Quiros, *The MSSM from Scherk-Schwarz supersymmetry breaking*, *Phys.Rev.* **D74** (2006) 055004, [hep-ph/0605024].

[119] G. von Gersdorff, *The MSSM on the Interval*, *Mod.Phys.Lett.* **A22** (2007) 385–398, [hep-ph/0701256].

[120] G. Bhattacharyya and T. S. Ray, *Naturally split supersymmetry*, *JHEP* **1205** (2012) 022, [arXiv:1201.1131].

[121] G. Larsen, Y. Nomura, and H. L. Roberts, *Supersymmetry with Light Stops*, *JHEP* **1206** (2012) 032, [arXiv:1202.6339].

[122] I. Antoniadis, S. Dimopoulos, and G. Dvali, *Millimeter range forces in superstring theories with weak scale compactification*, *Nucl.Phys.* **B516** (1998) 70–82, [hep-ph/9710204].

[123] R. Barbieri, L. J. Hall, and Y. Nomura, *Models of Scherk-Schwarz symmetry breaking in 5-D: Classification and calculability*, *Nucl.Phys.* **B624** (2002) 63–80, [hep-th/0107004].

[124] A. Delgado, G. von Gersdorff, P. John, and M. Quiros, *One loop Higgs mass finiteness in supersymmetric Kaluza-Klein theories*, *Phys.Lett.* **B517** (2001) 445–449, [hep-ph/0104112].

[125] R. Contino and L. Pilo, *A Note on regularization methods in Kaluza-Klein theories*, *Phys.Lett.* **B523** (2001) 347–350, [hep-ph/0104130].

[126] N. Weiner, *Ineffective supersymmetry: Electroweak symmetry breaking from extra dimensions*, hep-ph/0106021.

[127] H. D. Kim, *Softness of Scherk-Schwarz supersymmetry breaking*, *Phys.Rev.* **D65** (2002) 105021, [hep-th/0109101].

[128] M. Puchwein and Z. Kunszt, *Radiative corrections with 5-D mixed position / momentum space propagators*, *Annals Phys.* **311** (2004) 288–313, [hep-th/0309069].

[129] R. Barbieri, L. J. Hall, and Y. Nomura, *Softly broken supersymmetric desert from orbifold compactification*, *Phys.Rev.* **D66** (2002) 045025, [hep-ph/0106190].

[130] H. Murayama, Y. Nomura, S. Shirai, and K. Tobioka, *Compact Supersymmetry*, *Phys.Rev.* **D86** (2012) 115014, [arXiv:1206.4993].

[131] C. Han, F. Wang, and J. M. Yang, *Natural SUSY from SU(5) Orbifold GUT*, *JHEP* **1311** (2013) 197, [arXiv:1304.5724].

[132] A. Muck, L. Nilse, A. Pilaftsis, and R. Ruckl, *Quantization and high energy unitarity of 5-D orbifold theories with brane kinetic terms*, *Phys.Rev.* **D71** (2005) 066004, [hep-ph/0411258].

[133] R. S. Chivukula, D. A. Dicus, H.-J. He, and S. Nandi, *Unitarity of the higher dimensional standard model*, *Phys.Lett.* **B562** (2003) 109–117, [hep-ph/0302263].

[134] J. Huang and J. March-Russell, *Unified Maximally Natural Supersymmetry*, arXiv:1507.xxxx.

[135] Z. Chacko, M. A. Luty, and E. Ponton, *Massive higher dimensional gauge fields as messengers of supersymmetry breaking*, *JHEP* **0007** (2000) 036, [hep-ph/9909248].

[136] A. Lewandowski and R. Sundrum, *RS1, higher derivatives and stability*, *Phys.Rev.* **D65** (2002) 044003, [hep-th/0108025].

[137] G. von Gersdorff, M. Quiros, and A. Riotto, *Scherk-Schwarz supersymmetry breaking with radion stabilization*, *Nucl.Phys.* **B689** (2004) 76–90, [hep-th/0310190].

[138] R. Rattazzi, C. A. Scrucca, and A. Strumia, *Brane to brane gravity mediation of supersymmetry breaking*, *Nucl.Phys.* **B674** (2003) 171–216, [hep-th/0305184].

[139] W. D. Goldberger and M. B. Wise, *Modulus stabilization with bulk fields*, *Phys.Rev.Lett.* **83** (1999) 4922–4925, [hep-ph/9907447].

[140] A. E. Nelson and T. S. Roy, *New Supersoft Supersymmetry Breaking Operators and a Solution to the μ Problem*, *Phys.Rev.Lett.* **114** (2015) 201802, [arXiv:1501.03251].

[141] T. Cohen, J. Kearney, and M. Luty, *Natural Supersymmetry without Light Higgsinos*, *Phys.Rev.* **D91** (2015) 075004, [arXiv:1501.01962].

[142] G. Perez, T. S. Roy, and M. Schmaltz, *Phenomenology of SUSY with scalar sequestering*, *Phys.Rev.* **D79** (2009) 095016, [arXiv:0811.3206].

[143] I. Garcia Garcia and J. March-Russell, *Rare Flavor Processes in Maximally Natural Supersymmetry*, *JHEP* **1501** (2015) 042, [arXiv:1409.5669].

[144] D. Ghilencea, S. Groot Nibbelink, and H. P. Nilles, *Gauge corrections and FI term in 5-D KK theories*, *Nucl.Phys.* **B619** (2001) 385–395, [hep-th/0108184].

[145] R. Barbieri, R. Contino, P. Creminelli, R. Rattazzi, and C. Scrucca, *Anomalies, Fayet-Iliopoulos terms and the consistency of orbifold field theories*, *Phys.Rev.* **D66** (2002) 024025, [hep-th/0203039].

[146] G. D. Kribs and A. Martin, *Supersoft Supersymmetry is Super-Safe*, *Phys. Rev.* **D85** (2012) 115014, [arXiv:1203.4821].

[147] A. Hebecker and J. March-Russell, *The Flavor hierarchy and seesaw neutrinos from bulk masses in 5-d orbifold GUTs*, *Phys.Lett.* **B541** (2002) 338–345, [hep-ph/0205143].

[148] L. J. Hall, J. March-Russell, T. Okui, and D. Tucker-Smith, *Towards a theory of flavor from orbifold GUTs*, *JHEP* **0409** (2004) 026, [hep-ph/0108161].

[149] C. Froggatt and H. B. Nielsen, *Hierarchy of Quark Masses, Cabibbo Angles and CP Violation*, *Nucl.Phys.* **B147** (1979) 277.

[150] M. A. Luty, *2004 TASI lectures on supersymmetry breaking*, hep-th/0509029.

[151] L. Randall and R. Sundrum, *Out of this world supersymmetry breaking*, *Nucl.Phys.* **B557** (1999) 79–118, [hep-th/9810155].

[152] P. J. Fox, A. E. Nelson, and N. Weiner, *Dirac gaugino masses and supersoft supersymmetry breaking*, *JHEP* **0208** (2002) 035, [hep-ph/0206096].

[153] D. S. M. Alves, J. Galloway, M. McCullough, and N. Weiner, *Goldstone Gauginos*, arXiv:1502.03819.

[154] D. Marti and A. Pomarol, *Supersymmetric theories with compact extra dimensions in N=1 superfields*, *Phys.Rev.* **D64** (2001) 105025, [hep-th/0106256].

[155] H. E. Haber and R. Hempfling, *The Renormalization group improved Higgs sector of the minimal supersymmetric model*, *Phys.Rev.* **D48** (1993) 4280–4309, [hep-ph/9307201].

[156] S. P. Martin, *Extra vector-like matter and the lightest Higgs scalar boson mass in low-energy supersymmetry*, *Phys.Rev.* **D81** (2010) 035004, [arXiv:0910.2732].

[157] P. Batra, A. Delgado, D. E. Kaplan, and T. M. Tait, *The Higgs mass bound in gauge extensions of the minimal supersymmetric standard model*, *JHEP* **0402** (2004) 043, [hep-ph/0309149].

[158] A. Maloney, A. Pierce, and J. G. Wacker, *D-terms, unification, and the Higgs mass*, *JHEP* **0606** (2006) 034, [hep-ph/0409127].

[159] C. Cheung and H. L. Roberts, *Higgs Mass from D-Terms: a Litmus Test*, *JHEP* **1312** (2013) 018, [arXiv:1207.0234].

[160] H. K. Dreiner, S. Heinemeyer, O. Kittel, U. Langenfeld, A. M. Weber, et al., *Mass Bounds on a Very Light Neutralino*, *Eur.Phys.J.* **C62** (2009) 547–572, [arXiv:0901.3485].

[161] H. Dreiner, C. Hanhart, U. Langenfeld, and D. R. Phillips, *Supernovae and light neutralinos: SN1987A bounds on supersymmetry revisited*, *Phys.Rev.* **D68** (2003) 055004, [hep-ph/0304289].

[162] **Planck** Collaboration, P. Ade et al., *Planck 2015 results. XIII. Cosmological parameters*, arXiv:1502.01589.

[163] D. Atwood, C. Burgess, E. Filotas, F. Leblond, D. London, et al., *Supersymmetric large extra dimensions are small and/or numerous*, *Phys.Rev.* **D63** (2001) 025007, [hep-ph/0007178].

[164] C. Burgess, J. Matias, and F. Quevedo, *MSLED: A Minimal supersymmetric large extra dimensions scenario*, *Nucl.Phys.* **B706** (2005) 71–99, [hep-ph/0404135].

[165] J. Matias and C. Burgess, *MSLED, neutrino oscillations and the cosmological constant*, *JHEP* **0509** (2005) 052, [hep-ph/0508156].

[166] M. Cicoli, C. Burgess, and F. Quevedo, *Anisotropic Modulus Stabilisation: Strings at LHC Scales with Micron-sized Extra Dimensions*, *JHEP* **1110** (2011) 119, [arXiv:1105.2107].

[167] I. Antoniadis, K. Benakli, and A. Laugier, *D-brane models with nonlinear supersymmetry*, *Nucl.Phys.* **B631** (2002) 3–42, [hep-th/0111209].

[168] E. Dudas and J. Mourad, *Consistent gravitino couplings in nonsupersymmetric strings*, *Phys.Lett.* **B514** (2001) 173–182, [hep-th/0012071].

[169] M. Klein, *Couplings in pseudosupersymmetry*, *Phys.Rev.* **D66** (2002) 055009, [hep-th/0205300].

[170] I. Antoniadis and M. Tuckmantel, *Nonlinear supersymmetry and intersecting D-branes*, *Nucl.Phys.* **B697** (2004) 3–47, [hep-th/0406010].

[171] D. S. M. Alves, J. Liu, and N. Weiner, *Hiding Missing Energy in Missing Energy*, arXiv:1312.4965.

[172] E. Izaguirre, M. Manhart, and J. G. Wacker, *Bigger, Better, Faster, More at the LHC*, *JHEP* **1012** (2010) 030, [arXiv:1003.3886].

[173] T. J. LeCompte and S. P. Martin, *Compressed supersymmetry after 1/fb at the Large Hadron Collider*, *Phys.Rev.* **D85** (2012) 035023, [arXiv:1111.6897].

[174] B. Bhattacherjee and K. Ghosh, *Degenerate SUSY search at the 8 TeV LHC*, arXiv:1207.6289.

[175] M. Drees, M. Hanussek, and J. S. Kim, *Light Stop Searches at the LHC with Monojet Events*, *Phys.Rev.* **D86** (2012) 035024, [arXiv:1201.5714].

[176] G. Belanger, M. Heikinheimo, and V. Sanz, *Model-Independent Bounds on Squarks from Monophoton Searches*, *JHEP* **1208** (2012) 151, [arXiv:1205.1463].

[177] B. Bhattacherjee, A. Choudhury, K. Ghosh, and S. Poddar, *Compressed supersymmetry at 14 TeV LHC*, *Phys.Rev.* **D89** (2014), no. 3 037702, [arXiv:1308.1526].

[178] E. A. Mirabelli and M. E. Peskin, *Transmission of supersymmetry breaking from a four-dimensional boundary*, *Phys.Rev.* **D58** (1998) 065002, [hep-th/9712214].

[179] R. Sundrum, *Effective field theory for a three-brane universe*, *Phys.Rev.* **D59** (1999) 085009, [hep-ph/9805471].

[180] N. Arkani-Hamed, T. Gregoire, and J. G. Wacker, *Higher dimensional supersymmetry in 4-D superspace*, *JHEP* **0203** (2002) 055, [hep-th/0101233].

[181] A. Hebecker, *5-D superYang-Mills theory in 4-D superspace, superfield brane operators, and applications to orbifold GUTs*, *Nucl.Phys.* **B632** (2002) 101–113, [hep-ph/0112230].

[182] I. Linch, William Divine, M. A. Luty, and J. Phillips, *Five-dimensional supergravity in N=1 superspace*, *Phys.Rev.* **D68** (2003) 025008, [hep-th/0209060].

[183] J. L. Hewett and D. Sadri, *Supersymmetric extra dimensions: Gravitino effects in selectron pair production*, *Phys.Rev.* **D69** (2004) 015001, [hep-ph/0204063].

[184] N. Kaloper, J. March-Russell, G. D. Starkman, and M. Trodden, *Compact hyperbolic extra dimensions: Branes, Kaluza-Klein modes and cosmology*, *Phys.Rev.Lett.* **85** (2000) 928–931, [hep-ph/0002001].

[185] J. Alwall, M. Herquet, F. Maltoni, O. Mattelaer, and T. Stelzer, *MadGraph 5 : Going Beyond*, *JHEP* **1106** (2011) 128, [arXiv:1106.0522].

[186] T. Sjostrand, S. Mrenna, and P. Z. Skands, *PYTHIA 6.4 Physics and Manual*, *JHEP* **0605** (2006) 026, [hep-ph/0603175].

[187] M. Drees, H. Dreiner, D. Schmeier, J. Tattersall, and J. S. Kim, *CheckMATE: Confronting your Favourite New Physics Model with LHC Data*, arXiv:1312.2591.

[188] **DELPHES 3** Collaboration, J. de Favereau et al., *DELPHES 3, A modular framework for fast simulation of a generic collider experiment*, *JHEP* **1402** (2014) 057, [arXiv:1307.6346].

[189] M. Cacciari and G. P. Salam, *Dispelling the N^3 myth for the k_t jet-finder*, *Phys.Lett.* **B641** (2006) 57–61, [hep-ph/0512210].

[190] M. Cacciari, G. P. Salam, and G. Soyez, *FastJet User Manual*, *Eur.Phys.J.* **C72** (2012) 1896, [arXiv:1111.6097].

[191] M. Cacciari, G. P. Salam, and G. Soyez, *The Anti-k(t) jet clustering algorithm*, *JHEP* **0804** (2008) 063, [arXiv:0802.1189].

[192] A. L. Read, *Presentation of search results: The CL(s) technique*, *J.Phys.* **G28** (2002) 2693–2704.

[193] C. Lester and D. Summers, *Measuring masses of semiinvisibly decaying particles pair produced at hadron colliders*, *Phys.Lett.* **B463** (1999) 99–103, [hep-ph/9906349].

[194] A. Barr, C. Lester, and P. Stephens, *m(T2): The Truth behind the glamour*, *J.Phys.* **G29** (2003) 2343–2363, [hep-ph/0304226].

[195] H.-C. Cheng and Z. Han, *Minimal Kinematic Constraints and m(T2)*, *JHEP* **0812** (2008) 063, [arXiv:0810.5178].

[196] **LEPSUSYWG,ALEPH,DELPHI,L3, and OPAL experiments** Collaboration, *Combined LEP Selectron/Smuon/Stau Results, 183-208 GeV*, Tech. Rep. LEPSUSYWG/04-01.1, CERN, Geneva, June, 2004.

[197] **ALEPH** Collaboration, A. Heister et al., *Search for scalar leptons in e+ e- collisions at center-of-mass energies up to 209-GeV*, *Phys.Lett.* **B526** (2002) 206–220, [hep-ex/0112011].

[198] **L3** Collaboration, P. Achard et al., *Search for scalar leptons and scalar quarks at LEP*, *Phys.Lett.* **B580** (2004) 37–49, [hep-ex/0310007].

[199] **OPAL** Collaboration, G. Abbiendi et al., *Search for anomalous production of dilepton events with missing transverse momentum in e+ e- collisions at s**(1/2) = 183-Gev to 209-GeV*, *Eur.Phys.J.* **C32** (2004) 453–473, [hep-ex/0309014].

[200] **DELPHI** Collaboration, J. Abdallah et al., *Searches for supersymmetric particles in e+ e- collisions up to 208-GeV and interpretation of the results within the MSSM*, *Eur.Phys.J.* **C31** (2003) 421–479, [hep-ex/0311019].

[201] **CMS** Collaboration, *Exclusion limits on gluino and top-squark pair production in natural SUSY scenarios with inclusive razor and exclusive single-lepton searches at 8 TeV.*, Tech. Rep. CMS-PAS-SUS-14-011, CERN, Geneva, 2014.

[202] **ATLAS** Collaboration, G. Aad et al., *Search for direct pair production of the top squark in all-hadronic final states in proton-proton collisions at* $\sqrt{s} = 8$ *TeV with the ATLAS detector*, *JHEP* **1409** (2014) 015, [arXiv:1406.1122].

[203] J. Bagger and A. Galperin, *A New Goldstone multiplet for partially broken supersymmetry*, *Phys.Rev.* **D55** (1997) 1091–1098, [hep-th/9608177].

[204] G. Pradisi and F. Riccioni, *Geometric couplings and brane supersymmetry breaking*, *Nucl.Phys.* **B615** (2001) 33–60, [hep-th/0107090].

[205] J. A. Bagger and D. V. Belyaev, *Brane-localized Goldstone fermions in bulk supergravity*, *Phys.Rev.* **D72** (2005) 065007, [hep-th/0406126].

[206] K. Benakli and C. Moura, *Brane-Worlds Pseudo-Goldstinos*, *Nucl.Phys.* **B791** (2008) 125–163, [arXiv:0706.3127].

[207] J. Scherk and J. H. Schwarz, *Spontaneous Breaking of Supersymmetry Through Dimensional Reduction*, *Phys.Lett.* **B82** (1979) 60.

[208] J. Scherk and J. H. Schwarz, *How to Get Masses from Extra Dimensions*, *Nucl.Phys.* **B153** (1979) 61–88.

[209] S. Ferrara, C. Kounnas, M. Porrati, and F. Zwirner, *Superstrings with Spontaneously Broken Supersymmetry and their Effective Theories*, *Nucl.Phys.* **B318** (1989) 75.

[210] M. Porrati and F. Zwirner, *Supersymmetry Breaking in String Derived Supergravities*, *Nucl.Phys.* **B326** (1989) 162.

[211] D. E. Kaplan and N. Weiner, *Radion mediated supersymmetry breaking as a Scherk-Schwarz theory*, hep-ph/0108001.

[212] T. Gherghetta and A. Riotto, *Gravity mediated supersymmetry breaking in the brane world*, *Nucl.Phys.* **B623** (2002) 97–125, [hep-th/0110022].

[213] L. Covi, L. Roszkowski, and M. Small, *Effects of squark processes on the axino CDM abundance*, *JHEP* **0207** (2002) 023, [hep-ph/0206119].

[214] K. J. Bae, E. J. Chun, and S. H. Im, *Cosmology of the DFSZ axino*, *JCAP* **1203** (2012) 013, [arXiv:1111.5962].

[215] M. Baryakhtar, E. Hardy, and J. March-Russell, *Axion Mediation*, *JHEP* **1307** (2013) 096, [arXiv:1301.0829].

[216] K. J. Bae, K. Choi, and S. H. Im, *Effective Interactions of Axion Supermultiplet and Thermal Production of Axino Dark Matter*, *JHEP* **1108** (2011) 065, [arXiv:1106.2452].

[217] S. Abel and B. Schofield, *Brane anti-brane kinetic mixing, millicharged particles and SUSY breaking*, *Nucl.Phys.* **B685** (2004) 150–170, [hep-th/0311051].

[218] S. Abel, M. Goodsell, J. Jaeckel, V. Khoze, and A. Ringwald, *Kinetic Mixing of the Photon with Hidden U(1)s in String Phenomenology*, *JHEP* **0807** (2008) 124, [arXiv:0803.1449].

[219] N. Arkani-Hamed, S. Dimopoulos, G. Dvali, and J. March-Russell, *Neutrino masses from large extra dimensions*, *Phys.Rev.* **D65** (2002) 024032, [hep-ph/9811448].